

**Biodegradation of RDX in**  
***Rhodococcus* spp.**

Chun Shiong Chong

Ph D

University of York  
Department of Biology  
August 2011

# Abstract

The manufacture, use and storage of explosives over decades have seriously contaminated the environment. Hexa-hydro-1,3,5-trinitro-1,3,5-triazine (Royal Demolition Explosive - RDX) is one of the most widely used explosives. RDX is a man-made compound, recalcitrant to degradation and proven to be toxic to organisms. Bacteria capable of utilising RDX as a sole nitrogen source for growth have been isolated from RDX polluted sites including *Rhodococcus rhodochrous* 11Y. The RDX degrading genes, *xplA* and *xplB* encoding a novel flavodoxin fused cytochrome P450 and its reductase partner respectively, were first identified in *R. rhodochrous* 11Y. This unusual P450 system has now been found in almost all of the RDX degrading bacteria isolated so far. To date, XplA/B remains the only characterised RDX degrading P450 system and is encoded on an operon in strain 11Y, which also contains a putative permease (transporter) and transcriptional regulator. This gene cluster is highly conserved amongst other RDX degrading bacteria from geographically distinct regions including the United Kingdom, Belgium, Australia and North America, suggesting the *xplA/B* gene cluster may have been rapidly distributed across the globe by horizontal gene transfer.

The first aim of this study was to characterise *Rhodococcus erythropolis* HS4, a bacterium that degrades RDX slowly but did not contain *xplA* and *xplB*. A number of approaches have been employed to characterise this strain, which includes whole cell assays, western analysis, cell free extract activity assays, PCR amplification and affinity purification of protein in *R. erythropolis* HS4. While whole cells of HS4 showed low RDX degrading activity, no RDX activity was observed in HS4 cell free extracts. Attempts to purify an RDX degrading enzyme from *R. erythropolis* HS4 were unsuccessful.

The second aim of this project was to characterise the RDX degrading gene cluster in *R. rhodochrous* 11Y. Four genes encoding *xplB*, *xplA*, a putative permease and a MarR type regulator, were individually deleted using an unmarked gene deletion system (pK18mobsacB). The *xplB* knockout strain metabolised RDX more slowly than the wild-type suggesting XplA was able to obtain reducing equivalents from another source in the *xplB* knockout strain. The *xplA* knockout strain did not show RDX activity in whole cell and growth experiments. Neither *xplA* nor its gene product XplA was

detected in the *xplA* knockout strain. The findings suggested no alternative RDX degrading system is present in strain 11Y. The permease knockout did not show significant difference in the RDX removal rate compared to wild-type. Another attempt to characterise the permease in 11Y was to express it in *E. coli*. No significant difference of RDX uptake between the permease-expressing clone and the control (non-expressing clone) in the uptake assays. The regulator knockout strain had a lower RDX degradation rate than wild-type in the presence of nitrate/nitrite. Also, when the regulator knockout and wild-type strains were previously exposed to nitrate/nitrite, the knockout showed lower RDX degrading activity. Further investigation of *xplA* regulation in strain 11Y showed that XplA activity was induced by nitrogen-limiting conditions and further induced by RDX. This was the first observation on the XplA activity could be induced by low nitrogen availability in medium. These results suggested that the regulator is indirectly involved in controlling the expression of XplA in 11Y, which is linked to central nitrogen metabolism.

# Table of Contents

<b>Abstract</b>	<b>2</b>
<b>Table of Contents</b>	<b>4</b>
<b>List of Figures</b>	<b>11</b>
<b>List of Tables</b>	<b>15</b>
<b>List of Abbreviations</b>	<b>16</b>
<b>Acknowledgements</b>	<b>18</b>
<b>Author's Declaration</b>	<b>20</b>
<b>Publications arising from this work</b>	<b>21</b>
<b>Chapter 1 Introduction</b>	<b>22</b>
1.1 An overview of explosives	22
1.2 Contamination of the environment by explosives	26
1.3 Remediation technologies	29
1.3.1 Incineration	29
1.3.2 Bioremediation	29
1.3.2.1 Composting	29
1.3.2.2 Biostimulation	30
1.3.2.3 Phytoremediation	30
1.4 Microbial transformation of TNT	32
1.5 RDX	34

1.5.1 Microbial degradation of RDX	35
1.6 RDX degradation by commercial enzymes	40
1.7 <i>Rhodococcus rhodochrous</i> 11Y	41
1.8 Characterisation of XplA and XplB	43
1.9 The XplA-heme structure	45
1.10 RDX degrading gene cluster	48
1.11 Aims	51
<b>Chapter 2</b>	
<b>General methods</b>	<b>52</b>
2.1 Suppliers	52
2.2 Media	52
2.2.1 Minimal medium	52
2.2.2 Luria-Bertani Peptone (LBP) medium	52
2.2.3 Luria-Bertani (LB) medium	52
2.2.4 Tryptone medium	54
2.2.5 RDX dispersion agar	54
2.3 Bacterial strains and plasmids	54
2.4 Growth and resting cell experiments	54
2.4.1 Growth experiment and RDX degradation	54
2.4.2 Resting cell assays	54
2.5 Protein techniques	56
2.5.1 Preparation of cell free extracts	56
2.5.2 Protein quantification	56

2.5.3 SDS-PAGE gel analysis	56
2.5.4 Western blot analysis	57
2.5.5 Specific activity of XplA in cell free extracts	58
2.6 Molecular biology techniques	59
2.6.1 Gel electrophoresis of DNA	59
2.6.2 Polymerase chain reaction (PCR)	59
2.6.3 Digestion, dephosphorylation and ligation of DNA	60
2.6.4 Preparation of competent cells (calcium chloride method)	60
2.6.5 Preparation of competent cells (for knockout experiment)	60
2.6.6 Plasmid transformation (Heat shock)	60
2.6.7 Quantitative real-time PCR (qPCR) analysis	61
2.6.8 Sequencing	61
2.7 Analytical techniques	62
2.7.1 HPLC analysis	62
2.7.2 Griess assay	62
<b>Chapter 3</b>	
<b>RDX degradation in <i>Rhodococcus erythropolis</i> strain HS4</b>	<b>63</b>
3.1 Introduction	63
3.2 Materials and methods	65
3.2.1 Assay development for RDX degrading activity	65
3.2.2 Protein purification using Protein A SpinTrap column	65
3.2.3 PCR amplification	65
3.3 Results	66

3.3.1 Whole cell assays of <i>R. erythropolis</i> HS4	66
3.3.2 Assay development to detect RDX degrading activity (XplA) in cell free extracts	67
3.3.3 RDX activity in cell free extracts of strain HS4	70
3.3.4 Western blot analysis of strain HS4 cell free extracts	71
3.3.5 Purification trial of a putative RDX degrading enzyme in strain HS4	72
3.3.6 Lost of RDX activity in new batches of strain HS4	76
3.3.7 Zone of clearance on RDX dispersion agar	76
3.3.8 PCR amplification of <i>xplA</i> and <i>xplB</i> homologue	78
3.3.9 Sequencing of 16S rRNA gene in latest <i>Rhodococcus erythropolis</i> strain HS4	79
3.4 Discussion	80

## Chapter 4

### **Heterologous expression of a putative permease from *R. rhodochrous* strain 11Y** **83**

4.1 Introduction	83
4.2 Materials and methods	85
4.2.1 Ligation dependent cloning	85
4.2.2 Ligation independent cloning (LIC)	86
4.2.3 XplA and permease expression	87
4.2.4 His-tagged permease expression	87
4.2.5 Preparation of total protein fraction	87
4.2.6 Membrane protein isolation	88
4.2.7 Permease purification	88

4.2.8 RDX uptake assay	89
4.3 Results	90
4.3.1 Sequence analysis of the putative permease from <i>R. rhodochrous</i> 11Y	90
4.3.2 <i>Permease</i> and <i>xplA</i> expression in strain 11Y	91
4.3.3 PCR of <i>permease</i> homologue	92
4.3.4 Cloning and expression of permease and XplA	93
4.3.4.1 Resting cell assays	93
4.3.4.2 XplA activity in cell free extracts	95
4.3.4.3 RDX uptake assays	97
4.3.4.4 Growth of induced and uninduced Rosetta 2 pLICP2	98
4.3.4.5 Permease detection in the total protein fraction	99
4.3.4.6 Permease detection in the membrane protein fraction	100
4.3.4.7 Effect of temperature on the expression of the permease	101
4.3.4.8 Effect of IPTG concentration on permease expression	102
4.3.4.9 Purification of permease and peptide mass fingerprinting	103
4.3.4.10 Whole cell RDX uptake assays	104
4.4 Discussion	105

## Chapter 5

### Construction and characterisation of rhodococcal knockout strains 109

5.1 Introduction	109
5.2 Materials and methods	112
5.2.1 Inserts preparation	112



5.2.2 Plasmids construction	112
5.2.3 Screening, selection and validation of positive clones	114
5.2.4 Transconjugation	115
5.2.5 Second cross-over	115
5.2.6 Screening and selection of gene deleted strain	115
5.3 Results	116
5.3.1 Construction of knockout strains	116
5.3.1.1 Empty plasmid validation	116
5.3.1.2 Construct validation	117
5.3.1.3 Transconjugation	118
5.3.1.4 Gene-deleted strains	121
5.3.2 Characterisation of the knockout strains	123
5.3.2.1 Characterisation of the <i>xp/A</i> knockout strain	123
5.3.2.2 Western blot analysis	124
5.3.2.3 Resting cell assays of the <i>xp/A</i> knockout strain	125
5.3.2.4. Growth of the <i>xp/A</i> knockout strain on RDX dispersion agar	126
5.3.2.5 Characterisation of the <i>xp/B</i> knockout strain	127
5.3.2.6 Resting cell assays for the <i>xp/B</i> knockout strain	128
5.3.2.7 Quantitative RT-PCR and western blot analysis for the <i>xp/B</i> knockout strain	129
5.3.2.8 Characterisation of the permease knockout strain	130
5.3.3 Initial investigation of <i>xp/A</i> regulation in strain 11Y	132
5.3.3.1 Studies under nitrogen-limiting conditions and RDX	132
5.3.3.2 Putative promoter prediction of the <i>xp/A</i> operon	137

5.3.3.3 Sequence analysis of the MarR-like regulator in 11Y	141
5.3.3.4 RDX removal by whole cells of RDX-grown regulator knockout strain	142
5.3.3.5 RDX removal by the regulator knockout strain exposed to different nitrogen sources	143
5.3.3.6 A comparison of RDX degradation and growth of the wild-type and regulator knockout strains in the presence of alternative nitrogen sources	145
5.4 Discussion	150
<b>Chapter 6</b>	
6.1 Final discussion	154
Appendix A: Typical protein assay standard curve	159
Appendix B: Typical RDX standard curve	160
Appendix C: Typical nitrite standard curve	161
Appendix D: Sequencing analysis for knockouts	162
<b>References</b>	<b>166</b>

# List of Figures

Figure 1.1.	Example of explosives synthesised from nitration reaction.	25
Figure 1.2.	Explosives detected in the contaminated sites at the Camp Edwards, Massachusetts Military Reservation, MA.	28
Figure 1.3.	TNT degradation pathways.	33
Figure 1.4.	Proposed anaerobic RDX degradation pathways with anaerobic sludge.	38
Figure 1.5.	RDX degradation pathway in <i>Rhodococcus</i> strain DN22.	39
Figure 1.6.	The gene cluster isolated from strain 11Y contains genes responsible for RDX degradation.	42
Figure 1.7.	Proposed RDX degradation pathway by XplA and XplB.	44
Figure 1.8.	Topology of XplA-heme revealing the well conserved secondary elements.	46
Figure 1.9.	The active site and XplA-heme environment.	47
Figure 1.10.	The putative transport channels are shown in grey.	47
Figure 1.11.	Sequence comparison of gene clusters flanking <i>xplA/B</i> isolated from <i>Rhodococcus rhodochrous</i> 11Y (cluster A) and <i>Microbacterium sp.</i> MA1 (cluster B).	50
Figure 1.12.	RDX gene clusters flanking <i>xplA</i> isolated from <i>Gordonia sp.</i> strain KTR9.	50
Figure 3.1.	Clearance zone formed by isolated RDX degrading bacteria of <i>Rhodococcus</i> strains on RDX dispersion agar.	63
Figure 3.2.	RDX removal by whole cells of strains HS4 and 11Y after 20 hours of incubation at 20 °C.	66
Figure 3.3.	RDX activity in cell free extracts of strain 11Y under aerobic condition after 90 minutes of incubation.	68
Figure 3.4.	RDX (grey) and nitrite (white) concentration after 90 minutes of incubation with cell free extracts of 11Y under aerobic conditions at 20 °C.	69
Figure 3.5.	Analysis of HS4 cell free extracts for RDX degradation after 20 h at 20 °C under aerobic conditions.	70
Figure 3.6.	Western blot analysis of cell free extracts of strains 11Y and HS4.	71
Figure 3.7.	Principle of purification of protein using XplA antibody.	72

Figure 3.8.	Purification of IgGs in rabbit serum using Protein A HP SpinTrap column.	73
Figure 3.9.	Purification of protein from HS4 that is active towards XplA antibody.	74
Figure 3.10.	SDS-PAGE (a) and western blot (b) following purification of XplA from 11Y cell free extracts.	75
Figure 3.11.	RDX dispersion agar for strains 11Y and HS4.	76
Figure 3.12.	Growth of strain HS4 from glycerol stock on RDX (5 mM) dispersion agar.	77
Figure 3.13.	PCR amplification using primers specific to <i>xplA</i> and <i>xplB</i> genes with different primers combination.	78
Figure 4.1.	Topology of the putative rhodococcal permease.	83
Figure 4.2.	Quantitative real time PCR analysis for <i>xplA</i> and <i>permease</i> in strain 11Y with <i>gyrB</i> as an endogenous control.	91
Figure 4.3.	PCR amplification using primers specific to <i>permease</i> .	92
Figure 4.4.	Resting cells incubation (HPLC analysis).	94
Figure 4.5.	Resting cells incubation (Griess assay).	94
Figure 4.6.	RDX removal using cell free extracts of XplA co-expressed with permease (clone AP) compared to the XplA expressing control (clone A).	96
Figure 4.7.	RDX uptake in cells of the permease expressing clone (clone P) and Rosetta 2 (empty vector).	97
Figure 4.8.	Effect of IPTG induction on growth of Rosetta 2 pLICP2.	98
Figure 4.9.	SDS-PAGE and western blots of total proteins of Rosetta 2 pLICP2.	99
Figure 4.10.	Detection of His-tagged permease.	100
Figure 4.11.	Permease expression at different induction temperature.	101
Figure 4.12.	Effect of IPTG concentration in permease expression.	102
Figure 4.13.	Purification of permease using Nickel column.	103
Figure 4.14.	Uptake of RDX by induced and uninduced Rosetta 2 pLICP2.	104
Figure 5.1.	Organisation of the RDX degradation gene cluster in <i>R. rhodochrous</i> 11Y.	109

Figure 5.2.	The principle of the construction of a gene-deleted strain using the unmarked gene deletion system.	111
Figure 5.3.	Generation of inserts.	112
Figure 5.4.	Plasmid map of pK18mobsacB.	113
Figure 5.5.	Undigested and digested plasmid of pK18mobsacB from two selected colonies.	116
Figure 5.6.	Plasmid digestions.	117
Figure 5.7.	The 100 selected colonies growing on kanamycin containing agar.	118
Figure 5.8.	Sucrose sensitive colonies after transconjugation process.	119
Figure 5.9.	Detection of <i>sacB</i> .	120
Figure 5.10.	Sucrose resistant colonies on sucrose containing agar.	121
Figure 5.11.	Detection of <i>sacB</i> .	122
Figure 5.12.	Identification of the gene-deleted strains.	122
Figure 5.13.	Growth of the <i>xplA</i> knockout strain and wild-type on RDX minimal medium.	123
Figure 5.14.	Western blot analysis of cell free extracts of <i>xplA</i> knockout and wild-type strains.	124
Figure 5.15.	Resting cell assays for wild-type and the <i>xplA</i> knockout strains of <i>R. rhodochrous</i> 11Y.	125
Figure 5.16.	The <i>xplA</i> knockout and wild-type strains on RDX dispersion agar.	126
Figure 5.17.	Growth of the <i>xplB</i> knockout and wild-type strains on RDX as a sole nitrogen source.	127
Figure 5.18.	Resting cell assays for wild-type of <i>R. rhodochrous</i> 11Y and the <i>xplB</i> knockout strains.	128
Figure 5.19.	SDS-PAGE and western blot of cell free extracts of strain 11Y wild-type and the <i>xplB</i> knockout strains.	129
Figure 5.20.	Growth of the permease knockout strain and WT on RDX as a sole nitrogen source.	130
Figure 5.21.	RDX removal by the permease knockout and wild-type strains at a lower RDX concentration.	131
Figure 5.22.	RDX degradation by whole cells of <i>R. rhodochrous</i> 11Y under different nitrogen conditions.	133

Figure 5.23. Western blot analysis of cell free extracts of strains 11Y from different nitrogen treatments.	134
Figure 5.24. Specific XplA activity in cells treated with different nitrogen sources.	135
Figure 5.25. Transcript levels of <i>xplA</i> at different time points of the whole cell studies.	136
Figure 5.26. The RDX degrading gene cluster in strain 11Y.	137
Figure 5.27. Nucleotide and amino acid sequence of MarR-like regulator (ORF 27) and initial part of the putative permease (ORF 29).	138
Figure 5.28. Nucleotide and amino acid sequence of the putative dihydrodipicolinate reductase (ORF 30) and initial part of the <i>xplB</i> (ORF 31).	140
Figure 5.29. The alignment of MarR-like regulator of 11Y with its homologues.	141
Figure 5.30. RDX removal by the regulator knockout and wild-type strains.	144
Figure 5.31. Effect of nitrogen on RDX degradation in strain 11Y wild-type.	145
Figure 5.32. Growth profile of strain 11Y wild-type.	146
Figure 5.33. Effect of nitrogen on RDX degradation by growing cells of the regulator knockout strain.	147
Figure 5.34. Growth profile of the regulator knockout.	148
Figure 5.35. Comparison of RDX degradation between regulator knockout and wild-type strains.	149
Figure 6.1. XplA/B gene cluster in <i>R. rhodochrous</i> 11Y.	155

# List of Tables

Table 1.1.	Key events of the discovery and development of explosives.	24
Table 1.2.	Physical and chemical properties of RDX.	34
Table 2.1.	List of primers used for amplification of DNA fragments.	53
Table 2.2.	Bacterial strains used in this study.	55
Table 4.1.	Selected 11Y putative permease homologues with highest sequence identity.	90
Table 5.1.	Primers used to check inserts size.	114
Table 5.2.	Growth and the treatment media.	132
Table 5.3.	Resting cell assays for regulator knockout and wild-type strains.	142
Table 5.4.	Growth and treatment media.	143

# List of Abbreviations

<b>BLAST</b>	basic local alignment search tool
<b>BSA</b>	bovine serum albumin
<b>CoA</b>	coenzyme A
<b>dATP</b>	deoxyadenosine triphosphate
<b>DDM</b>	n-dodecyl- $\beta$ ,D-maltoside
<b>DMSO</b>	dimethyl sulfoxide
<b>DNA</b>	deoxyribonucleic acid
<b>dNTP</b>	deoxyribonucleotide triphosphate
<b>DNX</b>	hexahydro-1,3-dinitroso-5-nitro-1,3,5-triazine
<b>dTTP</b>	deoxythymidine triphosphate
<b>EDTA</b>	ethylenediaminetetraacetic acid
<b>EPA</b>	Environmental Protection Agency
<b>ESTCP</b>	Environmental Security Technology Certification Program
<b>FAD</b>	flavin adenine dinucleotide
<b>FMN</b>	flavin mononucleotide
<b>GST</b>	glutathione S-transferase
<b>GTN</b>	glycerol trinitrate
<b>HMX</b>	octahydro-1,3,5,7-tetranitro-1,3,5,7-tetrazocine
<b>HPLC</b>	high performance liquid chromatography
<b>IgG</b>	Immunoglobulin G
<b>IPTG</b>	Isopropyl $\beta$ -D-1-thiogalactopyranoside
<b>LB</b>	Luria-Bertani medium
<b>LBP</b>	Luria-Bertani peptone medium
<b>LIC</b>	ligation independent cloning
<b>MEDINA</b>	methylenedinitramine
<b>MMR</b>	Massachusetts Military Reservation
<b>MNX</b>	hexahydro-1-nitroso-3,5-dinitro-1,3,5-triazine



<b>MS</b>	mass spectrometry
<b>NADPH</b>	nicotinamide adenine dinucleotide phosphate
<b>NDAB</b>	4-nitro-2,4-diazabutanal
<b>NED</b>	N-(1-naphthyl)-ethylenediamine dihydrochloride
<b>NR</b>	nitroreductase
<b>OD</b>	optical density
<b>ORF</b>	open reading frame
<b>PAGE</b>	polyacrylamide gel electrophoresis
<b>PCB</b>	polychlorinated biphenyl
<b>PCR</b>	polymerase chain reaction
<b>PEG</b>	polyethylene glycol
<b>PETN</b>	pentaerythritol tetranitrate
<b>PMSF</b>	phenylmethylsulfonyl fluoride
<b>qPCR</b>	quantitative polymerase chain reaction
<b>RBS</b>	ribosomal binding site
<b>RDX</b>	hexahydro-1,3,5-trinitro-1,3,5-triazine
<b>RNA</b>	ribonucleic acid
<b>SDS</b>	sodium dodecyl sulfate
<b>TBS</b>	tris buffered saline
<b>TEMED</b>	tetramethylethylenediamine
<b>TMHMM</b>	transmembrane hidden Markov model
<b>TNT</b>	trinitrotoluene
<b>TNX</b>	hexahydro-1,3,5--trinitroso-5-nitro-1,3,5-triazine
<b>Tris</b>	tris(hydroxymethyl)aminomethane
<b>tRNA</b>	transfer RNA
<b>UV</b>	ultra violet

# Acknowledgements

It has been a golden opportunity for me to do my PhD in CNAP in the Department of Biology. I would like to thank the following people for their help throughout my PhD studies in York.

To Prof. Neil Bruce, for his excellent supervision, for being close to me as a friend and sharing all of the wonderful scientific and non-scientific experiences. The Bruce group is a brilliant research group.

To Dr. Astrid Lorenz, for the precious time when working together in the lab, for proofreading my chapters and for passing on to me all the beautiful clothes for my daughter. Jia Xin is always excited whenever she sees the clothes. To Dr. Liz Rylott, who guided me throughout my PhD studies. Her passions in research always inspires me. Also thanks to her for proofreading my chapters.

Many thanks to Drs. Cyril Bontemps, Rosamond Jackson, Florian Fisch, Federico Sabbadin, Christopher Mulligan, James Edwards, Hazel Housden, Emily Beynon, Fernando Gandia-Herrero, Helen Sparrow and Julia Schuckel for their interest in my research and useful discussions. To Andy for being my brilliant English teacher in writing and speaking (with a Yorkshire accent!). To William Eborall for proofreading parts of my chapters. To Margaret for coordinating my TAP meetings and sending my reports to my sponsor. To Mariya, Dana and others in M2 for being good company. To Drs. Ng C. Leong and Jack Lim for sharing their thesis-writing experiences and their interest in my project. To prayer meeting members: Joe, Lorenzo, Linda for prayer support.

To Drs. Marjan van der Woude and James Chong for helpful input during the TAP meetings.

To Universiti Teknologi Malaysia and Ministry of Higher Education, Malaysia for sponsorship.

To members from the York Chinese Church for constant support.

To my family members: father, mother, brothers and sisters. And to my loving wife: Chee Hooi and my dear daughter: Jia Xin. Thanks for your love, care and prayers. I love you all.

*Give thanks to the Lord, for He is good;  
His love endures forever.  
(Psalm 118:1)*

# Author's Declaration

I declare that I am the sole author for majority of the work in this dissertation and that it is original except where indicated by special reference in the text, and works involving in characterisation of the knockout strains derived from *R. rhodochrous* 11Y in chapter 5 was performed in conjunction with Dr. Astrid Lorenz. No part of the dissertation has been submitted for any other degree to any other institution.

# Publications arising from this work

Rylott EL, Jackson RG, Sabbadin F, Seth-Smith HMB, Edwards J, Chong CS, Strand SE, Grogan G & Bruce NC (2011). The explosive-degrading cytochrome P450 XplA: Biochemistry, structural features and prospects for bioremediation. *Biochimica et Biophysica Acta (BBA) - Proteins & Proteomics* 1814: 230-236.

Chong CS, Lorenz A, Rylott EL, Bontemps C, Andeer PF, Stahl DA, Strand SE & Bruce NC (2011). Analysis of RDX degrading gene cluster in *Rhodococcus rhodochrous* 11Y. Manuscript in preparation.

# Chapter 1

## Introduction

### 1.1 An overview of explosives

The development of organic chemistry has led to the synthesis of broad ranges of novel organic compounds, one group of which are explosives. An explosive is defined as “a chemical compound, or a mixture of compounds, that can be initiated to generate rapid expanding gases, heat, light and an enormous pressure” (Akhavan, 2004). The discovery and development of explosives have been described in detail by Akhavan (Akhavan, 2004) and briefly in Table 1.1.

Blackpowder was probably the first explosive composition that was, almost certainly accidentally, discovered by Chinese alchemists in 220 B.C. Blackpowder was made up from charcoal, sulphur and potassium nitrate (Akhavan, 2004). The recipe for blackpowder was introduced into Europe where it was first made in 1249, by Robert Bacon (England). Later, Hungary, Germany, England and Sweden all used blackpowder in mining and tunnelling operations.

The discovery of nitric and sulfuric acids allowed chemists to produce explosives via a nitration technique (Bailey and Murray, 2000), resulting in production of three classes of powerful explosives: nitrate esters, nitroaromatics and nitramines (Figure 1.1).

Glycerol trinitrate (GTN) was the first nitrate ester explosive and was discovered by an Italian Ascanio Sobrero in 1846. Few years later, Immanuel Nobel developed a method to generate GTN by mixing of glycerol, nitric acid and sulfuric acid. Although it was a powerful explosive, it was chemically unstable; an undesirable characteristic which led to the accidental demolition of a GTN factory (Akhavan, 2004). The second nitrate ester explosive, pentaerythritol tetranitrate (PETN) was developed by nitration of pentaerythritol in 1894. Similar to GTN, PETN was chemically unstable and was used in combination with other more stable explosives such as trinitrotoluene (TNT).

Picric acid (2,4,6-trinitrophenol) is a nitroaromatic explosive. It was initially used as dye for wool and silk. Its property as explosive was discovered in 1830 by Welter who demonstrated its synthesis by reacting nitric acid with indigo or phenol. Picric acid is a strong acid, soluble in benzene, acetone and water, and more stable than GTN. Since 1894, it has been used as a military explosive worldwide. The problem with picric acid is that it easily reacts with the shell walls resulting in corrosion (Akhavan, 2004). Another example of a nitroaromatic explosive is 2,4,6-trinitrotoluene (TNT), discovered by Joseph Wilbrand in 1863. By sequential nitration reactions of toluene, mononitrotoluene, then dinitrotoluene and finally TNT can be produced. TNT was the dominant explosive used in World War I (Lewis et al., 2004) and is still being used today. This is due to the advantageous properties of TNT including its high thermal stability, low production costs and ability to be pressed and moulded into shells. In addition, it is compatible with other explosives. Examples of military and commercially used explosive compositions that include TNT are Minol-2 (40 % TNT, 40 % ammonium nitrate and 20 % aluminium), Pentolites (50 % PETN and 50 % TNT) and Picratol (52 % Picric acid and 48 % TNT).

The hexahydro-1,3,5-trinitro-1,3,5-triazine: Royal Demolition Explosive (RDX) is a powerful nitramine explosive (Figure 1.1). Its explosive property was first observed by Herz in 1920 and its high chemical and thermal stabilities meant that it became widely used during World War II. A technical problem was that due to its high melting point, RDX was difficult to pour into shells. To overcome this problem, RDX was mixed with TNT to lower the melting temperature to make the explosive mixture pourable. Octahydro-1,3,5,7-tetranitro-1,3,5,7-tetrazocine; High Melting Explosive (HMX) is also a member of the nitramine explosives. HMX has a higher melting point than RDX (RDX melting temperature: 200 °C; HMX melting temperature: 275 °C). HMX has similar characteristic to RDX in that they are both chemically stable and have similar explosive power.

Decades of military activities across the globe including World War I and II have caused widespread land and groundwater contaminations. TNT and RDX are the most widely used explosives and these explosives are difficult to degrade and thus persist in the environment for decades. The scale of contamination by explosives is described in the following section.

**Table 1.1. Key events of the discovery and development of explosives.**

Date	Event
220 BC	Blackpowder accidentally discovered by Chinese alchemists
1169	Fireworks were made by Chinese
1249	Blackpowder was first synthesised in England
1320	Blackpowder was introduced to central Europe
1830	Picric acid was discovered as an explosive
1846	Glycerol trinitrate was discovered by Ascanio Sobrero
1863	Glycerol trinitrate was manufactured by Immanuel Nobel
1863	TNT was produced by Joseph Wilband
1891	TNT was manufactured in Germany
1894	PETN was synthesised in Germany
1902	Picric acid was replaced by TNT in Germany
1920	RDX was discovered as an explosive by Herz
1925	RDX was largely produced in U.S.
1945	HMX was synthesised by Bachmann



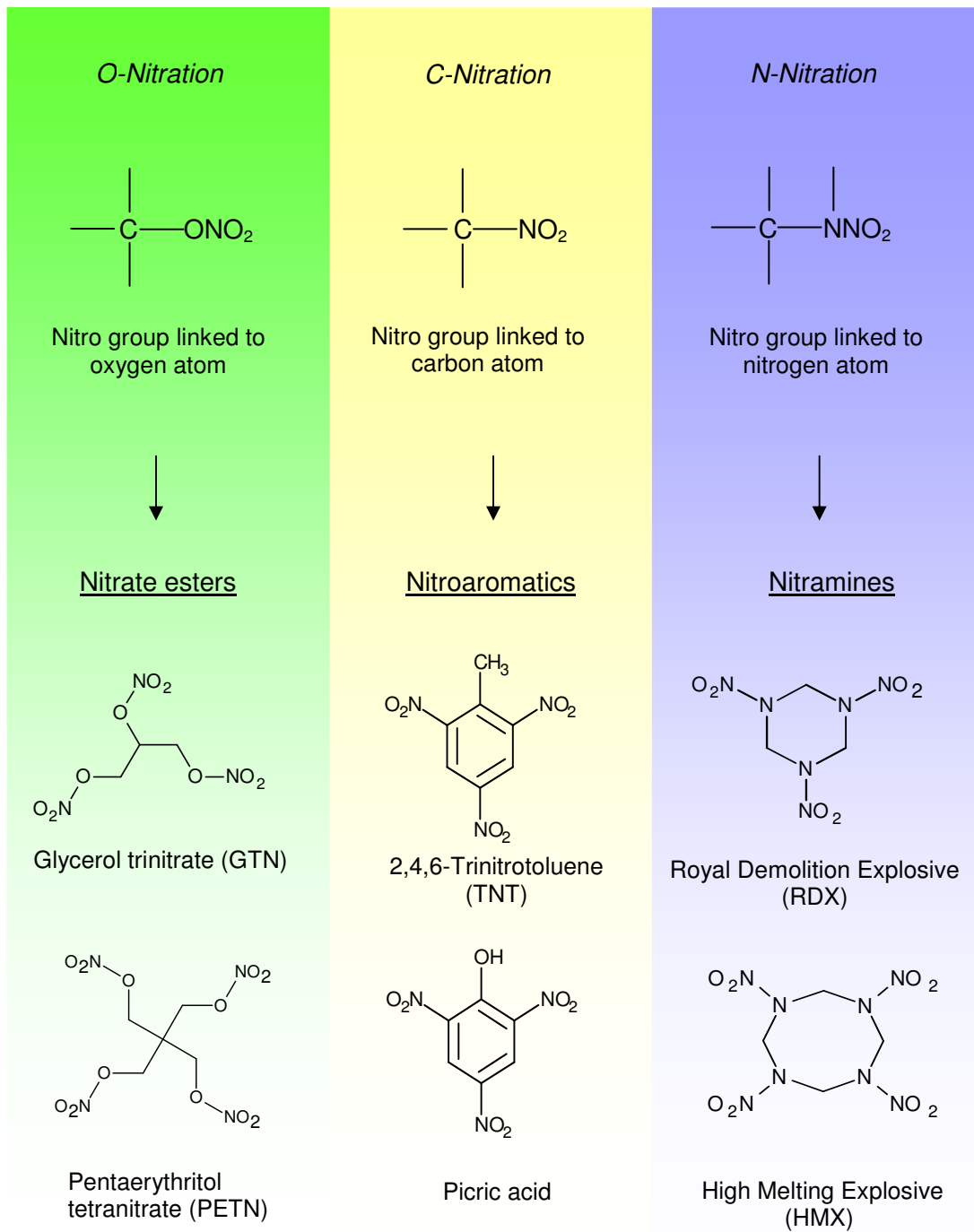


**Figure 1.1. Example of explosives synthesised from nitration reaction.** Figure taken from (Akhavan, 2004) and (Symons, 2005).

## 1.2 Contamination of the environment by explosives

The precise figure on the amount of explosives produced globally is unclear, but it is known that more than 5.5 billion pounds of explosives are produced each year in United States (U.S. Government Accountability Office, 2005). The U.S. Department of Defense predicts the production and use of explosives will be continuing on this scale (Wiesmann et al., 2007). The massive production, use and storage of explosives have led to serious contamination of the environment. In the United States alone, approximately 50 million acres (20.2 million hectares) of soil have been contaminated by explosives (Clausen et al., 2004) and around 17,000 sites on U.S. military training ranges have been identified that require clean up (Gunnison et al., 1999). Current clean up methods are incomplete and expensive and the estimated treatment cost could reach U.S. \$165 billion (<http://www.dtic.mil/cgi-bin/GetTRDoc?AD=ADA435939&Location=U2&doc=GetTRDoc.pdf>).

The characterisation of explosives contaminated sites in the United States has been extensively carried out by the Department of Defense under an environmental research program, namely Strategic Environmental Research and Development Program (SERDP). Of the explosives polluted sites, military training ranges at Massachusetts Military Reservation (MMR) located near Falmouth, are amongst the better characterised sites (Clausen et al., 2004). Analysis of more than 15,000 environmental samples revealed MMR has been contaminated by explosives and their derivative compounds (Figure 1.2). The sole-source drinking water aquifer was also found to be polluted by RDX, affecting more than half a million residents and visitors around the MMR area. Due to the contamination of water supplies by the explosives, the U.S. Environmental Protection Agency (EPA) has restricted the military activity at MMR.

The U.S. EPA classifies TNT as a group C possible human carcinogen (Craig et al., 1995). Studies showed TNT to be mutagenic to *Salmonella typhimurium* (Berthe-Corti et al., 1998, Honeycutt et al., 1996), hamster and rat cell lines (Honeycutt et al., 1996). TNT has also been reported to be toxic to marine mussels (Rosen and Lotufo, 2007), plants (Gong et al., 1999, Hannink et al., 2001) and sea urchin (Nipper et al., 2001). Similar to TNT, RDX is classified as a class C possible carcinogen. The mutagenic effects of RDX and its breakdown compounds hexahydro-1-nitroso-3,5-dinitro-1,3,5-

triazine (MNX) and hexahydro-1,3,5--trinitroso-5-nitro-1,3,5-triazine (TNX) in *S. typhimurium* indicated these compounds weakly induced mutagenesis (Pan et al., 2007). RDX is toxic to tested organisms such as fish (Lotufo et al., 2010), plants (Rylott et al., 2006) and bacteria (Flokstra et al., 2008); however, it is less toxic compared to TNT. HMX is classified as a group D non-classifiable carcinogen (Craig et al., 1995). A study showed that at a nearly saturated concentration of HMX (10  $\mu$ M), it failed to cause toxic effects when exposed to mussels (Rosen and Lotufo, 2007). Bioconcentration analysis using fish (*Cyprinodon variegatus*) as model demonstrated low potential for HMX to bioaccumulate in the fish (Lotufo et al., 2010).

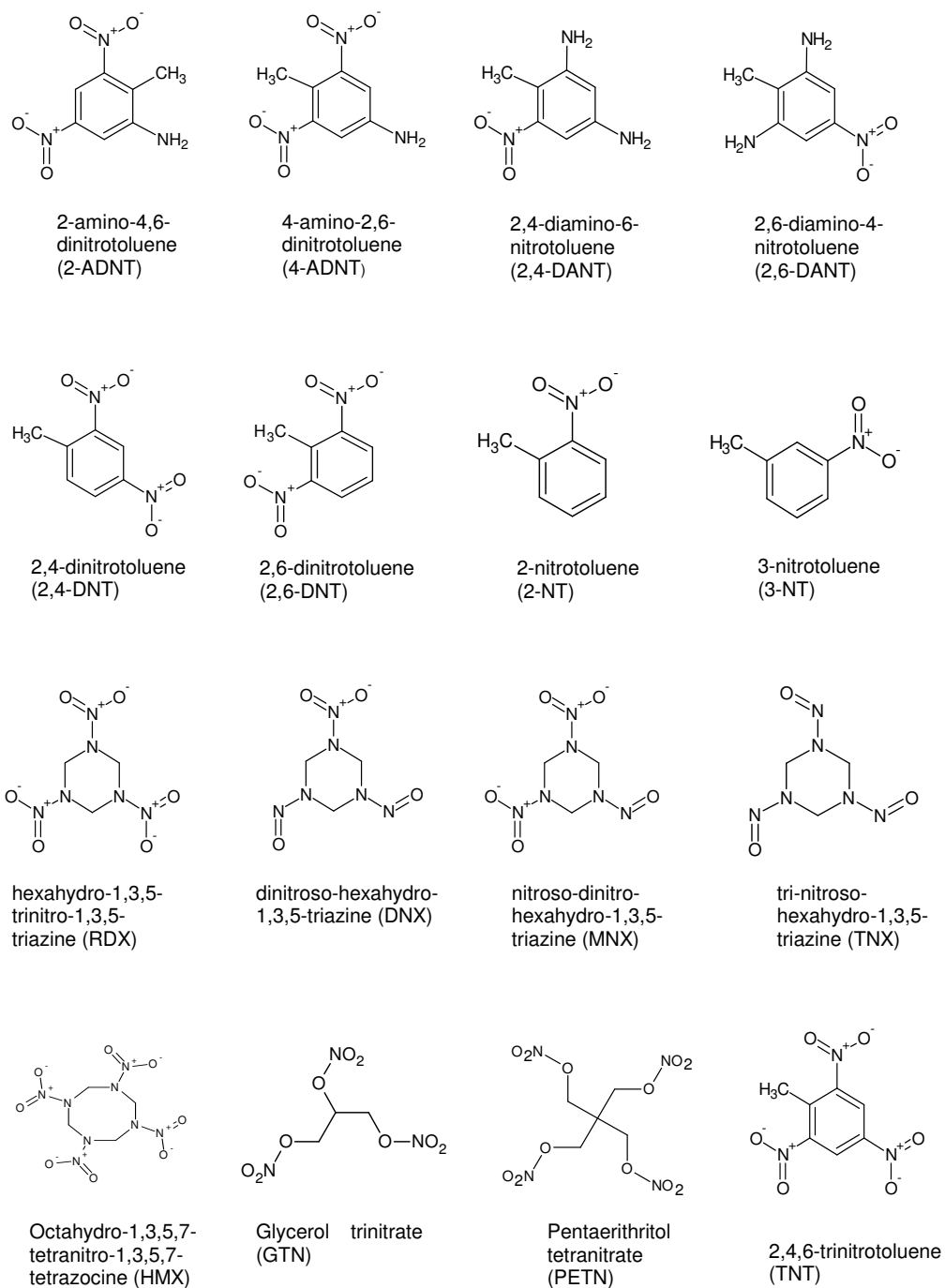


**Figure 1.2. Explosives detected in the contaminated sites at the Camp Edwards, Massachusetts Military Reservation, MA (Clausen et al., 2004).**

## **1.3 Remediation technologies**

### **1.3.1 Incineration**

Incineration is a waste treatment method that has been used to remediate explosive contaminated soils. It can remove explosives efficiently and is a time-saving treatment method. This method required high temperature (at least 850 °C) to convert waste materials into ash, gases and heat (Waterland et al., 1991). There are several drawbacks to this method: it produces toxic gases including dioxins, nitrous oxides, carbon monoxide, sulphur dioxide and hydrogen chloride (Beychok, 1987, van Ham, 1998), the humic component of the soil is destroyed leaving the soil biologically barren, the soil has to be transported to the incinerator and the cost for this method is very high; estimates range between U.S. \$400 to U.S. \$1400 per ton (Craig et al., 1995). Although incineration is an efficient treatment, the cost would be incredibly high if all of the soils contaminated with explosives were treated using this technology.

### **1.3.2 Bioremediation**

#### **1.3.2.1 Composting**

Composting is a biological treatment technique that has been used to remediate explosives contaminated soils. The contaminated soils are mixed with organic waste, such as agricultural waste, manures, fruit or vegetable processing wastes to provide nutrient source for the indigenous microorganisms (Craig et al., 1995). Efficient composting depends on a variety of factors including pore space in the compost system, moisture content, waste particle size, temperature, pH and aeration (Ro et al., 1998, McMahon et al., 2008). The treatment cost of this technique (U.S. \$100 per ton) is cheaper than incineration (Ro et al., 1998) and, unlike incineration, composting does not produce hazardous gases and is therefore well accepted by public. However, like incineration, it is difficult to treat large (>hectares) of soil with this method. Pilot scale studies have demonstrated that composting can effectively remove explosives from soils (Craig et al., 1995), but the fate of the explosives during composting is still an important aspect that remains to be investigated. As the transformation or degradation of explosives in the contaminated soils by composting mainly depends on the microbial activities, understanding the biotransformation and mineralisation pathways of explosives in single pure culture isolated from explosives contaminated sites is

essential. The knowledge gained from these studies would enhance our understanding about the fate of the explosives in the composting process.

### **1.3.2.2 Biostimulation**

Biostimulation is a biological approach to remediate explosive contaminated sites by adding nutrients and/or electron donors (acetate, soluble starch, ethanol and other carbon materials) (Davis et al., 2004). Numerous ex situ techniques have been employed to remediate explosive contaminated groundwater including bioreactors, granular activated carbon units and UV-oxidation reactors (Fuller et al., 2007, ESTCP, 2008). However, these techniques have high costs due to the pumping and re-injection of treated water to the water source. In situ biostimulation method offers a cheaper technique over other treatments. One example is using organic mulch. Organic mulch is a complex carbon material that typically contains indigenous bacteria. It has been employed to treat explosive-contaminated groundwater over a decade (ESTCP, 2008). Indigenous microorganisms in the organic mulch breakdown the complex organic materials to release soluble carbon sources which are further utilised by the same or other microorganisms as an electron donor for treating the explosives via the reductive pathways (Figure 1.4). Bench-scale and on-site studies using organic mulch permeable reactive barriers have revealed promising results in remediating the polluted groundwater (Ahmad et al., 2007, ESTCP, 2008).

### **1.3.2.3 Phytoremediation**

Phytoremediation refers to the use of plants to clean-up pollutants from the environment. This technique is an inexpensive alternative treatment to incineration and composting. Plants are robust and have good root systems to reach the pollutants; however, often contaminants are phytotoxic to plants. These limitations can be overcome by genetic engineering approach: expressing recombinant bacterial genes in plants to produce transgenic plants that are able to detoxify or degrade the contaminants. A number of studies demonstrated that transgenic plants dramatically improved the tolerance and biotransformation ability of plants to contaminants (Rugh et al., 1998, French et al., 1999, Hannink et al., 2001, Rylott et al., 2006, Hannink et al., 2007, Jackson et al., 2007, Rylott and Bruce, 2009). The enzyme nitroreductase (NR) from *Enterobacter cloacae* has been shown to be able to biotransform TNT (Bryant and DeLuca, 1991). NR-expressing plants significantly increased TNT biotransformation

rates by 30-fold when compared to untransformed plants grown in liquid medium. The NR-expressing plants also appeared healthy and gained weight at TNT concentration of 0.5 mM (Hannink et al., 2001) while unmodified plants died.

The cytochrome P450 enzyme XplA, and, reductase partner, XplB were isolated and shown to be responsible for RDX degradation in *Rhodococcus rhodochrous* 11Y (Seth-Smith et al., 2002, Jackson et al., 2007). Rylott and co-workers (2006) successfully expressed XplA individually and together with XplB in *Arabidopsis* plants. Soil studies showed that the XplA-expressing plants were able to grow healthily in the presence of up to 2,000 mg RDX/kg soil while unmodified plants exhibited signs of toxicity. Double transgenic plants that expressing both XplA and XplB were able to further enhance the RDX degradation (Jackson et al., 2007). HPLC analysis demonstrated up to three times more RDX accumulated in root tissues of unmodified plants than transgenic plants. Low level of RDX accumulation in transgenic plants and higher tolerance towards RDX suggested XplA degrades RDX in plants.

## 1.4 Microbial transformation of TNT

The nitroaromatic TNT is recalcitrant to degradation and persists in the environment. Bacteria are able to transform TNT under both aerobic and anaerobic conditions (French et al., 1998, Pak et al., 2000, Esteve-Nunez et al., 2001, Eyers et al., 2008, Rylott et al., 2011) but so far no reports suggest that complete degradation of TNT occurs. The mineralisation of TNT is challenging as multiple electro-withdrawing nitro groups are present in TNT, prevent oxidative attack on the ring that generally leads to the ring cleavage of aromatic compound.

The majority of TNT-transforming bacteria tend to reduce one or two of the nitro groups of TNT to produce nitroso, hydroxylamino and amino derivatives (Route 1, Figure 1.3). Azo dimers formed from hydroxylamino and amino derivatives of TNT have also been observed (Lewis et al., 1997). Nitroreductases are responsible for the TNT transformation illustrates in Route 1, Figure 1.3 (Rylott et al., 2011). Another TNT transformation pathway was found to be catalysed by members of the Old Yellow Enzyme family (Williams et al., 2004). It involves a hydrogenation reaction of the aromatic ring to produce a Meisenheimer complex. (Route 2, Figure 1.3). Recent studies further elucidate the TNT transformation pathway by these flavoprotein oxidoreductase, demonstrating that diarylamines and nitrite are formed from the condensation of hydroxyamino derivatives with dihydride Meisenheimer complexes (Figure 1.3)(Wittich et al., 2008, Wittich et al., 2009).



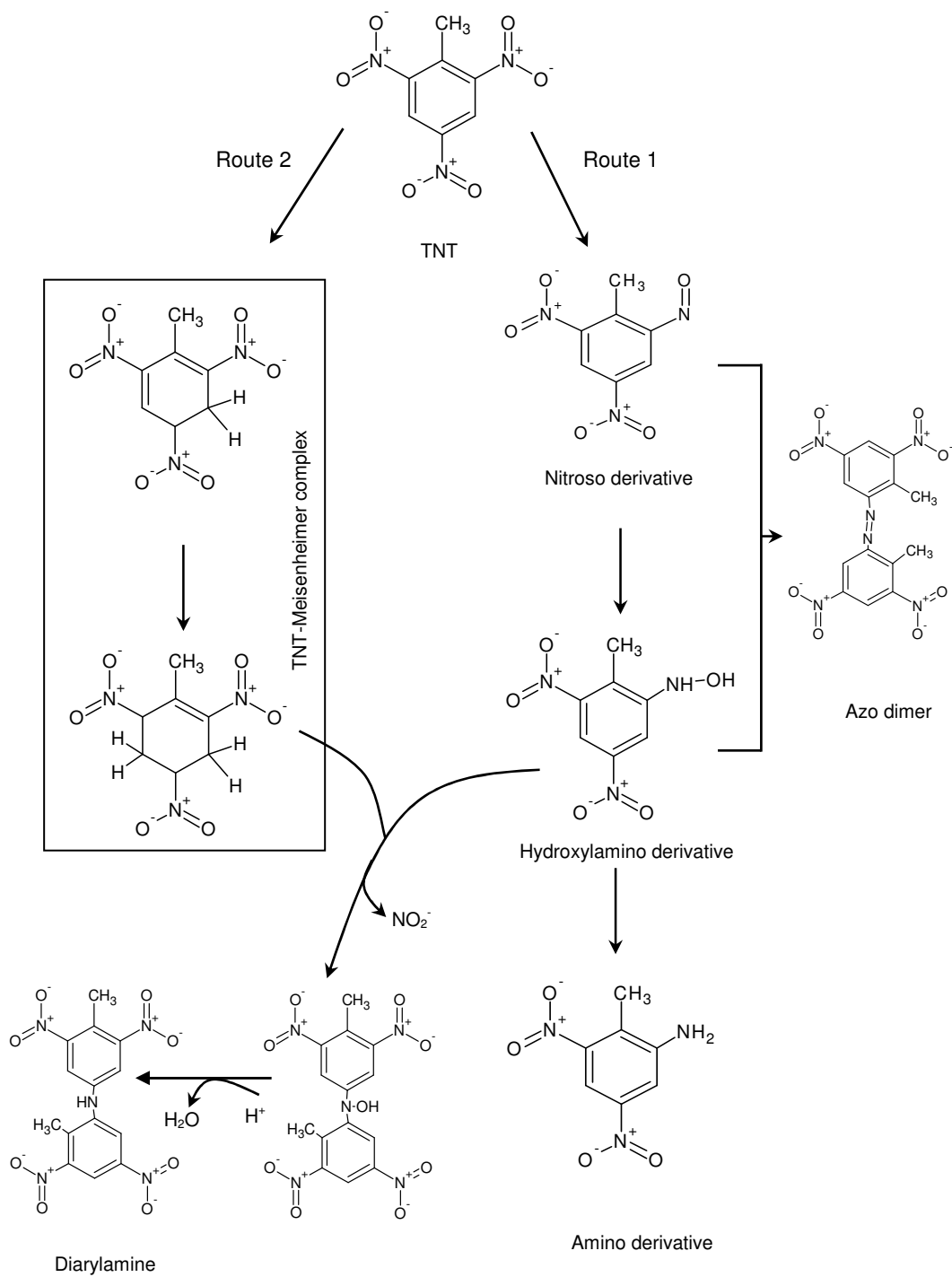


**Figure 1.3. TNT degradation pathways.** Route 1. TNT transformation via reduction of nitro groups. Route 2. TNT transformation via hydrogenation of TNT to produce Meisenheimer complex (Lewis et al., 1997, French et al., 1998, Wittich et al., 2008).

## 1.5 RDX

Royal Demolition Explosive (RDX), also known as hexogen, cyclonite and T4, is one of the most powerful explosives. It was extensively used during the World War II and nowadays more than 4000 military items are reported to contain RDX (U.S. EPA, 2011). RDX has a low soil sorption coefficient ( $K_{oc}$ ) values indicating that it is not easily retained by soil and easily migrates through soils to reach groundwater (Table 1.2). The power index of RDX is 169 % relatively to picric acid (Table 1.2). The structure of RDX is unique because of the attachment of the nitro group to the central ring via nitrogen-nitrogen bonds (Fig 1.1). To date, the nitrogen-nitrogen bond formation occurs rarely in nature. This unusual feature makes RDX resistant to biological attack.

**Table 1.2. Physical and chemical properties of RDX (EPA, 2011).**

Property	Value
Physical description	White Crystalline Solid
Molecular weight (g/mol)	222
Water solubility (mg/L at 20 °C)	42
Soil organic carbon-water coefficient ( $K_{oc}$ )	1.8
Melting point (°C)	206
Power index (%)	169

### 1.5.1 Microbial degradation of RDX

Although RDX is recalcitrant to degradation, bacteria in the environment are still able to adapt themselves to transform RDX, and as a result utilise it as a nitrogen source for growth. Documentation of microbial RDX degradation began around 30 years ago. To date, three RDX biodegradation pathways have been postulated: two-electron reduction, single-electron reductive denitration and direct RDX ring cleavage.

The two-electron reductive pathway was proposed by McCormick and co-workers (1981). When sewage sludge was incubated in medium containing 450  $\mu\text{M}$  RDX anaerobically, all of the RDX was removed after four days of incubation. The nitroso-derivatives: hexahydro-1-nitroso-3,5-dinitro-1,3,5-triazine (MNX), hexahydro-1,3-dinitroso-5-nitro-1,3,5-triazine (DNX) and hexahydro-1,3,5-trinitroso-5-nitro-1,3,5-triazine (TNX) were detected, indicating the pathway occurred via RDX reduction (Figure 1.4; Route 1). Further transformation of these metabolites produced ring cleavage products, namely formaldehyde, methanol ( $\text{CH}_3\text{OH}$ ) and hydrazine ( $\text{H}_2\text{N-NH}_2$ ). These nitroso metabolites were also observed by Hawari and co-workers (2000) when similar experiments were performed using municipal anaerobic sludge. In addition, two novel intermediate products were also detected by liquid chromatographic/mass spectroscopic: methylenedinitramine (MEDINA) and bis(hydroxymethyl)nitramine, suggesting another putative RDX transformation pathway via direct ring cleavage of RDX (Figure 1.4; Route 2). The authors suggested that both metabolites were further transformed to produce nitramine ( $\text{NH}_2\text{NO}_2$ ) and formaldehyde (HCHO). Nitramine was likely to be transformed spontaneously in water to yield  $\text{N}_2\text{O}$  and the formaldehyde was further transformed to  $\text{HCOOH}$  and eventually to  $\text{CO}_2$  in sludge (Hawari et al., 2000).

Pure bacterial isolates of *Klebsiella pneumoniae* strain SCZ-1 (Zhao et al., 2002), *Clostridium bifermentans* strain HAW-1 (Zhao et al., 2003), *Citrobacter* sp. (Kitts et al., 1994) and *Morganella* sp. (Kitts et al., 1994) were found to transform RDX via this reductive route yielding nitroso-RDX (MNX, DNX and/or TNX) and different RDX mineralisation activities were observed in these isolates (between 3 % and 72 %). It was proposed that a type I nitroductase enzyme initiated the transformation of RDX via two-electron reductive pathway in sludge (Hawari et al., 2000). *Enterobacter cloacae* type I nitroreductase was expressed in *Escherichia coli* (*E. coli*) and whole cell assays demonstrated approximately 5-fold higher RDX nitroreductase activity in induced cells

compared to uninduced cells. *In vitro* studies confirmed type I nitroreductase could transform RDX, however, details for intermediates were not provided by the authors (Kitts et al., 2000).

The single-electron reductive denitration of RDX was found to be another pathway in RDX degradation (Crocker et al., 2006). This route involves a one-electron transfer step subsequently releasing a nitro group from RDX. The removal of the nitro group leads to the formation of an unstable free-radical RDX followed by ring cleavage to release other intermediate products (Crocker et al., 2006). The degradation products via the denitration pathway were slightly different under aerobic and anaerobic conditions, with production of 4-nitro-2,4-diazabutanal (NDAB) and MEDINA under aerobic and anaerobic conditions, respectively. *Klebsiella pneumoniae* strain SCZ-1 was able to transform RDX via both denitration and reduction pathways under anaerobic conditions (Zhao et al., 2002). Strain SCZ-1 degraded RDX to produce methanol (12 % of total carbon), nitrous oxide (60 % of total nitrogen), carbon dioxide (72 % of total carbon) and transient products of formaldehyde, MNX and MEDINA.

More than 25 isolates have now been isolated that are able to transform RDX aerobically via the denitration pathway (Coleman et al., 2002, Seth-Smith et al., 2002, Thompson et al., 2005, Nejidat et al., 2008, Seth-Smith et al., 2008, Andeer et al., 2009). Almost all of the isolates belong to the *Rhodococcus* genus in the *Corynebacterineae* (Coleman et al., 2002, Nejidat et al., 2008, Seth-Smith et al., 2008, Seth-Smith et al., 2002, Bernstein et al., 2011). Examples are *Rhodococcus rhodochrous* 11Y, *Rhodococcus* sp. strain DN22 and *Rhodococcus* strain YH1. Biodegradation of RDX in *Rhodococcus* sp. strain DN22 is amongst the better characterised strains (Fournier et al., 2002, Annamaria et al., 2010). Resting cell studies of strain DN22 under aerobic condition generated metabolites of  $\text{NO}_2^-$ ,  $\text{NO}_3^-$ , MEDINA, NDAB,  $\text{N}_2\text{O}$ ,  $\text{CO}_2$ ,  $\text{NH}_3$  and HCHO. The authors proposed initial denitration taking place resulting in production of single-denitrated and double-denitrated metabolites (I and II, Figure 1.5). Following the ring cleavage, NDAB, MEDINA, diformylamide and formamide were produced. NDAB was found to be stable under ambient conditions, but MEDINA was unstable and readily decomposed to HCHO and  $\text{N}_2\text{O}$ . Diformylamide and formamide via the secondary biotic reactions were further degraded to yield  $\text{NH}_3$ , HCOOH and  $\text{CO}_2$  (Figure 1.5). Experiments with radio-labeled oxygen atom in water ( $\text{H}_2^{18}\text{O}$ ) and oxygen gas ( $^{18}\text{O}_2$ ) revealed oxygen atoms in both

water and oxygen gas were not directly involved in the initial denitration process, but one  $^{18}\text{O}$  atom from oxygen gas was incorporated in  $\text{NO}_3^-$ . Also, an  $^{18}\text{O}$  atom from water was detected in the ring cleavage product NDAB (Annamaria et al., 2010).

Involvement of a cytochrome P450 in RDX biodegradation was initially proposed by Coleman and co-workers (Coleman et al., 2002). The authors found that RDX degradation in strain DN22 was inhibited when metyrapone (P450 inhibitor) was added in the resting cell assays. Seth-Smith et al., (Seth-Smith et al., 2002) was the first group to successfully isolate the gene responsible for RDX degradation, *xplA*, which encodes a novel flavodoxin fused cytochrome P450 from *R. rhodochrous* 11Y, and was later used for the phytoremediation studies described above. *xplA* is conserved amongst the RDX degrading bacteria (Coleman et al., 2002, Nejidat et al., 2008, Andeer et al., 2009). The RDX degrading P450, XplA has been functionally characterised and the structure of XplA heme domain has been successfully resolved (Jackson et al., 2007, Sabbadin et al., 2009), which are described in following sections.

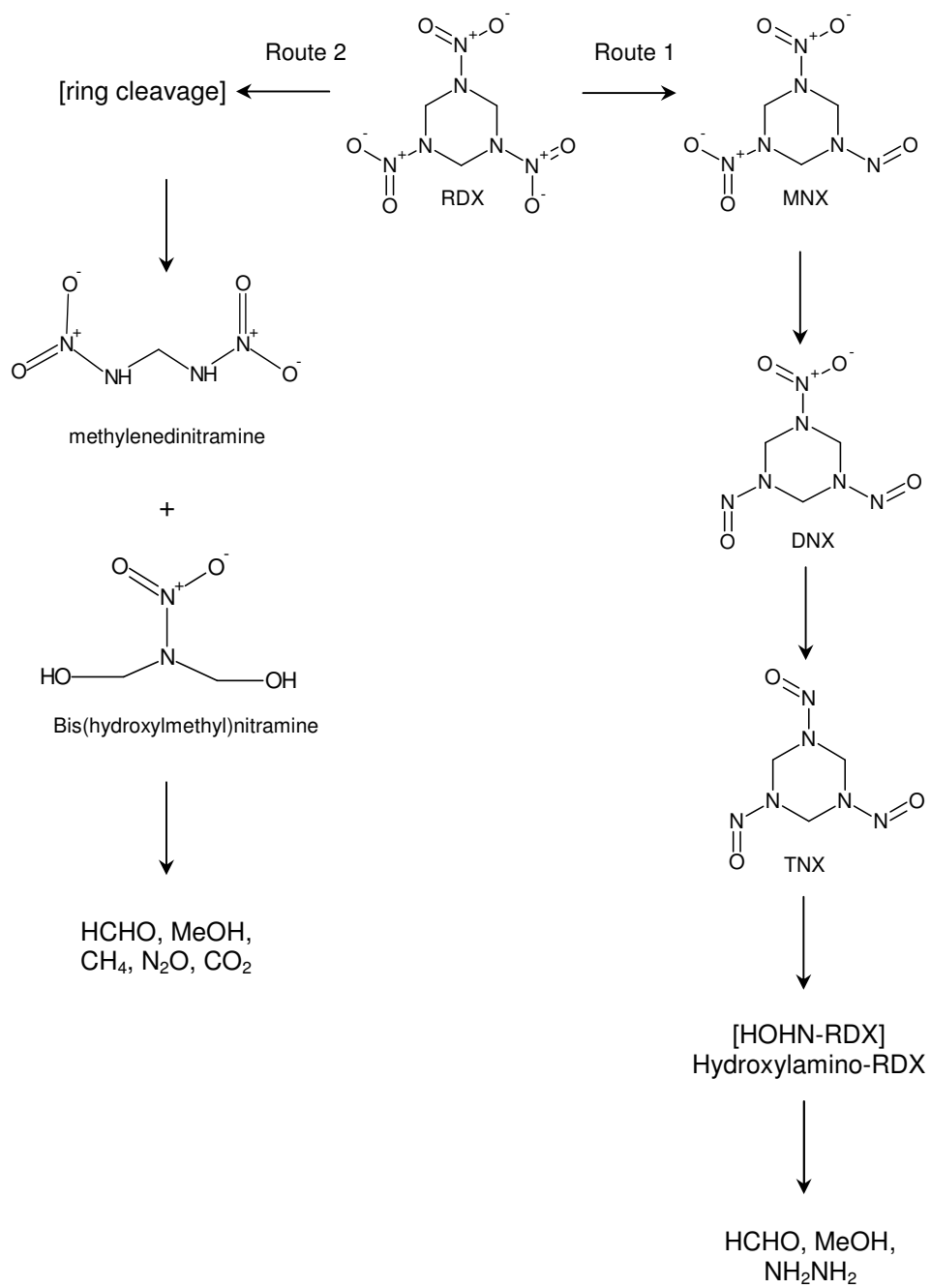
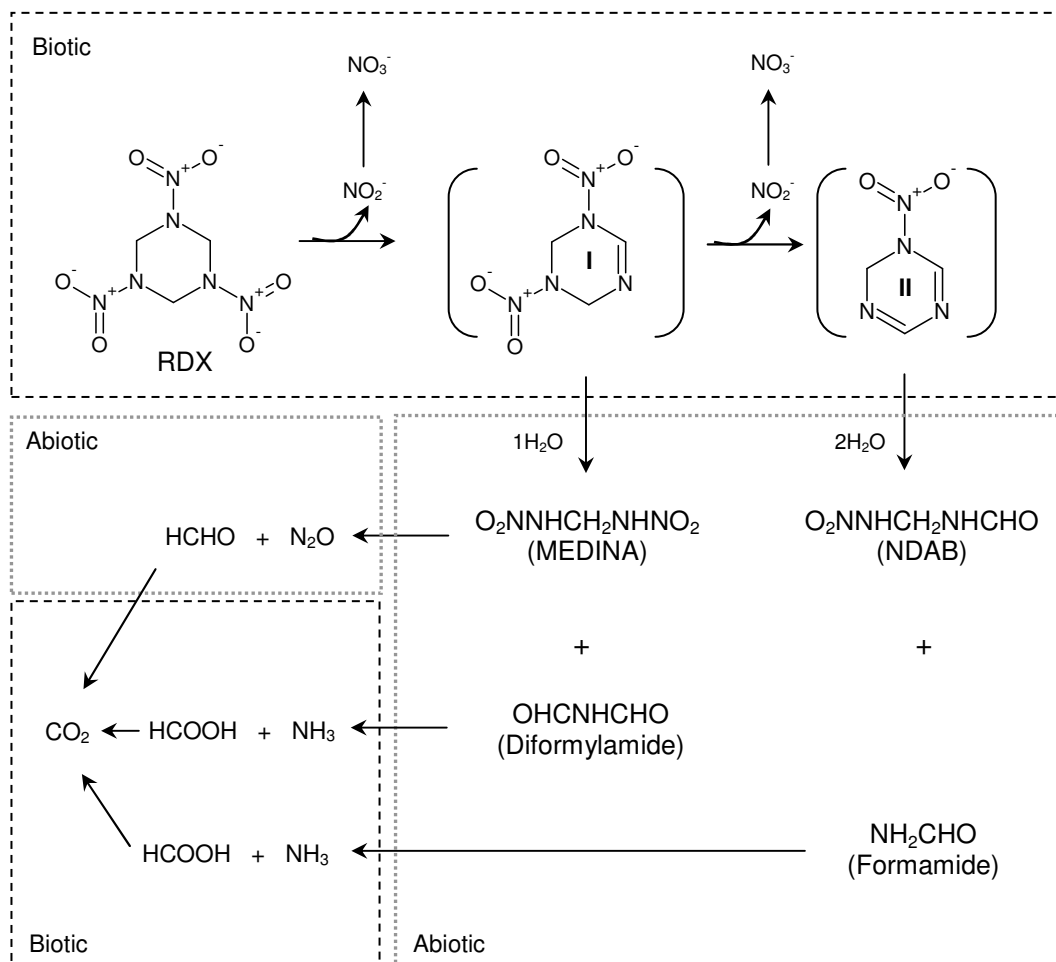


Figure 1.4. Proposed anaerobic RDX degradation pathways with anaerobic sludge (McCormick et al., 1981, Hawari et al., 2000).



**Figure 1.5. RDX degradation pathway in *Rhodococcus* strain DN22 (Annamaria et al 2010).** Intermediates in brackets indicate hypothetical denitrated (I and II) compounds. Dashed lines (grey) refers to abiotic reactions; dashed lines (black) refers to biotic reactions. Figure is taken from Annamaria et al., (2010).

## 1.6 RDX degradation by commercial enzymes

Some commercially available enzymes have been employed to investigate the transformation pathways of RDX (Bhushan et al., 2002, Bhushan et al., 2003). An NADPH dependent nitrate reductase from *Aspergillus niger* was shown to be able to catalyse the transformation of RDX under anaerobic conditions. This was the first report that a nitrate oxidoreductase was able to transform nitramine compounds (Bhushan et al., 2002). The activity of this enzyme toward RDX was inhibited in presence of nitrate.

Analysis of the intermediate compounds showed the MNX and a ring cleavage metabolite MEDINA were formed. These compounds then disappeared in the reaction mixtures followed by the appearance of nitrous oxide, formaldehyde and ammonium ion. No DNX and TNX were observed throughout the experimental time. Similar experiments were conducted using MNX as substrate and showed that DNX and TNX were not detected, suggesting that the ring cleavage occurred via MNX (Bhushan et al., 2002), which also indicates the possibility of another route of RDX transformation under anaerobic condition compared with the previously described pathway (Figure 1.4; Route 1).

Another RDX degrading commercially available enzyme is rabbit liver cytochrome P450 2B4 (Bhushan et al., 2003). This enzyme was initially found to be able to remove the alkyl group from pentoxyresorufin. Incubation of P450 2B4 with RDX and NADPH in presence of oxygen showed a similar distribution of RDX intermediates to that of *Rhodococcus* strain DN22. Based on the detection of metabolites and mass balance analyses, it was proposed that RDX degradation by P450 2B4 underwent initial two steps of denitration followed by ring cleavage to produce NDAB and formaldehyde (Bhushan et al., 2003).



## 1.7 *Rhodococcus rhodochrous* 11Y

*Rhodococcus rhodochrous* strain 11Y was isolated from soil taken from a polluted explosives manufacturing facility based on its ability to use RDX as a sole nitrogen source for growth. To isolate the gene that was responsible for RDX degradation in strain 11Y, a gene library from this strain was constructed and cloned into the *Escherichia coli* - *Rhodococcus* shuttle vector pDA71. This library was transferred into *Rhodococcus* strain CW25, a non-RDX degrading strain (Seth-Smith, 2002).

Following the screening of library clones in liquid minimal medium with RDX as the sole nitrogen source, and further selection on RDX dispersion agar, four recombinant CW25 strains that were able to degrade RDX were isolated. The pDA71 construct from these strains was sequenced and was found to possess a 7.5 kb of insert was present in all four of the recombinant CW25 strains. The construct was designated as pHSX1. Sequence analysis of the 7.5 kb insert revealed the presence of three open reading frames encoding a cytochrome P450 system, a reductase and acetyl CoA synthase (Figure 1.6).

Further subcloning to produce pHSX1a and pHSX1b was performed (Figure 1.6). The recombinant CW25 containing pHSX1b was found to be able to degrade RDX confirming that the cytochrome P450 system was responsible for RDX degradation and the P450 was named *xpIA*, for *explosive* degrading. The gene encoding the neighbouring reductase was named *xpIB*.

Sequence analysis revealed that *xpIA* encodes a new class of cytochrome P450 system which comprises a flavodoxin domain fused to the N-terminus of this P450 system (Seth-Smith et al., 2002). The *xpIB* gene adjacently upstream of *xpIA* encodes an open reading frame, with highest similarity to bovine mitochondrial adrenodoxin reductase (27 % identity and 42 % similarity) (Seth-Smith, 2002).

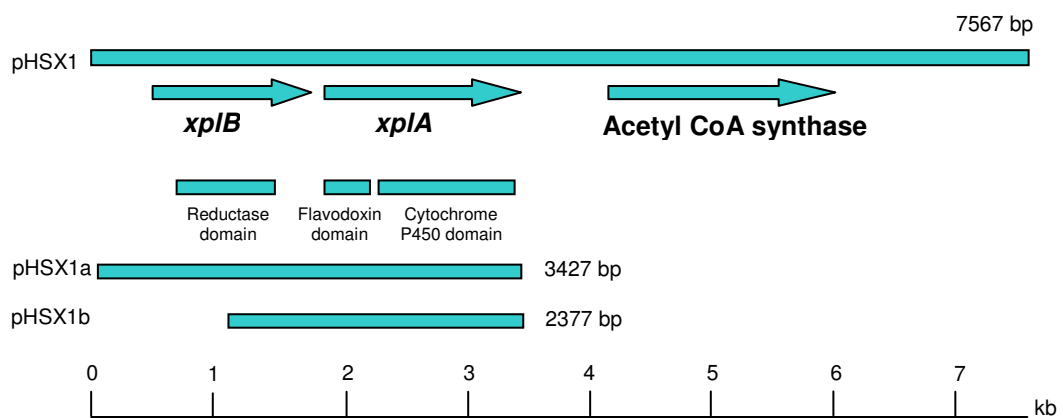


**Figure 1.6. The gene cluster isolated from strain 11Y contains genes responsible for RDX degradation (Seth-Smith, 2002).**

## 1.8 Characterisation of XplA and XplB

Soluble expression of 11Y XplA in *E. coli* was achieved and the characteristics of purified XplA as a cytochrome P450 were confirmed by spectral analysis in which the Soret peak was shown to shift from 420 nm to 448 nm when reduced in the presence of carbon monoxide (Jackson et al., 2007). Trypsin digestion and tandem mass spectrometry (MS/MS) analysis revealed the presence of flavodoxin and P450 domains, thus confirming XplA is a flavodoxin fused cytochrome P450 (Rylott et al., 2006). Active XplB was obtained as a GST fusion and cleavage of the GST from purified XplB-GST fusion caused protein precipitation. The flavin cofactors from XplA and XplB were released after a boiling step and HPLC analysis confirmed that XplA contains flavin mononucleotide (FMN) and XplB contains flavin adenine dinucleotide (FAD) (Jackson et al., 2007).

*In vitro* assays using XplA and XplB demonstrated RDX degradation pathways depend on the presence or absence of oxygen (Figure 1.7). Under aerobic conditions, the ratios of nitrite to RDX was 2.49:1.00 and the formaldehyde to RDX was 1.26:1.00 at 70 min. While NDAB was detected and continued to accumulate to a ratio of 1:1 (NDAB:RDX); MEDINA was not detected. Under anaerobic conditions, the ratios of nitrite to RDX was 1.4:1.0 and formaldehyde to RDX was 1.96:1.00. MEDINA was detected with a ratio of 0.68:1.00, as a transient metabolite (Jackson et al., 2007). Based on the metabolite distribution, it was proposed that under aerobic condition, two steps of denitration of RDX occur resulting in the release of two moles of nitrite followed by spontaneous ring cleavage to produce NDAB and formaldehyde. Under anaerobic condition, a single step of denitration of RDX was followed by ring cleavage to produce MEDINA and formaldehyde. These pathways are found to be in agreement with previously described RDX degradation pathways by resting cells (Fournier et al., 2002, Annamaria et al., 2010).

A wider range of substrate screening revealed that XplA does not transform HMX and TNT and no hydroxylation activity was detected when the common P450 substrates testosterone or paclitaxel were used. However, XplA was able to oxidise methyl tolyl and methyl phenyl sulphides to sulfoxide products implying it could act as a monooxygenase albeit poorly. Inhibition studies demonstrated TNT and methyl tolyl sulphide inhibited RDX activity (Jackson et al., 2007).

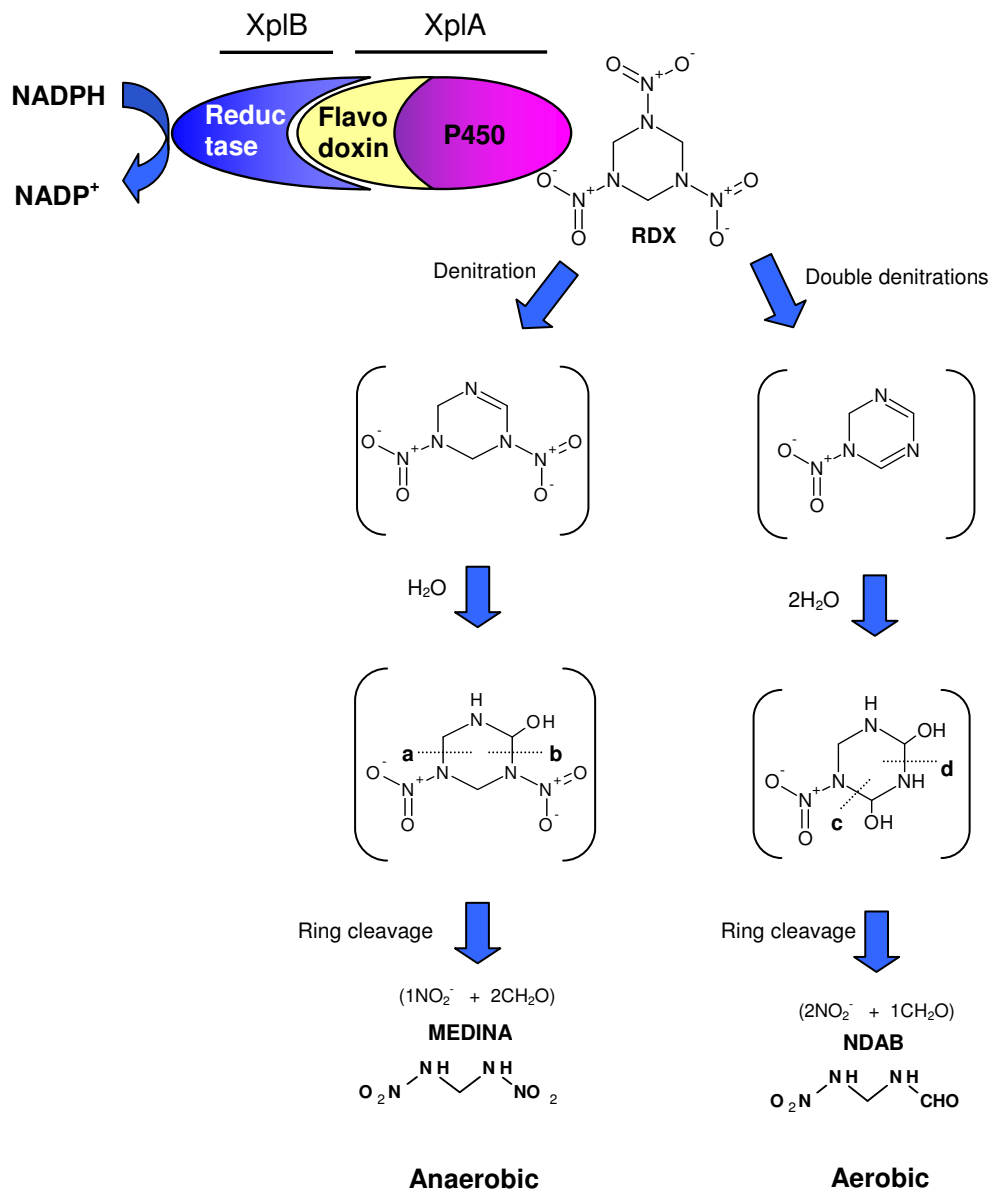


**Figure 1.7. Proposed RDX degradation pathway by XplA and XplB**

XplA is unusual in that it possesses a flavodoxin domain fused at the N terminus of the P450. Electrons transfer from NADPH to the heme domain via the reductase (XplB) then to the flavodoxin domain of XplA. The presence of oxygen alters the route of degradation. Under anaerobic condition, methylenedinitramine (MEDINA), nitrite and formaldehyde are produced. Under aerobic condition, 4-nitro-2,4-diazabutanal (NDAB), nitrite and formaldehyde are produced.

## 1.9 The XplA-heme structure

The heme domain of P450 XplA is a prism structure with dimensions of 50 x 50 x 60 Å. The overall structure of XplA-heme is conserved across other P450 hemes, including the  $\alpha$  helices-rich large domain and  $\beta$  strands-rich small domain (Fig. 1.8). However, XplA-heme possesses a number of unique features that make it differ from other P450s. While the long I helix, which directly contacts the heme, is conserved in other P450s, a break in the central region of the I helix in XplA-heme is observed (Fig. 1.8).

The iron in the active site is coordinated in the 5-position by the conserved Cys-503 (Fig. 1.9). The active site environment of XplA contains Trp-230, Trp-224, Phe-540, Leu-238, Val-387, Val-391, Ala-395, Pro-437 and methionine cluster (Met-318, Met-322, Met-394), forming a highly hydrophobic pocket. Interestingly, Met-394 and Ala-395 replaces the pair, commonly an acidic residue followed by threonine (or serine) in other P450s and are thought to be involved in oxygen activation. Due to the fact the RDX denitration by XplA does not require oxygen; the absence of threonine is important in RDX degradation. Site directed mutagenesis to directly replace Ala-395 to threonine increased  $K_m$  (4-fold higher than wild-type enzyme) and significantly decreased of  $K_{cat}$  (50-fold lower than wild-type enzyme). When Met-394 was mutated to leucine, a two fold decrease was observed in  $K_{cat}/K_m$  compared with wild-type enzyme (Sabbadin et al., 2009).

Two putative channels for ligand transport are found leading to the XplA-heme active site (Fig. 1.10). It is observed that in the larger channel, a chain of seven water molecules leads from the surface of the enzyme into the side chain of Gln-438, located close to the heme active site. The second channel is bounded by the side chains of Arg-288 and Arg-545 and a positively charged patch is observed on the surface of this channel, probably responsible for the capturing of the RDX. Although the structure of RDX bound to XplA-heme could not be obtained, the XplA-heme soaked with RDX revealed significant movement of residues (Arg-288, Arg-543 and Arg-545) at second putative channel, suggesting that RDX is likely entering the heme area via this channel (Fig. 1.10).

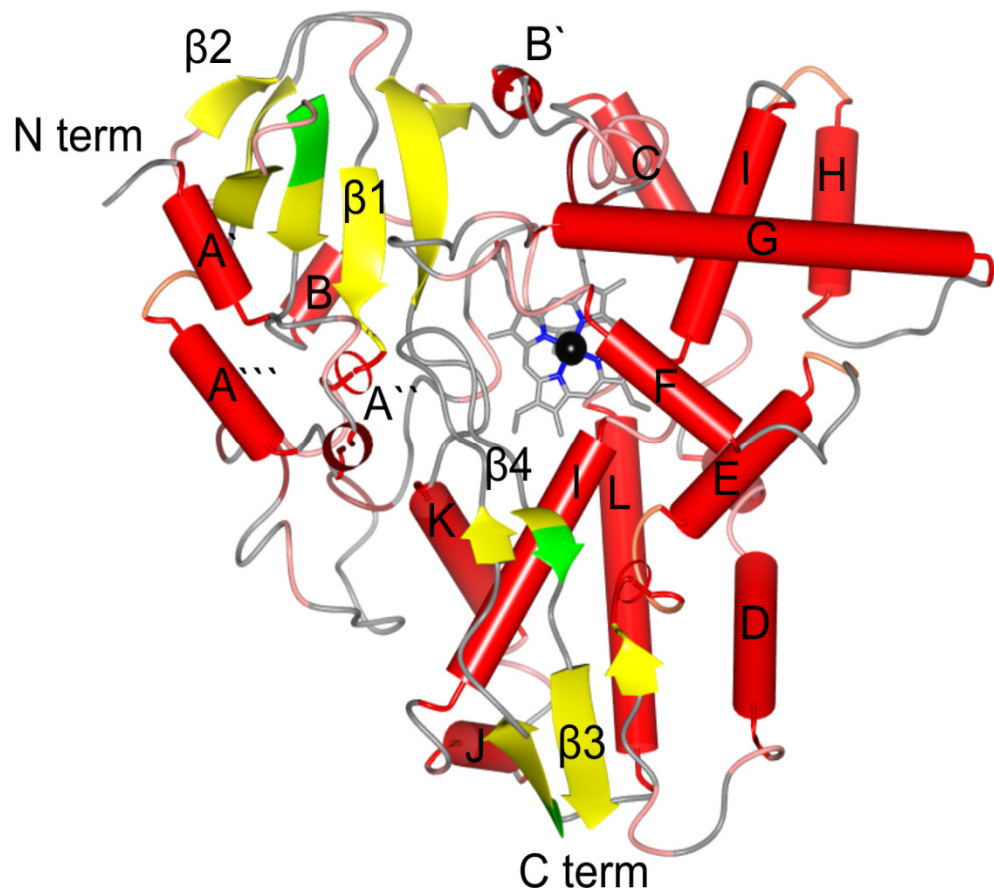


**Figure 1.8. Topology of XplA-heme revealing the well conserved secondary elements.** The  $\alpha$  helices are represented in red. The  $\beta$  strands are represented in yellow and green. The black circle refers to the iron at the heme active site. Figure is taken from Sabbadin (2010).

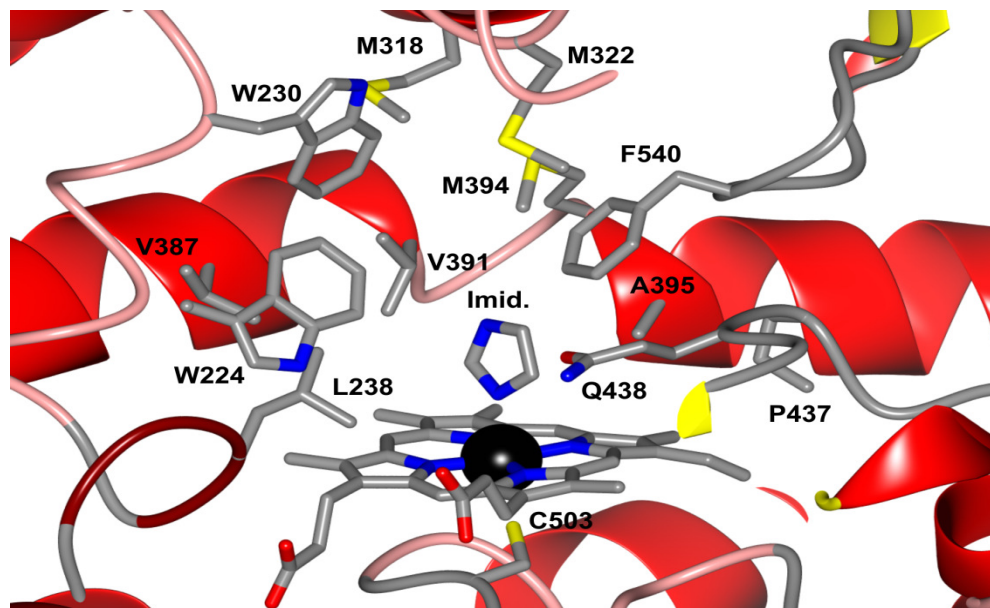


**Figure 1.9. The active site and XpIA-heme environment.** Imidazole is bound on the heme active site. Residues surrounding the heme including Trp-230, Trp-224, Phe-540, Leu-238, Val-387, Val-391, Ala-395, Pro-437 and methionine cluster (Met-318, Met-322, Met-394), forming a hydrophobic ceiling of the heme binding site. Figure is taken from Sabbadin (2010).

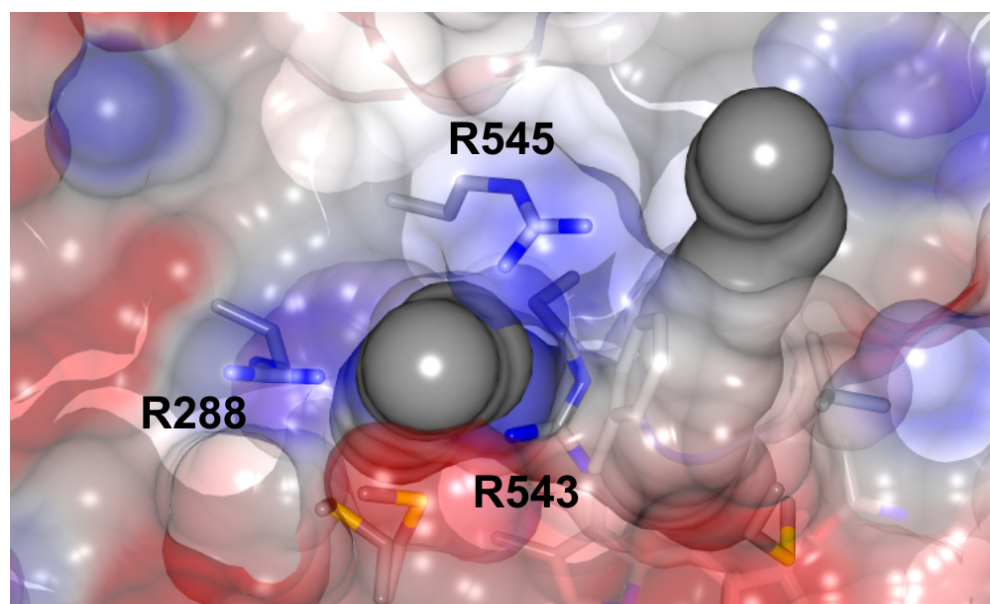


**Figure 1.10. The putative transport channels are shown in grey.** The movement of residues (Arg-288, Arg-543 and Arg-545) are observed in protein crystals soaked with RDX. Figure is taken from Sabbadin (2010).

## 1.10 RDX degrading gene cluster

Analysis using PCR with primers specific to the *xplA* and *xplB* sequences from *R. rhodochrous* strain 11Y yielded products in all of the *Rhodococcus* strains HS1-19 except strain HS4 (Seth-Smith et al., 2008). Partial sequencing of the PCR products showed more than 99 % nucleotide identity to *xplA* and *xplB*. Homologues (also with >99 % identity) of *xplA* and *xplB* have also been described for *Rhodococcus* sp. strain DN22 from Australia (Bhushan et al., 2003), strain YH1 from Israel (Nejdat et al., 2008), and *Gordonia* sp. strain KTR9 (Thompson et al., 2005) and *Williamsia* sp. strain KTR4, from North America (Indest et al., 2007). No XplA homologues have so far been detected in environments uncontaminated by explosives.

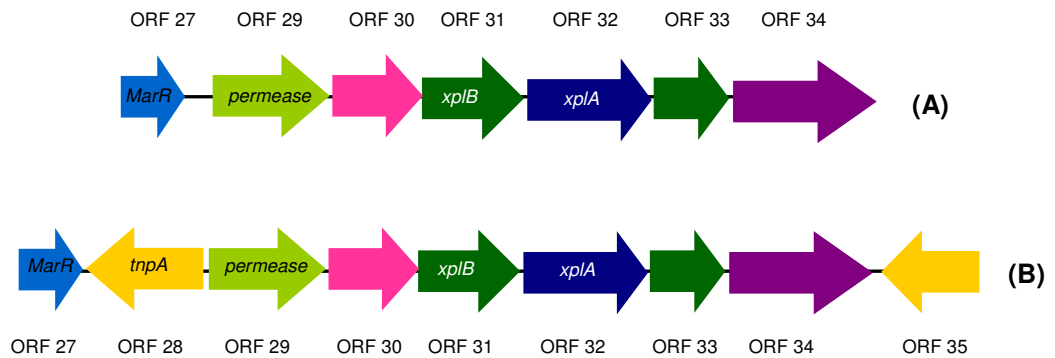
A fosmid library was constructed from *Microbacterium* sp. MA1, an RDX degrading bacterium from the U.S. and a 52 kb plasmid DNA sequence flanking *xplA/B* was isolated (Andeer et al., 2009). Sequence analysis of this DNA sequence flanking *xplA/B* revealed that the RDX degrading gene cluster from *Rhodococcus rhodochrous* 11Y in the U.K shares near identical sequences to the open reading frame (ORF) 30 to 34 in *Microbacterium* sp. MA1 (Figure 1.11) (Andeer et al., 2009).

By means of chromosome walking upstream of ORF 30 in *Rhodococcus rhodochrous* 11Y (Dr Cyril Bontemps and Dr Astrid Lorenz, personal communication), sequence analysis revealed ORF 27 and ORF 29 were also identical with the DNA sequence flanking *xplA/B* from *Microbacterium* sp. MA1 (Figure 1.11). The ORF 27 and ORF 29 encode a putative transcriptional regulator and a putative transporter, respectively. The putative regulator is characterised as a repressor with homology to the regulatory protein MarR, a multiple antibiotic resistance regulator. The putative transporter was found to display close homology to amino acid permease from *Mycobacterium vanbaalenii* PYR-1.

Another RDX degrading gene cluster was isolated from *Gordonia* sp. strain KTR9 (Indest et al., 2010). This gene cluster revealed the presence of four open reading frames encoding XplA, a fusion of glutamine synthase with XplB, a second cytochrome P450 (Cyp151C) and XplR, a GntR-type regulator (Figure 1.12). Whole cell studies demonstrated the XplA - expressing *E. coli* degraded RDX but the Cyp151C - expressing *E. coli* did not. The function of the XplB fusion and the putative regulator XplR was not investigated (Indest et al., 2010).



Recently, PCR analysis showed that the newly isolated RDX degrading *Rhodococcus* spp. (Belgium and UK) and strain *Rhodococcus* DN22 (Australia) also share near identical sequences from ORF 27 to 34 (Fig. 1.11) in *Rhodococcus rhodochrous* 11Y (Dana Sabir, personal communication). The highly conserved nature of the RDX degrading gene cluster from geographically distinct region suggests this gene cluster may have been transferred via a horizontal gene transfer mechanism.



ORF27: Putative transcriptional regulator with homology to regulatory protein MarR  
 ORF28: Transposase, *tnpA*. The only ORF in IS element ISMA1  
 ORF29: Putative transporter with homology to amino acid permease from *Mycobacterium vanbaalenii* PYR-1  
 ORF30: Putative dihydrodipicolinate reductase  
 ORF31: *xplB*, encodes a flavodoxin reductase partner for *xplA*  
 ORF32: *xplA*, encodes novel cytochrome P450 (CYP177A1, XplA) with flavodoxin domain  
 ORF33: Aldehyde dehydrogenase C-terminus domain protein  
 ORF34: Acetyl CoA synthase  
 ORF35: Transposase pseudo gene

**Figure 1.11. Sequence comparison of gene clusters flanking *xplA/B* isolated from *Rhodococcus rhodochrous* 11Y (cluster A) and *Microbacterium sp.* MA1 (cluster B) (Andeer et al., 2009).**



**Figure 1.12. RDX gene clusters flanking *xplA* isolated from *Gordonia sp.* strain KTR9. *xplR*, *cyp151C*, *glnAxpIB* and *xplA* encoding a putative regulator, a cytochrome P450, fusion reductase and RDX degrading P450 enzyme, respectively (Indest et al., 2010).**

## 1.11 Aims

As described in the previous sections, contamination of the environment by the explosive RDX is a global problem. Up to present, *xpIA* is the only P450 gene that has been identified as responsible for RDX degradation. The *XpIA/B* is encoded on an operon in *Rhodococcus rhodochrous* strain 11Y and the gene cluster is highly conserved amongst other RDX degrading bacteria from geographically distinct regions. The isolation of new RDX degrading gene(s) is an area of particular interest as other RDX degrading strains are likely to exist.

Therefore, the first aim of this project was to gain a better understanding of the RDX degrading system in *Rhodococcus erythropolis* strain HS4, which could potentially have an alternative RDX degrading system. Previous studies by Dr. Seth-Smith (2002) showed the RDX activity in strain HS4 was inhibited by metyrapone, an inhibitor of P450 enzyme. Southern blot and PCR analysis indicated that *xpIA* and *xpIB* were absent in strain HS4. Further characterisation of the RDX degradation in strain HS4 was attempted.

To date, the *xpIA/B* gene cluster has not been characterised. The second aim was to analyse the genes on the operon with respect to RDX metabolism in strain 11Y. An unmarked gene deletion system (van der Geize et al., 2001) was employed to sequentially knockout *xpIA*, *xpIB*, putative permease and the putative regulator on the 11Y gene cluster to produce four knockout strains. These knockout strains were characterised relative to wild-type. In addition, the putative permease was also heterologously expressed in *E. coli* and RDX uptake assays performed.

# Chapter 2

## General methods

### 2.1 Suppliers

All reagents, chemicals and DNA modifying enzymes were purchased from Sigma-Aldrich (Gillingham, UK), GE Healthcare (Pollards Wood, UK), Promega (Southampton, UK), New England Biolabs (Hitchin, UK), Merck (Nottingham, UK), Qiagen (West Sussex, UK), Fisher Scientific (Loughborough, UK), Expedeon (Cambridge, UK), Applied Biosystems (Paisley, UK) and Invitrogen (Paisley, UK).

RDX (>95 % purity) was kindly provided by the Defence Science and Technology Laboratory, Fort Halstead, U.K.

Oligonucleotide primers used in this study were synthesised by Sigma-Genosys Ltd (UK) (Table 2.1).

### 2.2 Media

#### 2.2.1 Minimal medium

Minimal medium (pH 7.2) contained 1.55 g/L  $\text{KH}_2\text{PO}_4$ , 4.95 g/L  $\text{K}_2\text{HPO}_4$ , 10 mM glycerol, 5 mM glucose, 5 mM succinate, trace elements (Rosenberger and Elsdén, 1960), and, 180  $\mu\text{M}$  RDX as a sole nitrogen source or unless specified.

#### 2.2.2 Luria-Bertani Peptone (LBP) medium

Complex medium (LBP) consisted of 1 % (w/v) Bacto-peptone, 0.5 % (w/v) yeast extract and 1 % (w/v) NaCl.

#### 2.2.3 Luria-Bertani (LB) medium

Complex medium (LB) consisted of 1 % (w/v) tryptone, 0.5 % (w/v) yeast extract and 1 % (w/v) NaCl.

**Table 2.1. List of primers used for amplification of DNA fragments.**

Name	Sequence	Target
<b>Primers for detection of xplA and xplB (Chapter 3 and 5)</b>		
xplA-HindIII	AAGCTTATGACCGACGTAACCTGTC	xplA
xplA-531F	GAACAACCCCTATCCCTGGT	xplA
xplA-XbaIR	TCTAGATCAGGACAGGACGATCGG	xplA
xplA-1033R	TCAGATAGCCGAAAGCGACT	xplA
xplB-KpnF1	GGTACCATGGACATCATGAGT	xplB
xplB-614	AGTTCGACCCGGTGATGAT	xplB
xplB-XbaR1290	TCTAGATCAGCAGACCGATTTC	xplB
xplB-1142R	ACTGTCCGGTCGATCACTTC	xplB
<b>Primers for qPCR (Chapter 4 and 5)</b>		
perm-F_RT852	GCCGCGACGACATGATC	permease
perm-R_RT906	CGTTTGGCATCGAACTTCTTG	permease
xplA-F_RT413	CCGAGTGGGCCAAACAGT	xplA
xplA-R_RT468	TCCTCCTCGTCGAGTTCGAT	xplA
gyrB-F_RT259	GCCGAGGAGCAGGAACAG	gyrB
gyrB-R_RT323	TAGTGGTAGACCGGGTCTTG	gyrB
<b>Primers for cloning and expression (Chapter 4)</b>		
Permease-F(Lic)	CCAGGGACCAGCAATGAGTCCGTGGCGAACTTCG	permease
Permease-R(Lic)	GAGGAGAAGGCGCGCTACTCCCCGGTCTTCTTCGGAATCG	permease
PermF1+NcoI	TCAAACCATGGATGAGTCCGTGGGCGA	permease
Perm-R1371+NdeI	GTTCCGCATATGGTCCGCTACTCCCCG	permease
xplA-F1+RBS+NheI	CCGAGCTAGCCGAGAAGGAGTGTGGAGAAT	xplA
xplARend+HindIII	TCGGATAAGCTTTCAGGACAGGACGATCG	xplA
<b>Primers for mutagenic plasmids construction (Chapter 5)</b>		
UpF822(perm)+EcoRI	ACGTCGGAATTCAGTGTGGGCGGACC	permease upstream
UpR30(perm)+NdeI	GAATTCATATGGGACGTATAACCGAG	permease upstream
DwnF0(perm)+NdeI	ATTCGCATATGAAGAAGACCGGGGAG	permease downstream
DwnR975(perm)+HindIII	GCGCAGAAGCTTCTGGGCAGATCGAC	permease downstream
UpF861(rp)+EcoRI	GGGGAAATCCGAGGATCGCCGTGA	regulator upstream
UpR75(rp)+NdeI	TGGTCCCATATGGCCCCGACACTCGACG	regulator upstream
DwnF116(rp)+NdeI	CTGGCGCATATGTCAAAAACCTTAT	regulator downstream
DwnR852(rp)+HindIII	ACAGACAAGCTTCGATCAGTGGCGCGG	regulator downstream
UpF816(xplA)+EcoRI	CGATCTGAATTCGCACCCGGACACCCCT	xplA upstream
UpR33(xplA)+NdeI	ATTCTCCATATGGGGTTCACTGCAGGG	xplA upstream
DwnF7(xplA)+NdeI	GTCTTGACATATGATCCGATCTCACCTGCC	xplA downstream
DwnR975(xplA)+HindIII	CCCAAGCTTGACGGTCCAGGGCGTTGT	xplA downstream
UpF1083(xplB)+EcoRI	ACCATGGAATTCACGAACATCAGAGCT	xplB upstream
UpR135(xplB)+NdeI	GTCGAGCATATGCACGTCGGGGATACG	xplB upstream
DwnF30(xplB)+NdeI	ACCCGACATATGACACCCGAGATGGAG	xplB downstream
DwnR849(xplB)+HindIII	CGTCCAAAGCTTCCAGTTTCGGCGTGA	xplB downstream
<b>Primers for detection of sacB, permease, regulator and 16S (Chapter 4 and 5)</b>		
sacBf 488	GGTCAGGTTACGCCACATTT	sacB
sacBr 1262	CCTTTCGCTTGAGGTACAGC	sacB
permF260	TGATCGCGCTGCTCGTCACCAT	permease
permR1086	CGAGGACGACCATCTGGAAGGCGAT	permease
permease-1F	ATGAGTCCGTGGCGAACTTCG	permease
permease-1395R	CTACTCCCCGGTCTTCTTCGGAAT	permease
rpF1	GTGACGAACGACGATCTGGTGAC	regulator
rpR543	ACAATGGTCATGTTCCGGTAACC	regulator
fD1	AGAGTTTGATCCTGGCTCAG	16S
rD2	AAGGAGGTGATCCAGCC	16S

## **2.2.4 Tryptone medium**

Tryptone medium (pH 6.5) contained 2 % (w/v) tryptone, 1 % (w/v) NaCl and 1 % (w/v) of yeast extract. After autoclaving, following chemicals were added: 10 % (w/v) PEG3350, 5 % (v/v) DMSO and MgCl<sub>2</sub> (0.2 M).

## **2.2.5 RDX dispersion agar**

The RDX dispersion agar contained 1.5 % (w/v) of agarose with minimal medium as described previously (2.2.1) and 5 mM of RDX as nitrogen source.

## **2.3 Bacterial strains and plasmids**

See Table 2.2 for details of bacterial strains used in this study.

The plasmid pLIC-YSBLIC 3C (University of York) was used for both cloning and expression. The plasmid pK18mobsacB required for the gene deletion was kindly provided by Professor Eltis Lindsay (University of British Columbia, Canada).

## **2.4 Growth and resting cell experiments**

### **2.4.1 Growth experiment and RDX degradation**

Microbial growth was monitored by measuring the OD<sub>600</sub> using a UV-160A recording spectrophotometer (Shimadzu Corp., Kyoto, Japan). For RDX measurement, samples were taken from the cultures at intervals over the incubation time. Cells were pelleted by centrifugating at 15,000 x g for 3 minutes and the supernatant was used to measure RDX concentration by HPLC (2.7.1).

### **2.4.2 Resting cell assays**

Cells (0.01 g/mL) were incubated in minimal medium contained RDX (100 μM) for 3 h. Samples were taken at different time points and 10 % of trichloroacetic acid (1.5 M) was added to stop the XpIA activity. Samples were then centrifuged (15,000 x g) for 3 minutes and the supernatant was used for RDX analysis measured by HPLC.

**Table 2.2. Bacterial strains used in this study.**

<b>Bacterial strain</b>	<b>Details</b>	<b>Source</b>
<i>Rhodococcus rhodochrous</i> strain 11Y	RDX degrading bacteria	Seth-Smith et al., 2002
<i>Rhodococcus erythropolis</i> strain HS4	RDX degrading bacteria	Seth-Smith et al., 2008
MarR (ORF 27) knockout strain	Derived from 11Y using unmarked gene deletion system (van der Geize et al 2001).	In this study
Permease (ORF 29) knockout strain	Derived from 11Y using unmarked gene deletion system (van der Geize et al 2001).	In this study
<i>xpIB</i> knockout strain	Derived from 11Y using unmarked gene deletion system (van der Geize et al 2001).	In this study
<i>xpIA</i> knockout strain	Derived from 11Y using unmarked gene deletion system (van der Geize et al 2001).	In this study
NovaBlue Singles	General cloning strain	Novagen-Merck
Rosetta 2 (DE3)	Used for expression of genes containing rare codons. Rosetta 2 (DE3) contains pRARE2 plasmid encoding tRNA genes for the rare codons AUA (Ile), AGG (Arg), AGA (Arg), CGG (Arg), CCC (Pro), GGA (Gly) and CUA (Leu).	Novagen-Merck

## **2.5 Protein techniques**

### **2.5.1 Preparation of cell free extracts**

Cells were resuspended in 40 mM potassium phosphate buffer (pH 7.2). Phenylmethylsulfonyl fluoride (PMSF 0.2 mM), a proteinase inhibitor, was added to cells prior to sonication (S-4000 Sonicator, Misonix). This was carried out by using a small probe operated at amplitude of 70 % for 3 s and 7 s cooling intervals for a total of 4 min. All steps were performed in an ice-water bath. Centrifugation (14,000 x g) to separate soluble and insoluble fraction was performed (SS 34 rotor; High Speed Sorvall RC5B+ centrifuge). The supernatant was taken and used for cell free extract assays and western blot analysis.

### **2.5.2 Protein quantification**

Total protein concentration was measured according to the protocol of the Coomassie (Bradford) Protein Assay Kit (Thermo Scientific Pierce). The protein assay standard curve was prepared using a series dilution of bovine serum albumin (BSA). Samples (10 µL) were mixed with 1000 µL Bradford reagent and read at the absorbance of 595 nm. The protein concentration (C) is determined based on the following equation: "C = A/0.0012", where A corresponds to the absorbance.

### **2.5.3 SDS-PAGE gel analysis**

Proteins were analysed using a SDS-PAGE gel (0.75 mm, 12 %). The gel contains two layers (separating and stacking layer). The separating layer was made up by Tris-HCl (375 mM, pH 8.8), SDS (0.1 % w/v), acrylamide (12 % w/v), N,N-methylene-bis-acrylamide (0.3 % w/v), TEMED (0.04 % v/v) and ammonium persulfate (0.1 % w/v). This layer was topped by a stacking layer, which the composition was the same as separating layer except for Tris-HCl (125 mM, pH 6.8), acrylamide (5 % w/v) and N,N-methylene-bis-acrylamide (0.1 % w/v). Samples were diluted (1:4) in loading buffer (SDS (2 % w/v), bromophenol blue (0.15 % w/v), Tris-HCl (60 mM, pH 6.8), glycerol (15 % v/v) and beta-mercaptoethanol (5 % v/v)) and heated at 100 °C for 5 min. The gels were run at 200 V for 50 min and stained with InstantBlue, a coomassie based staining solution (Expedeon, UK).



## 2.5.4 Western blot analysis

### XpIA detection

Initially, two gels were run and one of the gels was used for quantitative determination stained with InstantBlue. Another gel was used to develop the nitrocellulose membrane. This gel was first incubated in pre-chilled Towbin transfer buffer (25 mM Tris, 192 mM Glycin, 20 % (v/v) Methanol, pH 8.3) for approximately 15 minutes. Nitrocellulose membrane (Schleicher and Shuell BioScience, Protran BA 83, cellulosenitrate (E), 0.2  $\mu$ M, 200 x 200 mm, Dassel Germany) and filter paper (Whatman, 3 mm chromatography paper) were cut according to gel size. The membrane was incubated in pre-chilled Towbin transfer buffer for 25 minutes. The filter paper was briefly soaked in the transfer buffer before the gel/membrane sandwich complex.

To make the gel/membrane sandwich complex, three pieces of filter papers were placed onto the anode of the transfer unit, followed by the membrane, gel and another three pieces of pre-soaked filter paper. All steps were performed carefully to avoid any bubbles forming within the layers. This was followed by placing the cathode onto the sandwich complex and a current of 10 V was applied to allow the transfer for one hour. After the transfer of protein onto the membrane, the membrane was rinsed in TBS (Tris buffered saline 1x, 150 mM NaCl, 25 mM Tris-HCl, pH 7.5). The membrane was then blocked with 1x TBS containing 3 % (w/v) non-fat milk powder (Marvel) in the cold room overnight.

The membrane was then incubated with primary antibody, XpIA antibody (TBS 1x, 3 % (w/v) BSA, 10  $\mu$ L antibody/10 mL) for one hour, after which, following treatments were carried out: incubation of membrane with TBS, 0.1 % Tween 20 (x2) for 5 minutes, then, with TBS, 0.5 % Tween 20, 1M NaCl (x2) for 5 minutes and briefly rinsed with TBS and TBS containing 3 % (w/v) of BSA. The membrane was incubated with secondary antibody, goat anti-rabbit conjugated to alkaline phosphatase, in a dilution of 1/20000 for one hour, followed by several treatments: incubation with TBS, 0.1 % Tween 20 (x2) for 5 minutes, then, with TBS, 0.5 % Tween 20, 1M NaCl (x2) for 5 minutes and briefly rinsed with TBS, 0.1 % Tween 20 and TBS. The membrane was then incubated in 10 mM Tris pH 9.6 for 5 minutes. The membrane was developed using Sigma tablets containing of active compound of nitroblue tetrazolium and 5-bromo-4-chloro-3-indolyl phosphate dipotassium for approximately 10 minutes. The

reaction was stopped by washing the membrane with TBS, 0.1 % Tween 20, TBS and water.

### **His-tag protein detection**

This western blot analysis was performed based on procedure described above with some modification. After the membrane was blocked with 1x TBS containing 3 % (w/v) of non-fat milk powder overnight, it was incubated with anti-polyhistidine conjugated to peroxidase, in a dilution of 1/2000 for two hours. The membrane was then developed using peroxidase substrate 4-chloro-1-naphthol. All steps were performed at room temperature.

### **2.5.5 Specific activity of XplA in cell free extracts**

To determine the specific activity of XplA in the cell free extracts, activity assays were set up. The reaction contained cell free extracts (75  $\mu$ L), NADPH (300  $\mu$ M), Spinach ferredoxin reductase (Sigma) (0.1 U/mL) and RDX (100  $\mu$ M) in a final volume of 150  $\mu$ L. All of the reactions were performed aerobically at room temperature (20  $^{\circ}$ C) and the NADPH oxidation rate was monitored at absorbance 340 nm. The difference in NADPH concentration after three min of reaction time was calculated using the following equation:

$$\frac{\Delta C}{\Delta t} = \frac{K}{\epsilon}$$

$\Delta C$ : difference in [NADPH]

$\Delta t$ : reaction time (n min)

$K$ : change of absorbance over reaction time

$\epsilon$ : extinction coefficient of NADPH at 340 nm ( $6.2 \times 10^{-3} \mu\text{M}^{-1} \text{cm}^{-1}$ )

The specific activity of XplA in the cell free extracts was determined based on the following formula:

$$\text{Specific activity} = (\text{rate of reaction } [\mu\text{mol/L/min}] \times \text{volume of reaction [L]}) / \text{total protein [mg]}$$

## **2.6 Molecular biology techniques**

### **2.6.1 Gel electrophoresis of DNA**

DNA fragments were separated by agarose gel electrophoresis using 1 % (w/v) agarose in Tris-acetate-EDTA buffer (40 mM Tris-HCl, 18 mM glacial acetic acid and 1 mM ethylenediaminetetraacetic acid (EDTA)). The loading dye consisted of 0.15 % (w/v) bromophenol blue, 0.5 % (w/v) SDS, 0.15 M EDTA and 50 % (v/v) glycerol and was added to the sample to a final dilution of 20 % (v/v). DNA was visualised by adding 10 µg mL<sup>-1</sup> ethidium bromide to the gel and viewing under UV. Fragment size was determined by comparison to a 10 kb Smart Ladder (Eurogentec) or 1kb ladder (NEB) that had been run alongside the lanes of interest.

### **2.6.2 Polymerase chain reaction (PCR)**

Polymerase chain reaction was carried out for screening and cloning purposes.

For the screening purposes, GoTaq<sup>®</sup> DNA polymerase (Promega) was used, which contained 1x GoTaq buffer, 0.4 µM of dNTPs, 1.5 mM MgCl<sub>2</sub>, 0.4 µM of forward and reverse primers, 0.7 U GoTaq<sup>®</sup> DNA polymerase, 16 µL distilled H<sub>2</sub>O and 20-40 ng DNA template in a total volume of 25 µL.

For cloning purposes, Phusion DNA polymerase (New England Biolabs) was used. Reactions of 50 µL consisted of 1x HF buffer, 2.5 mM of dNTPs, 0.4 µM of forward and reverse primers, 1 U Phusion DNA polymerase, 36 µL distilled H<sub>2</sub>O and 40-80 ng DNA template.

PCR cycle started with an initial denaturation step of 95 °C for 5 minutes, followed by 30 cycles of denaturation step of 95 °C (30 s), annealing step (varied temperature-determined from primers melting temperature) and extension step of 72 °C (1-3 minutes). A final extension cycle at 72 °C for 10 minutes was performed.

The reaction was performed in a thermocycler (ThermoElectron Corp.).

### **2.6.3 Digestion, dephosphorylation and ligation of DNA**

Restriction endonuclease digestion of DNA (inserts fragments or plasmid), dephosphorylation of the linearised plasmid and DNA ligation were performed according to the manufacturer's protocol (NEB).

### **2.6.4 Preparation of competent cells (calcium chloride method)**

*E.coli* (Novablue) was inoculated in LB (10 mL) and grown overnight at 37 °C. Then, 5 mL of the pre-culture was inoculated into 450 mL of fresh LB medium and allowed to grow until OD<sub>600</sub> reached between 0.4 and 0.5. Cells were harvested by centrifugation at 4 °C for 15 minutes (13,000 x g) and resuspended in 50 mL sterile ice-cold calcium chloride (100 mM). This was followed by another centrifugation at 4 °C for 15 minutes (6,600 x g) and resuspended in 50 mL sterile ice-cold calcium chloride (100 mM). The cells were incubated on ice for 1h and harvested by centrifugation at 4 °C for 15 minutes (3,300 x g). Supernatant was decanted and cells were gently resuspended in 1 mL of ice-cold sterile CaCl<sub>2</sub> (100 mM). The competent cells were used immediately or ice-cold sterile glycerol was added to a final concentration of 15 % (v/v) for storage. Cells were aliquoted into 50 µL and stored at -80 °C.

### **2.6.5 Preparation of competent cells (for knockout experiment)**

A pre-culture (5 mL) of *E.coli* (S17-1) in LB was incubated overnight at 37 °C. Then, 0.5 mL of pre-culture was inoculated into 50 mL of pre-warmed medium and incubated at 37 °C to allow OD<sub>600</sub> reached between 0.3 and 0.4. This was followed by 3,000 x g centrifugation at 4 °C for 10 minutes and resuspended cells in 0.5 mL tryptone medium. Cells were aliquoted into 50 µL portions and stored at -80 °C for future use.

### **2.6.6 Plasmid transformation (Heat shock)**

An aliquot (50 µL) of competent cells was thawed on ice. 2-3 µL of plasmid DNA, ligation reaction or LIC reaction was added into the cells. Cells were incubated on ice for 5 minutes and heat shocked at 42 °C (1 minute). Then, 3 minutes incubation was performed on ice. LB (500 µL) was added and cells were incubated at 37 °C for 1 hour. After the incubation, cell suspension was spread on a selective LB agar plate and was incubated at 37 °C overnight.

### **2.6.7 Quantitative real-time PCR (qPCR) analysis**

For RNA isolation, cell pellets were treated with RNAprotect Bacterial Reagent (Qiagen) to stabilise the total RNA in bacteria. Then, cells were incubated with lysozyme (80 mg/mL) and proteinase K (2 mg/mL) at 25 °C for 2 h with 150 rpm shaking. Glass beads (40 mg) were added into the cells suspension and cells were ruptured using a FastPrep machine (Q-biogene) at force 6.5 setting for 40 seconds. The total RNA isolation was performed using RNeasy Mini Kit (Qiagen) according the manufacturer's instructions. The quantity and quality of total RNA was analyzed using NanoDrop spectrophotometer (Thermo Scientific).

SuperScript II reverse transcriptase (Invitrogen) and random hexamer primers (Applied Biosystems) were used to reverse transcript total RNA (2 µg) into cDNA and the cDNA was then purified by Wizard PCR clean-up kit (Promega). The concentration of cDNA was determined using NanoDrop spectrophotometer. The qPCR reactions were performed in Applied Biosystems ABI7000 Real-time Quantitative PCR system. The SYBR Green PCR master mix contained 12.5 µL power SYBR green mix (Applied Biosystems), 5 µL cDNA (5 ng/µL), 2 µL primer pair mix (10 µM each primer) and 5.5 µL nuclease free water. The cycle started with single step of 50 °C (2 min) and 95 °C (10 min), followed by 40 cycles of 95 °C (15 s) and 60 °C (1 min). The data was analysed by Applied Biosystems ABI7000 software with a DNA gyrase, subunit B (*gyrB*) as internal standard.

### **2.6.8 Sequencing**

The DNA sequencing was performed by Technology Facility, University of York. Sequence analyses were performed by ClustalW and BLASTn.

## **2.7 Analytical techniques**

### **2.7.1 HPLC analysis**

The HPLC system used in this study contained a 510 pump, a Waters Alliance 2695 separation module and a Waters 2996 Photodiode Array. Samples (50  $\mu\text{L}$ ) were separated using a Sunfire C18 5  $\mu\text{M}$  column (Waters, Wexford, Ireland) at a flow of 1 mL/min with the mobile solvent of 50:50 MeOH:H<sub>2</sub>O. The elution was monitored at 237 nm and the RDX standard curve (Appendix B) was used to convert the peak area to the concentration of RDX in the samples.

### **2.7.2 Griess assay**

Griess assay was used to measure nitrite content in samples. Samples (180  $\mu\text{L}$ ) were mixed with 50  $\mu\text{L}$  of sulphanilamide (10 mg/mL sulphanilamide in 0.68 M hydrochloric acid) and 20  $\mu\text{L}$  of *N*-(1-naphthyl)-ethylenediamine dihydrochloride (NED) (10 mg/mL NED in water). The reaction was incubated for two minutes at room temperature (20  $^{\circ}\text{C}$ ). The sample was measured at 540 nm and blanked against reagent. The concentration of nitrite was determined based on a standard curve of sodium nitrite (Appendix C).

## Chapter 3

# RDX degradation in *Rhodococcus erythropolis* strain HS4

### 3.1 Introduction

*Rhodococcus erythropolis* strain HS4 is one of the nineteen strains of *Rhodococcus* capable of utilising RDX as a sole nitrogen source that was isolated from an RDX contaminated site (Seth-Smith, 2002). Strain HS4 was able to remove RDX supplied as a sole nitrogen source from growth medium, but was not able to utilise RDX supplied as a sole carbon and nitrogen source. When strain HS4 was grown on RDX dispersion agar, a clearance zone around the colony formed (Fig. 3.1), which was not observed in non-RDX degrading strains.

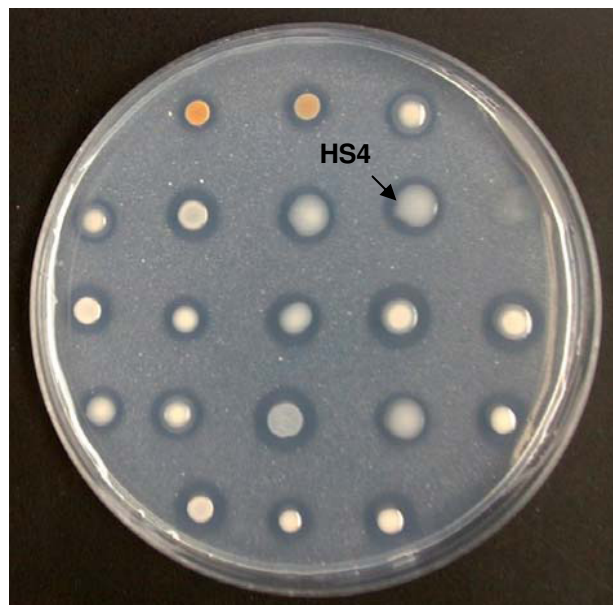


**Figure 3.1.** Clearance zone formed by isolated RDX degrading bacteria of *Rhodococcus* strains on RDX dispersion agar (Seth-Smith, 2002). The clearance zone around strain HS4 is clearly visible.

It was demonstrated that RDX degradation activity in strain HS4 was inhibited by metyrapone, a cytochrome P450 inhibitor, suggesting that a cytochrome P450 system is involved in RDX degradation in this strain. The novel RDX degrading cytochrome P450 system XplA/B was first identified in *Rhodococcus rhodochrous* 11Y (Seth-Smith et al., 2002). Unlike the other 18 strains, Southern blot analysis suggested that the genes *xplA* and *xplB* were not present in HS4 (Seth-Smith et al., 2008). Furthermore, no DNA amplification products were detected using PCR with *xplA* and *xplB* specific primers on strain HS4 gDNA. These findings suggested that there might be a different P450 system responsible for biodegradation of RDX in strain HS4 and investigation of this is detailed in this chapter.



## **3.2 Materials and methods**

### **3.2.1 Assay development for RDX degrading activity**

To prepare the cell free extracts, cultures were grown in minimal medium (see Chapter 2) with 200  $\mu\text{M}$  of RDX. When cells reached late-log phase, they were centrifuged (14,000  $\times$  g), washed twice and resuspended to a concentration of 0.05 g wet weight/mL in 40 mM of potassium phosphate buffer (pH 7.2). Phenylmethylsulfonyl fluoride (0.2 mM), a protease inhibitor, was added to cells prior to cells disruption.

To detect RDX degrading activity in cell free extracts, reactions were incubated in 1 mL of minimal medium with 90  $\mu\text{M}$  RDX at 20  $^{\circ}\text{C}$ ; with or without addition of ferredoxin reductase (0.1 U/mL) and an cofactor recycling system that consisted of alcohol dehydrogenase (0.72 U/mL), NADPH (300  $\mu\text{M}$ ) and isopropanol (30  $\mu\text{L}/\text{mL}$ ). Samples were centrifuged (10,000  $\times$  g) for 2 minutes before sample analysis. Nitrite and RDX were measured using the Griess assay and HPLC, respectively (details for Griess assay and HPLC analysis, see Chapter 2).

### **3.2.2 Protein purification using Protein A SpinTrap column**

Purification of an XplA-like from *Rhodococcus erythropolis* strain HS4 was performed using Protein A SpinTrap column according to the manufacturer's instructions (GE Healthcare Life Sciences Company, UK).

### **3.2.3 PCR amplification**

PCR amplification was carried out on DNA from strain HS4 for *xplA* and *xplB* using primers specific to these genes (see Chapter 2, Table 2.1). This was performed in a thermocycler (ThermoElectron Corp). The cycle started with an initial denaturation step of 94  $^{\circ}\text{C}$  30 s, followed by an annealing step of 50  $^{\circ}\text{C}$  30 s, an extension step of 72  $^{\circ}\text{C}$  1.5 min for 30 cycles and a final extension step at 72  $^{\circ}\text{C}$  for 10 min.

## 3.3 Results

### 3.3.1 Whole cell assays of *R. erythropolis* HS4

*R. erythropolis* strain HS4 were previously shown to be able to degrade RDX slowly (Seth-Smith, 2002). To test the RDX degradation activity in strain HS4, whole cell assays were performed along side strain 11Y (Fig. 3.2).

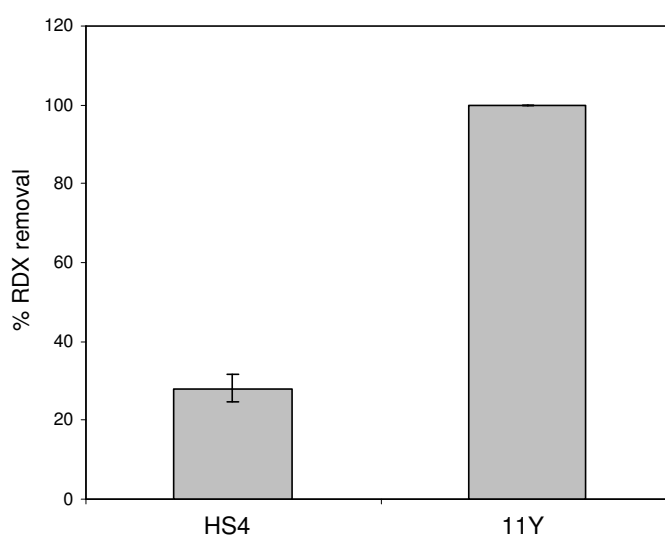


**Figure 3.2. RDX removal (%) by whole cells of strains HS4 and 11Y (0.05 g/mL) after 20 hours of incubation at 20 °C.** Initial RDX concentration was 100  $\mu$ M. Error bars show one standard deviation for duplicate samples.

Strain HS4 removed about 30 % of RDX after 20 hours of incubation, while all of the RDX was removed from the incubation mixtures by strain 11Y. The lower rates of RDX removal by HS4 was in agreement with previous observations described by Seth-Smith (Seth-Smith, 2002). Since whole cells of strain HS4 had less RDX activity compared to strain 11Y, cell free extracts of strain 11Y were used to develop an assay for the detection of XplA activity in cell free extracts.

### **3.3.2 Assay development to detect RDX degrading activity (XplA) in cell free extracts**

A previous study indicated that a cytochrome P450 system in both strains 11Y and HS4 was involved in RDX degradation (Seth-Smith, 2002); however, no RDX degrading activity in cell free extracts could be detected. More recent work on the characterisation of purified recombinant XplA revealed that the NADPH and reductase XplB were required for RDX degradation (Jackson et al., 2007). Also, active XplB was obtained as a GST fusion and the cleavage of the GST from the purified fusion protein caused precipitation suggesting XplB could be unstable in cell free extracts. It was found that a surrogate commercially supplied spinach leaf ferredoxin reductase can partner XplA for RDX activity (Edwards, 2006). These findings allowed the development of an assay for XplA activity in cell free extracts.

In this assay, the cofactor recycling system and ferredoxin reductase were included to ensure the supply of reducing equivalents was not limiting the reaction. The cofactor recycling system consisted of alcohol dehydrogenase, NADPH and isopropanol. Activity was detected by measuring the release of nitrite (Griess assay, section 2.7.2) and reduction of RDX (HPLC, section 2.7.1). The reactions of sulphanilamide and NED with nitrite (RDX breakdown product) forms a colour compound in the Griess assays, which can be measured at 540 nm. Whole cells of strain 11Y were used as a positive control. Boiled cell free extracts with ferredoxin reductase was the negative control and results are shown in Figures 3.3 and 3.4.

In the presence of ferredoxin reductase, in combination with a cofactor recycling system, 56 % of the 90  $\mu$ M RDX was degraded with the production of 96  $\mu$ M of nitrite over the incubation time of 90 min (Fig. 3.3b and Fig. 3.4). The addition of the cofactor recycling system-only in the absence of ferredoxin reductase showed approximately 11 % of the RDX had been degraded (Fig. 3.3c and Fig. 3.4). However, no biotransformation of RDX occurred in the absence of ferredoxin reductase and cofactor recycling system, suggesting parts of the reductase(s) in strain 11Y had lost activity after the cells were disrupted, and that NADPH plays an important role in RDX biodegradation. No RDX reduction was observed in the negative control containing boiled of both cell free extracts of 11Y and ferredoxin reductase, demonstrating that XplA in cell free extracts in combination with ferredoxin reductase were responsible for the RDX activity. In the positive control, all of the RDX was degraded after 90 min of

incubation (Fig. 3.4). Only low levels of nitrite were detected in 11Y whole cells and it is likely that this product was assimilated by the cells during the incubation period.

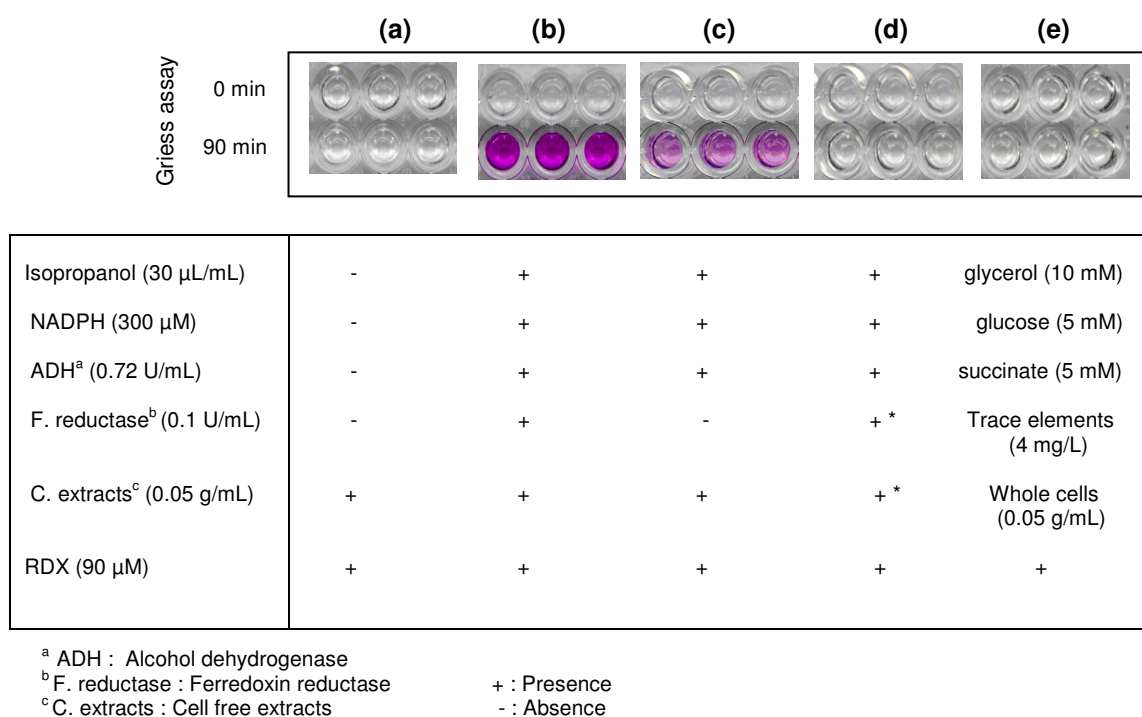
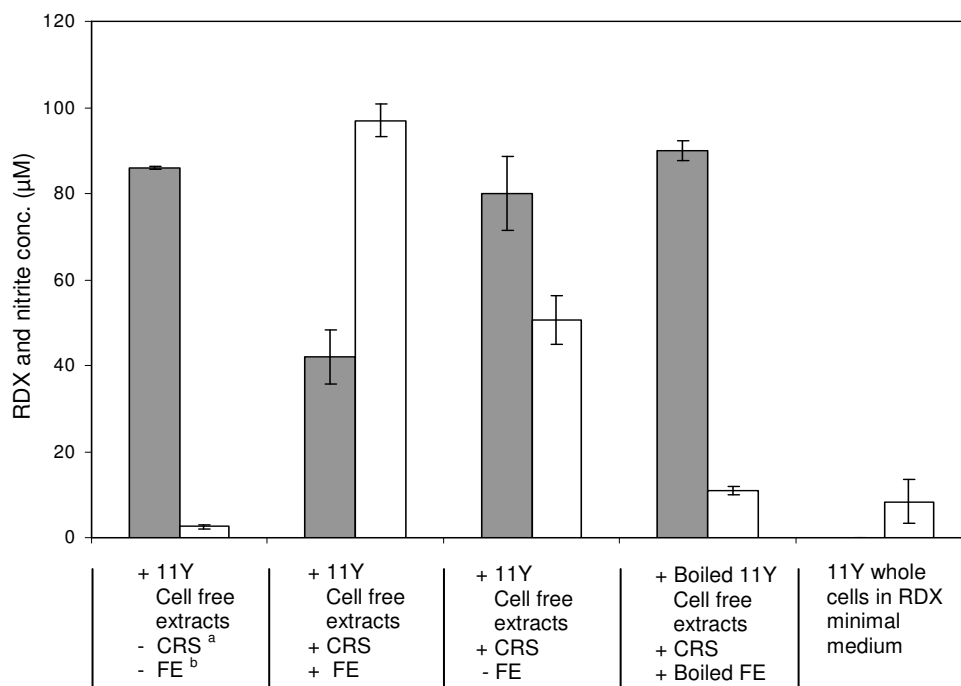


**Figure 3.3. RDX activity in cell free extracts of strain 11Y under aerobic condition after 90 minutes of incubation. (a)** Cell free extracts only (without addition of ferredoxin reductase and a cofactor recycling system). **(b)** Cell free extracts with addition of ferredoxin reductase and a cofactor recycling system. **(c)** Cell free extracts without addition of ferredoxin reductase. **(d)** Negative control (\*boiled ferredoxin reductase and cell free extracts). **(e)** Positive control (whole cells of strain 11Y). The initial RDX concentration for all reactions was 90  $\mu$ M.



<sup>a</sup> CRS : Cofactor recycling system consisting of alcohol dehydrogenase, NADPH and isopropanol.

<sup>b</sup> FE : Ferredoxin reductase

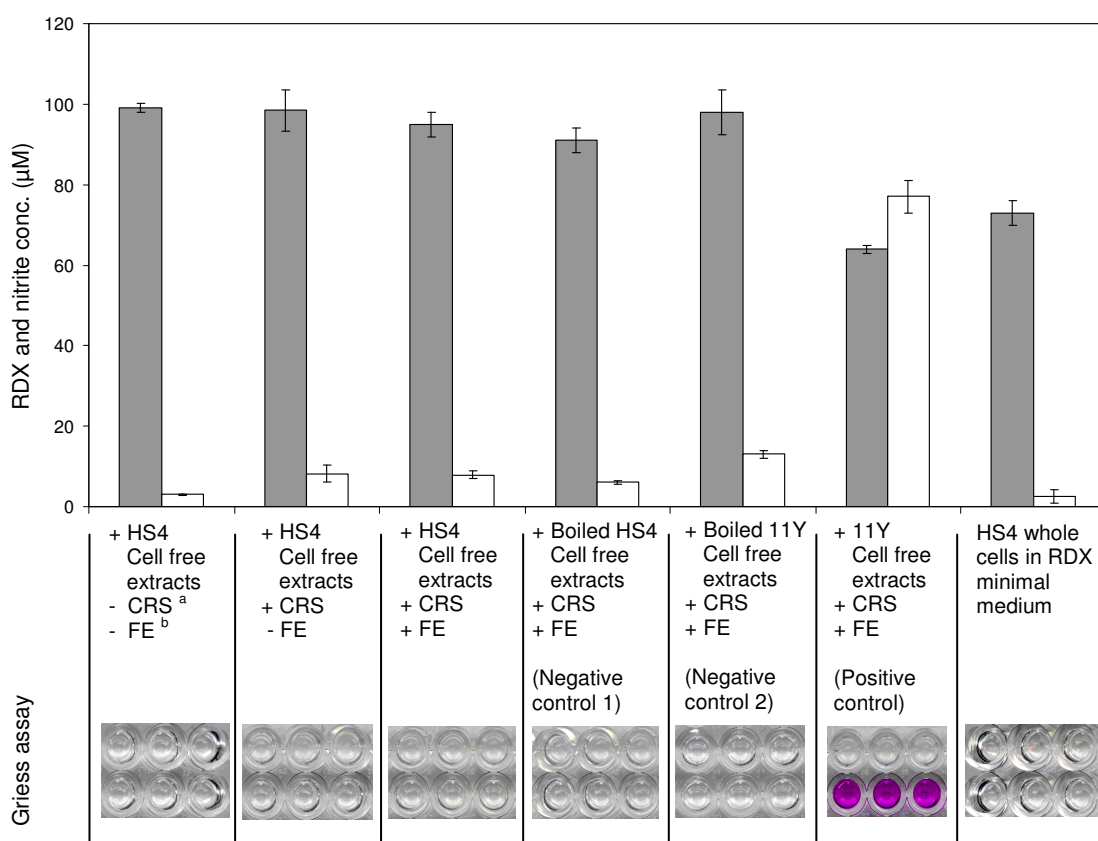
+ : Presence

- : Absence

**Figure 3.4. RDX (grey) and nitrite (white) concentration after 90 minutes of incubation with cell free extracts of 11Y under aerobic conditions at 20 °C. Error bars show one standard deviation for triplicate samples.**

### 3.3.3 RDX activity in cell free extracts of strain HS4

Following the development of an assay to detect RDX degradation in cell free extracts of 11Y, the assay was used to measure RDX degradation in cell free extracts of strain HS4, with strain 11Y used as a positive control. The results (Figure 3.5) showed that whilst RDX was degraded in extracts of strain 11Y, with the production of nitrite, no RDX degrading activity was observed in cell free extracts of strain HS4 despite the addition of ferredoxin reductase and a cofactor recycling system. No RDX degrading activity was detected in the negative controls by HPLC analysis and Griess assays. Whole cells of strain HS4 removed approximately 30  $\mu\text{M}$  RDX during the 20 h of incubation time.



<sup>a</sup> CRS : Cofactor recycling system consisted of alcohol dehydrogenase, NADPH and isopropanol.  
<sup>b</sup> FE : Ferredoxin reductase

**Figure 3.5. Analysis of HS4 cell free extracts for RDX degradation after 20 h at 20 °C under aerobic conditions.** Grey and white bars represent RDX and nitrite concentration respectively. Error bars show one standard deviation from triplicate samples.

### 3.3.4 Western blot analysis of strain HS4 cell free extracts

An antibody to the recombinant, purified XplA cloned originally from 11Y was used to investigate whether protein(s) in strain HS4 cell free extracts had cross-reactivity to anti-XplA antibodies. Extracts were run on gels for quantitative determination of protein following staining with InstantBlue (data not shown), and, using semi dry transfer onto nitrocellulose membrane, for western blotting (Fig. 3.6).

The primary (XplA) and secondary (goat anti-rabbit antibody conjugated to alkaline phosphatase) antibody incubations were followed by membrane development. A band with a molecular weight of ~58 kDa was detected from strain HS4 cell free extracts, a smaller molecular weight than XplA (70 kDa). The band was not clearly visible on the Coomassie-stained gel, so peptide sequencing was not performed at this stage. Given the apparent cross-reactivity of the XplA antibody with HS4, affinity purification of the HS4 protein of interest was attempted.

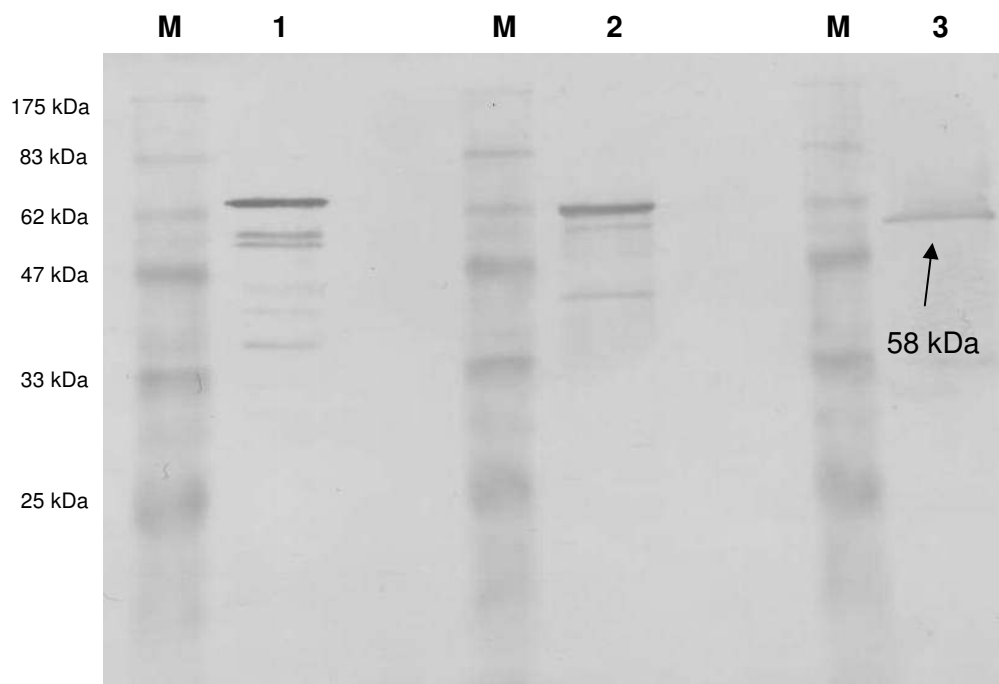


**Figure 3.6. Western blot analysis of cell free extracts of strains 11Y and HS4. (M);** Protein marker, **(1);** Purified recombinant-XplA (0.33 mg/mL), **(2);** Cell free extracts of strain 11Y (total protein of 1.9 mg/mL), **(3);** Cell free extracts of strain HS4 (total protein of 1.0 mg/mL).

### 3.3.5 Purification trial of a putative RDX degrading enzyme in strain HS4

Protein A HP SpinTrap columns (GE Healthcare) are a simple and small-scale antibody purification columns. The Protein A Sepharose HP has a high affinity for the F<sub>c</sub> region of IgGs antibodies. The XpIA antibody is an IgG type antibody and thus this column was chosen for protein purification. To start with, XpIA antibodies were bound covalently to Protein A Sepharose High Performance matrix by using the cross-linking agent dimethyl pimelimidate dihydrochloride in triethanolamine at pH 8.9. The unbound antibodies were removed before adding HS4 cell free extracts into the column. Elution was carried out after several washing steps. The eluates were analysed using SDS-PAGE. The general principle for purification of proteins using antibodies is shown in Figure 3.7.

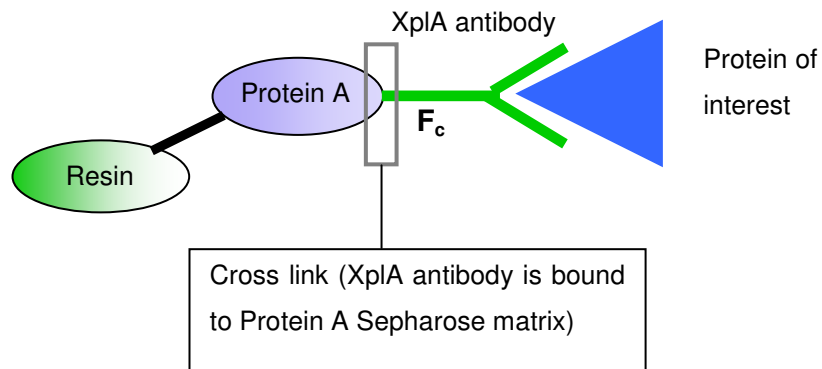


**Figure 3.7. Principle of purification of protein using XpIA antibody.**

The primary antibody that was used for the western blot (Fig. 3.6) was from crude rabbit serum. This means that besides polyclonal XpIA IgGs, there are other proteins in the serum. The rabbit serum was purified using Protein A to remove contaminants and to enable determination of the size of IgGs in the serum. This information is important as there is a possibility that the IgGs are of a similar molecular weight to the target



protein in HS4. To purify XplA IgG, a Protein A HP SpinTrap column was equilibrated with binding buffer (0.5 M Tris, 1.5 M NaCl, pH 7.5) then rabbit serum added. End-over-end mixing for 30 minutes was carried out, then the protein eluted. The results are shown in Figure 3.8.

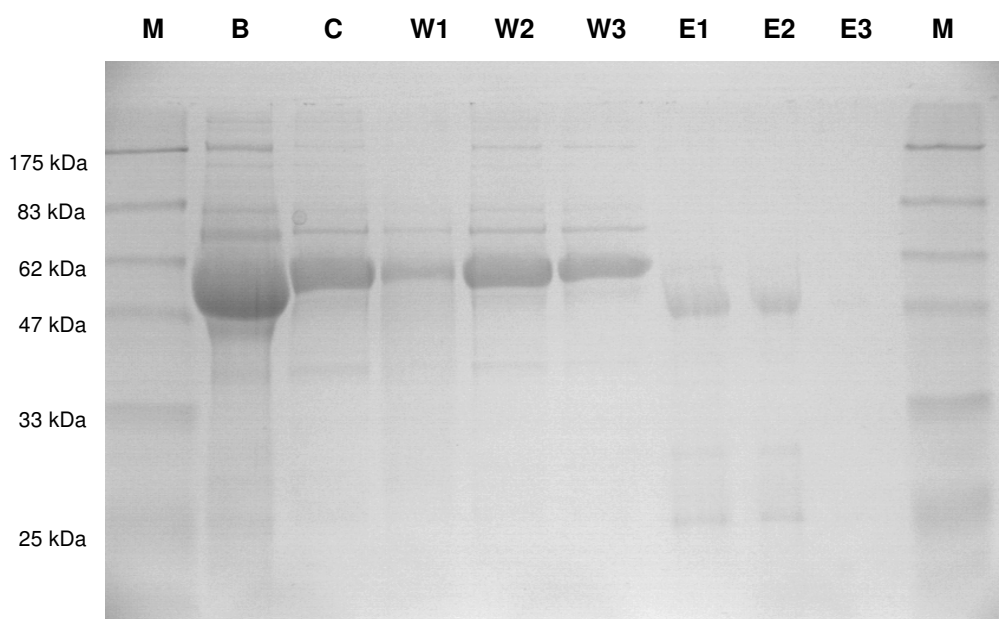


**Figure 3.8. Purification of IgGs in rabbit serum using Protein A HP SpinTrap column. (M)** Protein marker **(B)** rabbit serum before purification **(C)** excess antibody after binding to the column **(W1-W3)** washing steps before elution of binding IgGs **(E1-E3)** elution of IgGs using elution buffer (2.5 % of acetic acid).

Elution of a single band from the Protein A column suggests that IgGs were successfully purified from rabbit serum and these had an apparent molecular weight of approximately 47 kDa (Fig. 3.8; E1-E2). The molecular weight of the IgGs is quite close to that of the protein of interest, about 58 kDa (Fig. 3.6); however, cross-linking of the Protein A column with XplA antibody prior to the purification of the protein from HS4 cell free extracts should remove the IgG from subsequent SDS-PAGE analysis. A single band at the elution step confirmed that the column was working well for purification and so purification of the protein of interest from strain HS4 was then carried out.

To minimise impurities that may bind to the column and then co-elute with the target protein during the purification, cell free extracts were pre-cleared with a SpinTrap column that had not been coupled with any antibody as suggested by the manufacture. HS4 cell free extracts were incubated for four hours on the column before collection of the cleared cell free extracts, as suggested by the manufacture, and these cell free extracts were then used for purification.

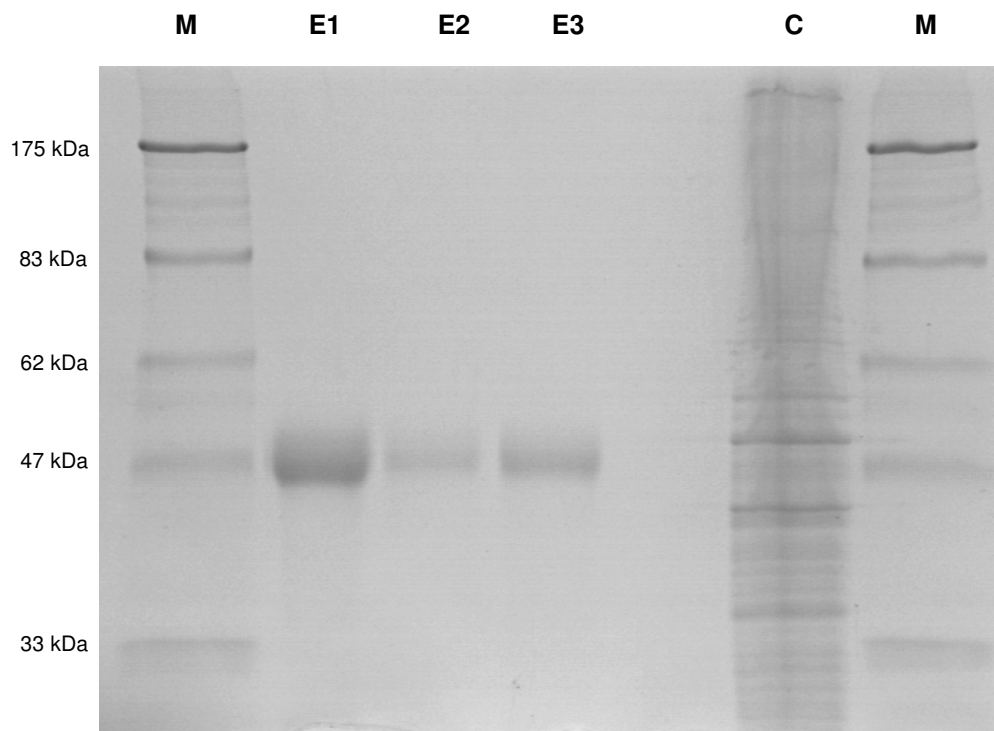


**Figure 3.9. Purification of protein from HS4 that is active towards XplA antibody (M)** Protein marker (**E1-E3**) elution of target protein using elution buffer (0.1 M Glycine-HCl, pH 2.9) (**C**) HS4 cell free extracts.

The elution steps in the protein purification show a band at molecular weight about 47 kDa instead of 58 kDa (Fig. 3.9). This means that the eluate most probably contains IgGs of XplA antibody, not the protein of interest from strain HS4. To investigate this further, the experiment was repeated using cell free extracts of strain 11Y to purify XplA, as a positive control system. Following application of strain 11Y cell free extracts to the column and washing steps, no XplA was detected in the elution fraction (Fig. 3.10a). To investigate where XplA was 'lost' during the process, western blot analysis was carried out on the column fractions (Fig. 3.10b).

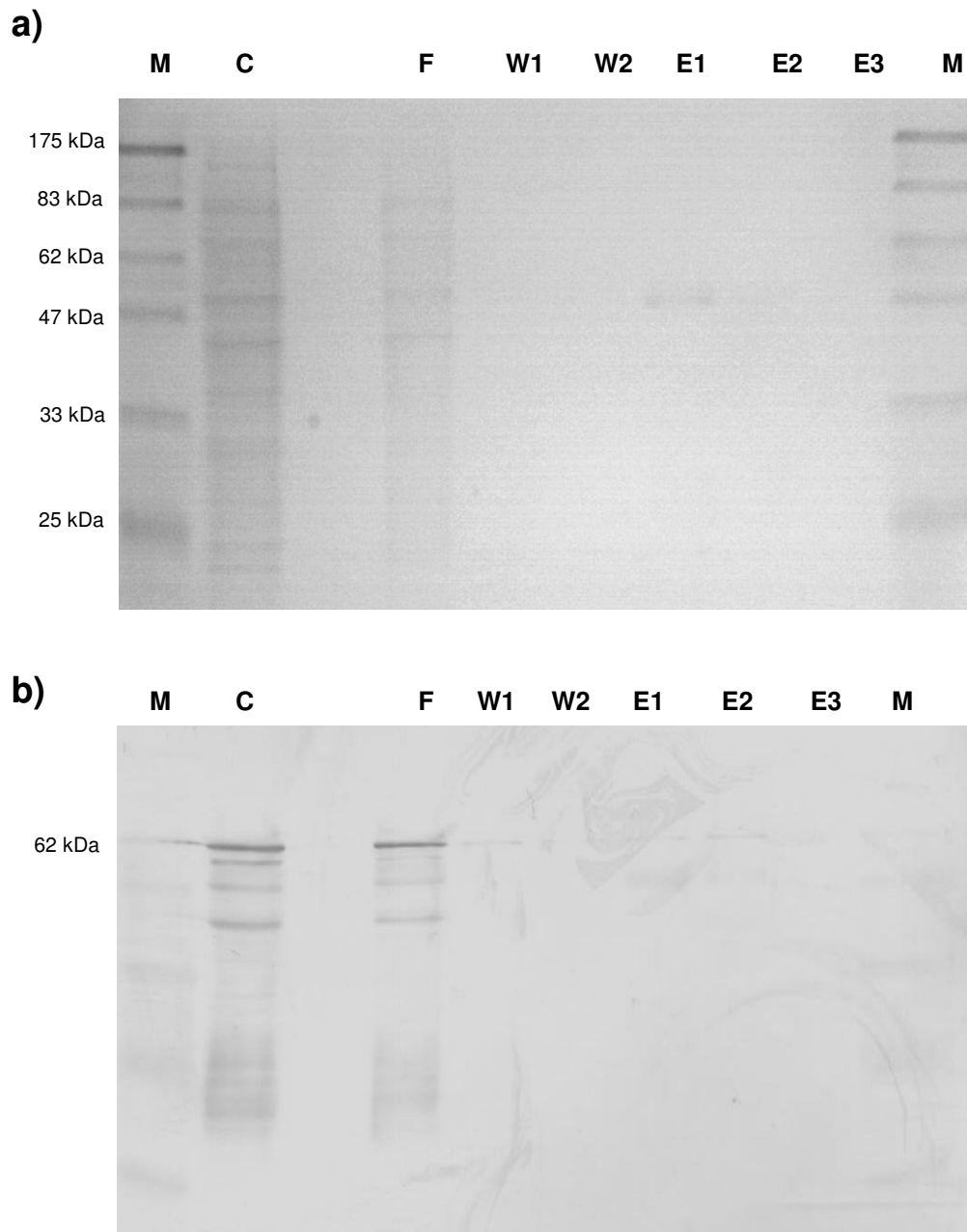


**Figure 3.10. SDS-PAGE (a) and western blot (b) following purification of XplA from 11Y cell free extracts. (M) Protein marker (C) 11Y cell free extracts (F) flow through (W1-W2) Washing steps before elution (E1-E3) elution of target protein using elution buffer (0.1 M Glycine-HCl, pH 2.9).**

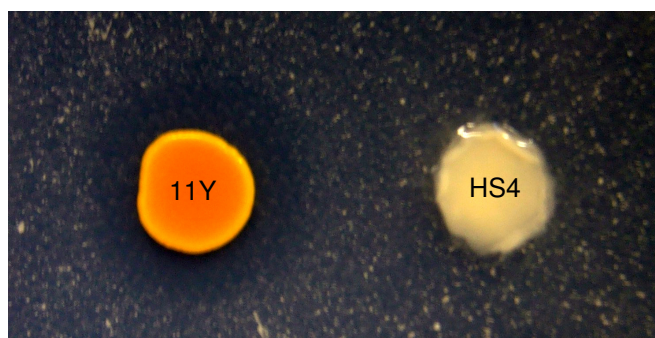
Western blot analysis showed that most of the XplA was present in the flow through.

### 3.3.6 Lost of RDX activity in new batches of strain HS4

Additional experiments were performed to try to improve the cross-linking of the XplA antibody to the column, this used the remaining original cell free extracts of strains 11Y and HS4 and new batches of strains HS4 and 11Y cell free extracts were prepared. It is unfortunate that the new batches of whole cell of HS4 from the original glycerol stock cultures did not show RDX activity despite the incubation time continued until a month (data not shown).

### 3.3.7 Zone of clearance on RDX dispersion agar

Strain HS4 has previously been shown to be able to form a zone of clearance on RDX dispersion agar (Seth-Smith, 2002), and it was this preliminary observation that suggested this strain was able to degrade RDX. This screen was repeated using the latest batch of strain HS4 and no zone of clearance was observed after four weeks of incubation time (Fig. 3.11). This confirmed strain HS4 had lost its activity towards RDX.



Latest RDX dispersion agar



RDX dispersion agar (Seth-Smith, 2002)

**Figure 3.11. RDX dispersion agar for strains 11Y and HS4.** No zone of clearance was observed in the latest RDX dispersion agar for strain HS4.

It was possible that the HS4 cells in the glycerol stock were a mixed population, or one that had somehow lost the ability to degrade RDX. To try to recover a line of strain HS4 that still has the ability to degrade RDX, the glycerol stock of strain HS4 was spread on RDX dispersion plates supplemented with 100  $\mu$ M of ammonium chloride to enhance the growth of the strain. None of the colonies produced a zone of clearance on the RDX dispersion plate after one month of incubation (Fig. 3.12). Incubation time was prolonged to four months and still no zones of clearance were observed.



**Figure 3.12. Growth of strain HS4 from glycerol stock on RDX (5 mM) dispersion agar.** No zone of clearance was observed in the any of the colonies that grew on the RDX dispersion plate supplemented with 100  $\mu$ M of ammonium chloride.

### 3.3.8 PCR amplification of *xplA* and *xplB* homologue

To look for the *xplA/B* genes in strain HS4, colony PCR amplification for *xplA* and *xplB* using different combination of primers was carried out (details for primers, see Chapter 2).

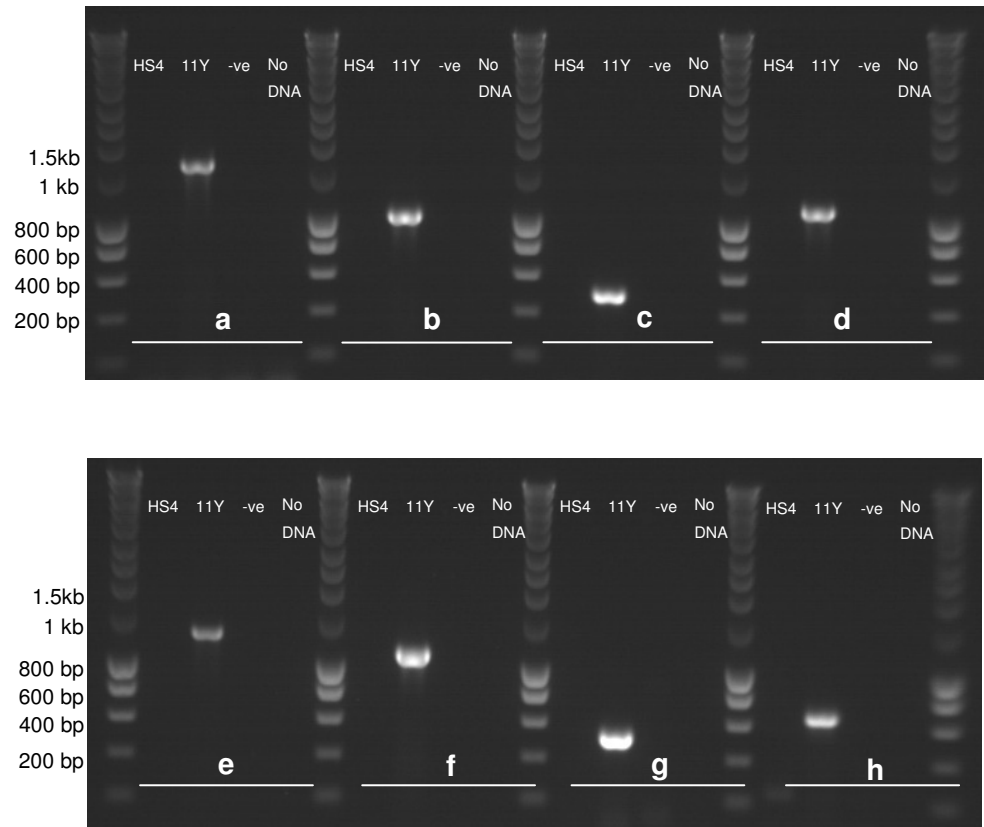


**Figure 3.13. PCR amplification using primers specific to *xplA* and *xplB* genes with different primers combination** (a) *xplA*-HindIIIIF + *xplA*-XbaIR; (b) *xplA*-HindIIIIF + *xplA*-1033R; (c) *xplA*-531F + *xplA*-1033R; (d) *xplA*-531F + *xplA*-XbaIR; (e) *xplB*-KpnF1 + *xplB*-XbaR1290; (f) *xplB*-KpnF1 + *xplB* 1142R; (g) *xplB*-614F + *xplB* 1142R; (h) *xplB*-614F + *xplB*-Xbar 1290.

Colony PCR showed that a product of the expected size using different combinations of primers was amplified in strain 11Y. However, no PCR product was amplified from strain HS4.

### **3.3.9 Sequencing of 16S rRNA gene in latest *Rhodococcus erythropolis* strain HS4**

To confirm whether the bacterium used in these studies is the *Rhodococcus erythropolis* strain HS4 and not a contaminant, 16S rRNA was amplified using universal primers. The sequence showed 99 % sequence identity with the *Rhodococcus* strain HS4 amplified by Dr Seth-Smith (data not shown).

### 3.4 Discussion

*Rhodococcus erythropolis* strain HS4 had previously been shown to be capable of degrading RDX and its activity inhibited was by metyrapone, a P450 inhibitor, suggesting that the enzyme involved in RDX degradation in this strain is a cytochrome P450 (Seth-Smith, 2002). Generally, the mechanism of a cytochrome P450 system involves the transfer of electrons from NAD(P)H to a reductase redox partner and the electron further transferred to the heme catalytic centre of the P450 enzyme to activate the enzyme. Therefore, ferredoxin reductase (a general surrogate partner for P450 enzymes) and cofactor recycling system were included in the assay development to detect RDX degrading activity in cell free extracts.

Incubation of cell free extracts of strain 11Y with ferredoxin reductase and the cofactor recycling system gave the highest RDX degrading activity (56 %). Lower RDX activity (11 %) was observed when cell free extracts were incubated with the cofactor recycling system in the absence of the ferredoxin reductase. Results clearly indicate that the P450 redox partner plays an important role in RDX biodegradation. No activity was shown in cell free extracts when the ferredoxin reductase and cofactor recycling system were absent in the reaction mixture. This shows that XplB might have lost significant activity throughout the cells disruption process. Enzymes are often degradation-sensitive molecules when released from their protected environment. As soon as cells are disrupted, pH fluctuations occur and enzyme-damaging activities such as proteases and free radicals are released. This could explain why whole cells of strain 11Y showed higher RDX activity than cell free extracts and perhaps why the addition of a reductase and cofactor recycling system was a crucial step to amplify the XplA activity in cell free extracts.

While initial experiments showed that whole cells of strain HS4 showed very low RDX degrading activity (30  $\mu$ M RDX degraded after 20 h of incubation), there was no activity observed when cell free extracts of the strain were incubated in various conditions as described in section 3.3.3. Despite the addition of a reductase and an cofactor recycling system, RDX degrading activity in cell free extracts could not be detected. This is perhaps not surprising as rates of RDX removal by whole cells of strain HS4 were low; 11Y showed reduced rates of RDX degrading activity in cell free extracts compared with whole cells and the enzyme(s) responsible for activity in HS4 strain



might have additionally been even more susceptible than 11Y to damage as a result of the cell disruption process.

Given that cell free extracts from the first incubations performed using HS4 had cross-reactivity with the XplA antibody, as shown by western blot analysis (section 3.3.4), affinity purification of the enzyme that is responsible for RDX activity in this strain was performed. Experimental development confirmed that the XplA IgGs were successfully purified from the serum and that most of the contaminants were removed in the washing step, suggesting the column was working well. However, when purification of the 58 kDa HS4 protein, which had cross-reactivity with XplA antibody, was performed, only a single band with a MW of 47 kDa was present in the elution fractions.

Since the XplA antibody in crude rabbit serum was developed using recombinant, purified XplA cloned from strain 11Y, this strain was used to optimise the affinity purification. However, attempts to purify XplA from cell free extracts of strain 11Y revealed that most of the XplA was present in the flow through (Fig. 3.10b). In conclusion, it is likely that the cross-linking of XplA antibody to the column failed. Given that subsequent experiments showed that strain HS4 had lost its activity toward RDX, optimisation of the cross-linking conditions was not further performed.

It was unfortunate that the most recent incubations of *Rhodococcus* strain HS4 from the original glycerol stock made by Dr. Seth-Smith in 2000 did not show activity toward RDX despite the application of a range of approaches. It is worth noting that strain HS4 was isolated about ten years ago and maintained in non-selective LB medium in the glycerol stock. Although unlikely, perhaps long term storage of strain HS4 in the non-selective rich medium and multiple freezing and thawing of the stock culture could have caused this strain to lose its ability to degrade RDX. Naphthalene-degrading bacteria were reported to lose their activity towards naphthalene after being repeatedly transferred to fresh LB medium for several months (Stuart-Keil et al., 1998). An *E. coli* carried plasmid was stabilised under selective conditions and was easily lost when the bacterium was grown under non-selective conditions (Maschke et al., 1992). While bacteria grown without selective pressure can lose degradation activity toward their substrate over generations, both the studies of Stuart-Keil et al., (1998) and Maschke et al., (1992) were performed at temperatures where generation times must have been

orders of magnitude higher. It would be surprising if this was how the RDX degrading activity in strain HS4 was lost.

In summary, the most recent incubations from glycerol stocks of *Rhodococcus* strain HS4 show no degradative activity toward RDX in whole cells, or cell free extract assays, and no band was detected in western blot analysis using cell free extracts from these incubations in the latest HS4 strain. Western blot analysis using cell free extracts of CW25, a non RDX degrader however, revealed a 58 kDa band (data not shown). This indicates that the 58 kDa band that was observed in previous HS4 cell free extracts is probably an artefact. Despite using a range of PCR techniques, no *xplA/B* products were amplified from strain HS4 DNA. Together these results show that this strain had lost RDX degrading ability, possibly encoded on a similar plasmid to that known to contain *xplA/B* in other strains of rhodococci. It was thus decided not to continue investigating this strain.

# Chapter 4

## Heterologous expression of a putative permease from *R. rhodochrous* strain 11Y

### 4.1 Introduction

The flavodoxin-fused cytochrome P450 (XplA) and a reductase partner (XplB) were identified as responsible for RDX degradation in *Rhodococcus rhodochrous* strain 11Y (Seth-Smith et al., 2002). Chromosome walking upstream of the genes *xplA* and *xplB* in the genome of *R. rhodochrous* strain 11Y revealed the presence of an open reading frame encoding a putative permease, which is 100 % identical to a putative transporter in the RDX degrader *Microbacterium* sp. MA1 from North America (Chapter 1). Sequence analysis using membrane protein topology prediction software showed this putative transporter contained twelve predicted transmembrane domains (Fig. 4.1).

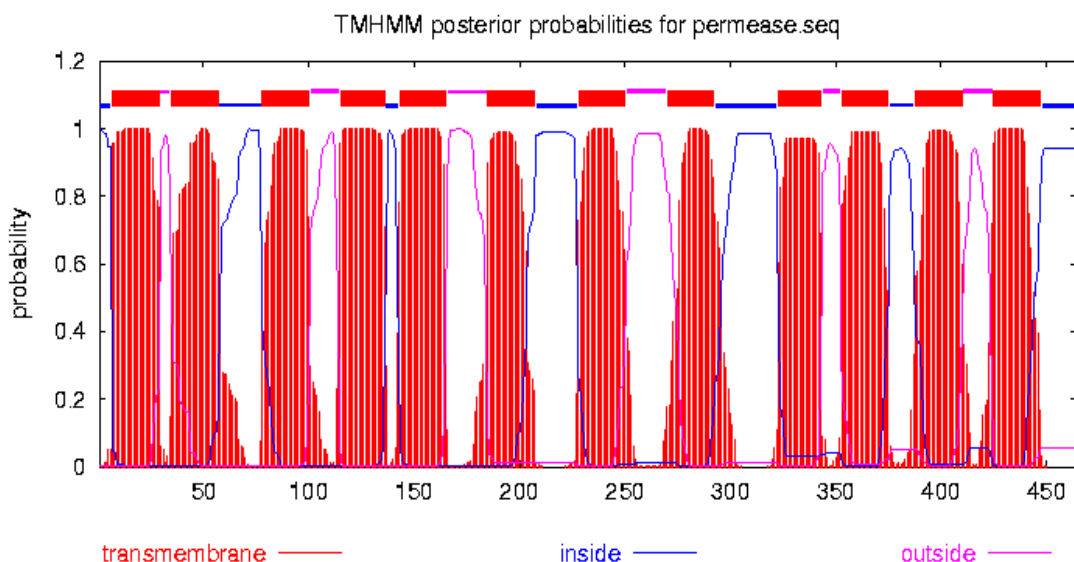


**Figure 4.1. Topology of the putative rhodococcal permease.** Prediction of transmembrane helices in the permease was carried out by using TMHMM algorithm (<http://www.cbs.dtu.dk/services/TMHMM/>).

Heterologous expression and functional characterisation of membrane proteins in *E. coli* have been well documented (Miroux and Walker, 1996, Masi et al., 2003, Drew et al., 2006, Beckham et al., 2010). Zolotarev and co-workers (2008) reported that heterologous expression of a permease in *E. coli* increased uptake of sulphate and confirmed the permease as a sulphate transporter. It is often found that genes located close to each other are likely to have related function in biosynthetic or biodegradation pathways (Williamson et al., 2006, Yu et al., 2007). To investigate the involvement of the putative permease as an RDX transporter in strain 11Y, the rhodococcal putative permease in *E. coli* was expressed heterologously. This chapter describes the heterologous expression and characterisation of the putative permease from *R. rhodochrous* 11Y.

## 4.2 Materials and methods

### 4.2.1 Ligation dependent cloning

The *permease* and *xplA* were cloned individually and together in *E. coli* NovaBlue Singles using the vector pET-YSBLIC3C (kindly donated by the Technology Facility at the University of York).

For plasmid preparation, pET-YSBLIC3C was digested in a total volume of 60  $\mu$ L containing 6  $\mu$ g pET-YSBLIC3C, 0.6  $\mu$ L BSA (10 mg/mL), 5 U of restriction enzymes using either '*Nco*I and *Nde*I' or '*Nhe*I and *Hind*III' and 1x multi-core buffer (Promega). Reactions were incubated at 37  $^{\circ}$ C for 3 h, separated on an agarose gel (1 % w/v) and purified using a QIAquick gel extraction kit (Qiagen). The digested plasmid was dephosphorylated using 5 U of phosphatase per  $\mu$ g of DNA before ligation.

The *xplA* gene was amplified using primers (Chapter 2) adapted with *Nhe*I and *Hind*III restriction sites. Similarly, the permease was amplified using primers (Chapter 2) creating PCR products with *Nco*I and *Nde*I restriction sites. The annealing temperature for all reactions was 63  $^{\circ}$ C with 1.30 minutes extension time at 72  $^{\circ}$ C for 30 cycles. The product sizes of *xplA* (1660 bp) and *permease* (1395 bp) were confirmed by gel electrophoresis. The PCR products were purified using Wizard PCR clean-up kit (Promega) and the DNA concentration was determined using NanoDrop UV-spectrophotometer (Thermo Scientific).

In order to create sticky ends for the ligation, the PCR products were digested by mixing 3  $\mu$ g of PCR products, 1x multi-core buffer (Promega), 0.6  $\mu$ L of BSA (10 mg/mL), 5 U of *Nhe*I and *Hind*III (for *xplA* insert) or 5 U of *Nco*I and *Nde*I (for permease insert) in a total volume of 60  $\mu$ L.

The ligation reaction consisted of 3 molar inserts to 1 molar plasmid, 0.4  $\mu$ L T4 ligase (Promega), 1x ligation buffer in a total volume of 20  $\mu$ L. The reaction was incubated at 16  $^{\circ}$ C overnight. Control of the ligation was the reaction without insert. Competent cells of *E. coli* NovaBlue Singles were transformed with 2  $\mu$ L of the ligation reaction, spread onto LB agar and grown overnight at 37  $^{\circ}$ C. The presence of the permease and *xplA* inserts in pET-YSBLIC3C was confirmed by colony PCR using primers specific to

target genes (Chapter 2). Ligated constructs were transformed into Rosetta 2 (DE3) for gene expression studies.

#### **4.2.2 Ligation independent cloning (LIC)**

The ligation independent cloning technique was employed to clone and express the His-tagged rhodococcal permease (Bonsor et al., 2006).

##### **Plasmid**

The plasmid pET-YSBLIC3C was linearised in 1 mL of restriction enzyme reaction containing 5 µg of the pET-YSBLIC3C, 20 U *Bse*RI and 1x buffer 2 (NEB) and was incubated at 37 °C for 1 h 50 min. The reaction mixture was separated on an agarose gel (1 % w/v) and the linearised plasmid was purified using a QIAquick gel extraction kit (Qiagen).

To produce single stranded T-overhangs on the linearised plasmid, a T4 polymerase reaction was conducted. The reaction consisted of 4.0 pmol of linearised plasmid, 1x T4 polymerase buffer, 20 U of T4 polymerase (Novagen), 2.5 mM dTTP, 5 mM DTT and water to final volume of 400 µL. The reaction was incubated at 22 °C for 30 min then at 75 °C for 20 min. The plasmid was then purified using QIAquick PCR purification kit (Qiagen). The concentration of plasmid determined using NanoDrop UV-spectrophotometer and stored at -20 °C.

##### **Insert**

The insert was generated using primers with LIC specific ends. The PCR reaction contained 1 µL of DNA, 0.4 µM forward primer (Forward: CCAGGGACCAGCA), 0.4 µM reverse primer (reverse: GAGGAGAAGGCGCG), 0.5 µL of dNTPs (25 mM), 1x of HF buffer (Finnzymes, UK), 1 U of Phusion polymerase (Finnzymes, UK) and water to 50 µL. The PCR cycle started with an initial denaturation step of 96 °C for 30 s, followed by an anneal step of 61 °C for 30 s, an extension step of 72 °C 1.5 min for 30 cycles and a final extension step at 72 °C for 10 min. PCR product were cleaned using QIAquick PCR purification kit.

To produce single stranded A-overhangs, the insert reaction was carried out. The reaction contained 0.2 pmol of the insert, 2  $\mu$ L T4 polymerase buffer, 2.5 mM dATP, 1  $\mu$ L dithiothreitol (100 mM), 0.4  $\mu$ L T4 polymerase and water in a total volume of 20  $\mu$ L. The reaction was incubated at 22  $^{\circ}$ C for 30 min and stopped by incubation at 75  $^{\circ}$ C for 20 min.

#### **LIC reaction**

Two  $\mu$ L insert reaction was added to one  $\mu$ L of pET-YSBLIC3C vector (50 ng/ $\mu$ L) and the mixture was incubated for 10 minutes at 22  $^{\circ}$ C. One  $\mu$ L EDTA (25 mM) was added to the reaction mixture for ligation. The reaction was left at room temperature for 10 minutes. Competent cells of *E. coli* NovaBlue Singles were transformed with 2  $\mu$ L of LIC reaction and grown on LB agar contained kanamycin (100  $\mu$ g/mL) to select for clones containing the plasmid with the insert. For expression studies, constructs were transformed into Rosetta 2 (DE3). Details for transformation see Chapter 2.

### **4.2.3 XplA and permease expression**

Cells expressing XplA or the permease, or both XplA and the permease were grown in LB medium supplemented with kanamycin (100  $\mu$ g/mL) and chloramphenicol (34  $\mu$ g/mL). As negative control, Rosetta 2 cells containing the empty vector were grown alongside. After overnight incubation at 37  $^{\circ}$ C with 250 rpm shaking, cells were cooled down to 20  $^{\circ}$ C, induced with IPTG (1 mM). Aminolevulinic acid (1 mM) and FeCl<sub>3</sub> (0.5 mM) were also added. Cells were then incubated at 20  $^{\circ}$ C for 17 hours and harvested and washed twice with 40 mM potassium phosphate buffer (pH 7.2).

### **4.2.4 His-tagged permease expression**

LB medium (50 mL) containing 100  $\mu$ g/mL kanamycin and 34  $\mu$ g/mL chloramphenicol was inoculated with 0.5 mL of an overnight culture. The cultures were grown to an OD<sub>600</sub> of 0.5 at 37  $^{\circ}$ C and IPTG (1 mM) was added. Cultures were left grown for another 3 or 18 h at 25  $^{\circ}$ C and cells were harvested by centrifugation at 14,000 x g (SS34 rotor, High Speed Sorvall RC5B+).

### **4.2.5 Preparation of total protein fraction**

Total protein solubilisation buffer contained 1 % (w/v) SDS, 2M urea, 1.25 % (v/v) 2-mercaptoethanol, 2.5 % (v/v) glycerol and 15 mM Tris (pH 6.8). A 200  $\mu$ L aliquot of

protein solubilisation buffer was added into cell pellet (~10 mg). Samples were incubated at 100 °C for 15 min prior to SDS-PAGE and western blot analysis.

#### **4.2.6 Membrane protein isolation**

Cell pellets were resuspended with buffer containing 50 mM potassium phosphate buffer, 10 % (v/v) glycerol, 10 mM MgSO<sub>4</sub> and 0.1 mg/mL DNase. Sonication was performed using the S-4000 Sonicator (Misonix) operated at an amplitude of 70 % with 3 s and 7 s cooling intervals for a total of 4 min. All steps were performed in an ice-water bath. Unbroken cells and cells debris were removed by centrifugation at 14,000 x g (SS34 rotor, High Speed Sorvall RC5B+) for 20 minutes at 4 °C. The supernatant was then centrifuged at 200,000 x g for 30 min in an ultracentrifuge (TLA100.3 rotor, Beckman Coulter). The pellets containing total membrane proteins were resuspended in 50 mM potassium phosphate buffer. The membrane fractions were snap-frozen in liquid nitrogen and stored at -80 °C.

#### **4.2.7 Permease purification**

This method was adapted from Mulligan (2008).

##### **Solubilisation reaction**

Membrane protein fractions were resuspended in solubilisation buffer consisting of 50 mM potassium phosphate (pH 7.8), 20 % (v/v) glycerol, 200 mM NaCl, 0.5 % (w/v) of n-dodecyl- $\beta$ ,D-maltoside (DDM) and 10 mM imidazole. The solubilisation reaction was incubated on ice for 30 min. Insoluble components were removed by centrifugation at 200,000 x g (TLA100.3 rotor, Beckman Coulter) for 20 min at 4 °C. After centrifugation, the supernatant fraction that contained the soluble membrane proteins was used for permease purification.

##### **Ni<sup>2+</sup> affinity chromatography**

The soluble membrane fraction was incubated in equilibrated Ni<sup>2+</sup>-NTA superflow resin (Qiagen, 0.1 mL/10 mg protein) for 1.5 hours in a disposable polystyrene column (Pierce). Unspecific bound proteins were removed by washing the column with buffer containing 50 mM potassium phosphate (pH 7.8), 20 % (v/v) glycerol, 200 mM NaCl, 0.05 % (w/v) of DDM and 20 mM imidazole. Proteins bound with the resin were eluted with elution buffer that consisted 50 mM potassium phosphate (pH 7.8), 20 % (v/v)



glycerol, 200 mM NaCl, 0.05 % (w/v) of DDM and 500 mM imidazole. Fractions of purification were analysed on SDS-PAGE gel electrophoresis.

#### **4.2.8 RDX uptake assay**

Induced cells were washed twice with potassium phosphate buffer (pH 7.2) and suspended in potassium phosphate buffer (pH 7.2) at a concentration of 0.05 g/mL or 0.25 g/mL. RDX (5  $\mu$ M or 80  $\mu$ M) was added into 500  $\mu$ L of cell suspension and the assays were carried out under continuous stirring using a magnetic stirrer (size of magnetic stir bar is 0.5 cm). Samples were taken at different time points for measurement of the RDX concentration using HPLC.

## 4.3 Results

### 4.3.1 Sequence analysis of the putative permease from *R. rhodochrous* 11Y

Protein sequence of the 11Y putative permease was analysed using the Basic Local Alignment Search Tool (<http://blast.ncbi.nlm.nih.gov/Blast.cgi>). The 11Y permease was found to share 100 % amino acid identity with the *Microbacterium* sp. MA1 permease. The *Mycobacterium vanbaalenii* PYR-1 amino acid permease shared 72 % amino acid identity and other transporters (Table 4.1) shared more than 67 % sequence identity with the 11Y permease. A conserved domain of a transmembrane amino acid transporter protein was also found to be located in the amino acid sequence of 11Y permease.

**Table 4.1. Selected 11Y putative permease homologues with highest sequence identity.**

Accession	Description	Gene (bp)	Protein (aa)	Protein sequence identity (%)
ACO88871.1	permease protein [ <i>Microbacterium</i> sp. MA1]	1395	464	100
YP_952672.1	amino acid permease-associated protein [ <i>Mycobacterium vanbaalenii</i> PYR-1]	1518	505	72
YP_890909.1	amino acid permease [ <i>Mycobacterium smegmatis</i> str. MC2 155]	1497	498	70
ZP_04686854.1	amino acid permease [ <i>Streptomyces ghanaensis</i> ATCC 14672]	1542	513	68
YP_003652340.1	amino acid permease-associated protein [ <i>Thermobispora bispora</i> DSM 43833]	1521	506	68

### 4.3.2 *Permease* and *xplA* expression in strain 11Y

Genes which are under the control of a specific regulation system may exhibit a similar expression pattern when exposed to certain conditions. To investigate whether the expression of the permease has a similar expression pattern to *xplA* in strain 11Y, quantitative real time PCR (qPCR) was performed. This was done in the presence and absence of RDX as it is thought it may have an inducing effect on these genes.

The results of the qPCR analysis showed when cells of strain 11Y were grown in 750  $\mu\text{M}$  of  $\text{NH}_4\text{Cl}$  with or without RDX, both the *xplA* and *permease* were expressed. Interestingly, when RDX was supplied as a sole nitrogen source, transcription of *xplA* and *permease* was 16-fold and 27-fold respectively, higher than when cells were grown in the absence of RDX (Fig. 4.2). The similar expression patterns of the *permease* and *xplA* in strain 11Y under the different conditions tested indicates that both genes are regulated by a similar mechanism.

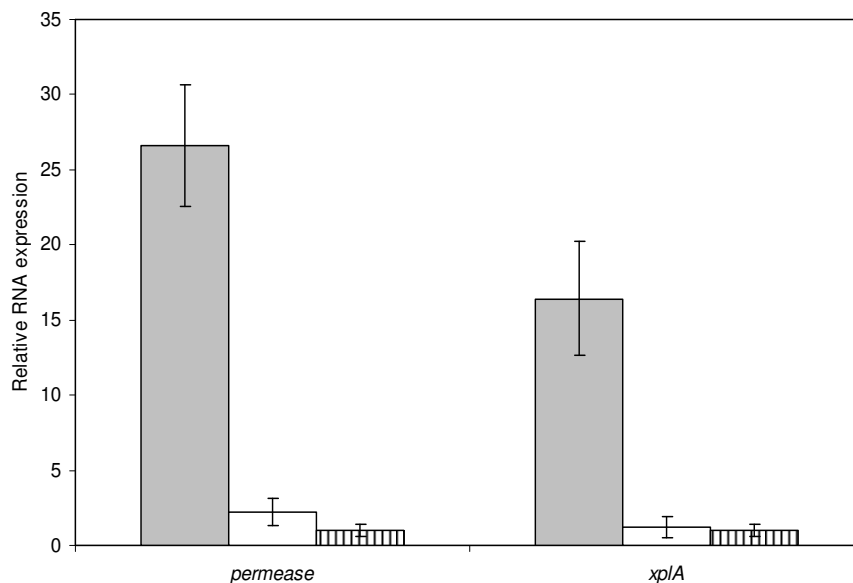


**Figure 4.2. Quantitative real time PCR analysis for *xplA* and *permease* in strain 11Y with *gyrB* as an endogenous control.** The relative RNA expression of *xplA* and *permease* when cells were grown in different nitrogen sources: RDX (grey bar), RDX +  $\text{NH}_4\text{Cl}$  (white bars) and  $\text{NH}_4\text{Cl}$  (vertical bars). The *gyrB* was used to normalise data. Error bars show one standard deviation for triplicate samples.

### 4.3.3 PCR of *permease* homologue

To examine whether the *permease* homologue is only present in the RDX degrading bacteria or if it is also found in related non-RDX degrading bacteria, colony PCR amplification using primers specific to the *permease* was performed. A total of thirteen RDX degrading bacteria that were available in our laboratory were chosen. Two *Rhodococcus* strains CW 25 and *Rhodococcus* strains 717, and *E. coli* (Rosetta 2) were used as examples of three non-RDX degrading bacteria.

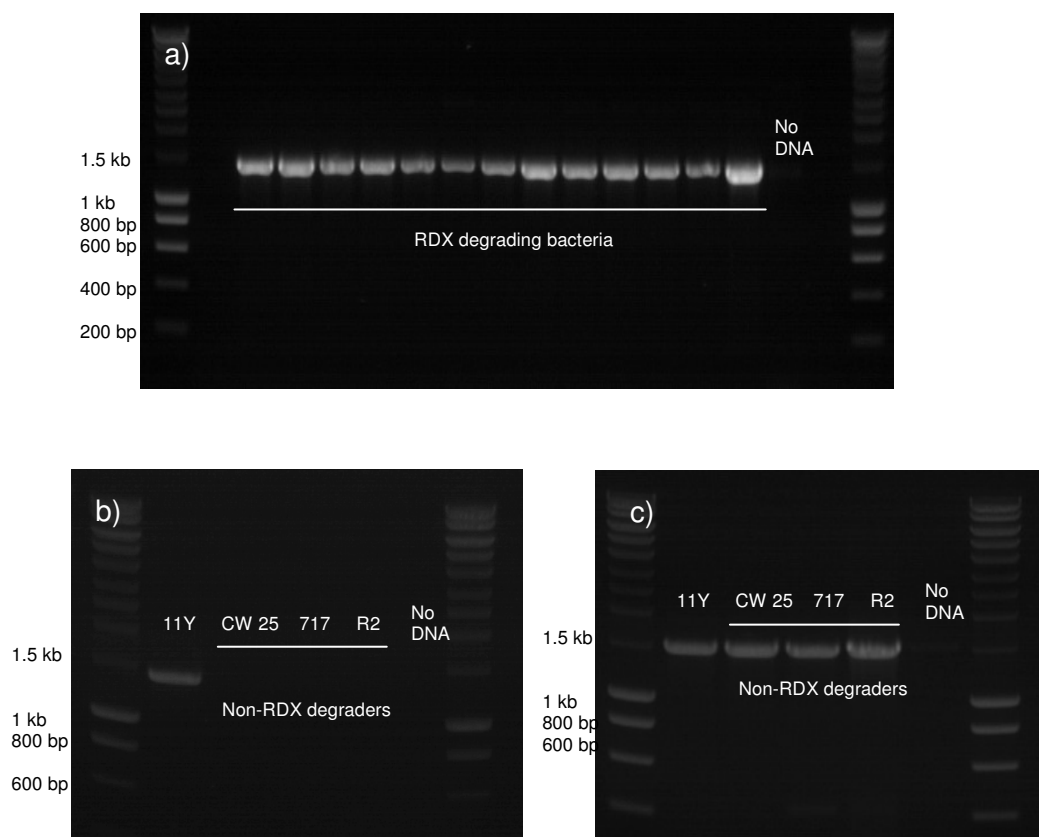


**Figure 4.3. PCR amplification using primers specific to *permease*.** (a) RDX degrading bacteria (*Rhodococcus* NCB 147-159); (b) Non-RDX degrading bacteria (*Rhodococcus* strain CW25, *Rhodococcus* strain 717 and *E. coli* Rosetta 2); (c) PCR amplification of 16S rRNA using universal primers confirmed template DNA from *Rhodococcus* strain CW25, *Rhodococcus* strain 717 and *E. coli* Rosetta 2 were of good quality for PCR amplification.

The PCR analysis showed (Figure 4.3) that all of the thirteen RDX degrading strains of *Rhodococcus* spp. carry the *permease* gene and no PCR product was observed in the non-RDX degraders.

#### 4.3.4 Cloning and expression of permease and XplA

As described in Section 4.3.2, *permease* and *xplA* were significantly upregulated when cells of *R. rhodochrous* 11Y were grown with RDX as the sole source of nitrogen. This upregulation might reflect the involvement of the permease in RDX transport. To test this, the permease was expressed in *E. coli* Rosetta 2 (DE3).

The *permease* and *xplA* were cloned individually and together into pET-YSBLIC3C (Section 4.2.1). The following constructs were obtained:

- pET-YSBLIC3C containing XplA only (pET-A)
- pET-YSBLIC3C containing the permease only (pET-P)
- pET-YSBLIC3C containing XplA and the permease (pET-AP)

The constructs were transformed into Rosetta 2 (DE3) and the following clones were obtained: XplA expressing (pET-A), permease expressing (pET-P) and XplA co-expressed with permease (pET-AP). The insert size of these clones was checked by PCR analysis using primer specific to *xplA* and *permease*.

##### 4.3.4.1 Resting cell assays

To investigate whether the presence of the permease enhanced RDX activity, resting cell assays were carried out. XplA expressing (pET-A), permease expressing (pET-P), XplA co-expressed with permease (pET-AP) and empty vector clones were incubated in minimal medium containing 80  $\mu$ M RDX as a sole nitrogen source for 3 hours. Samples were taken at different time points for RDX and nitrite analysis.

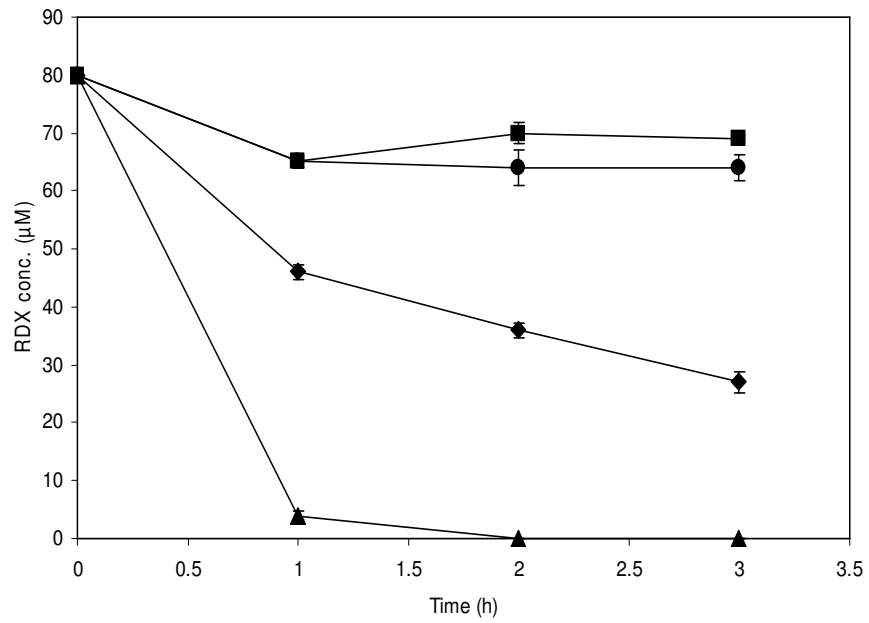


**Figure 4.4. Resting cells incubation (HPLC analysis).** XplA expressing clone (triangles), XplA co-expressed with permease clone (diamonds), permease expressing clone (squares) and Rosetta 2 with empty vector (circles). Error bars show one standard deviation for triplicate samples.

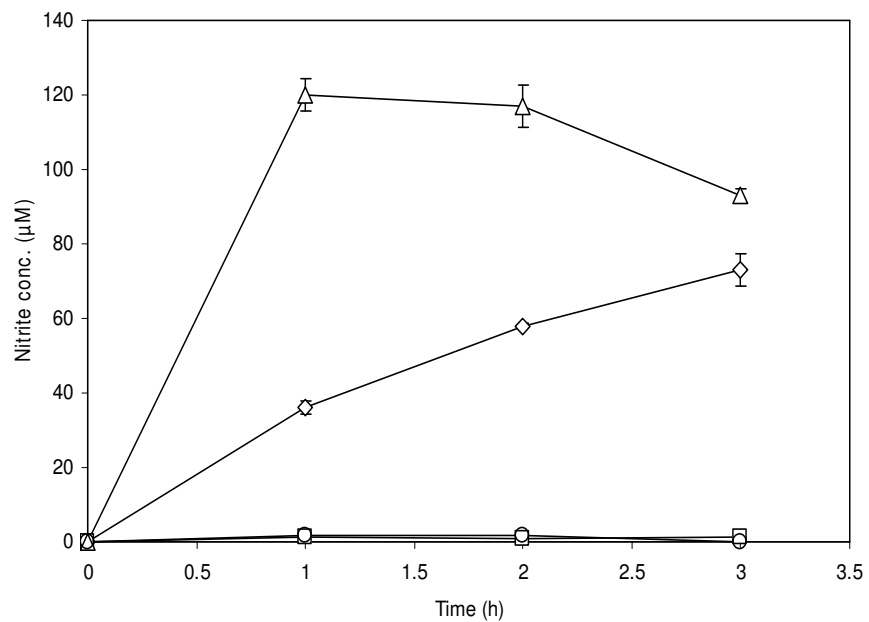


**Figure 4.5. Resting cells incubation (Griess assay).** XplA expressing clone (triangles), XplA co-expressed with permease clone (diamonds), permease expressing clone (squares) and Rosetta 2 with empty vector (circles). Error bars show one standard deviation for triplicate samples.

HPLC analysis (Fig. 4.4) revealed that after 1 hour of incubation, approximately 95 % (76  $\mu$ M) of RDX was degraded by the XplA expressing (pET-A) clone and 120  $\mu$ M of nitrite (degradation product) detected (Fig. 4.5). Complete RDX degradation by this clone was observed after 2 hours of incubation (Fig. 4.4). For XplA co-expressed with permease (pET-AP) clone, 42 % (34  $\mu$ M) of the RDX was degraded, with 36  $\mu$ M of nitrite production after 1 hour of incubation and approximately 66 % (53  $\mu$ M) of RDX after 3 hours.

For the permease expressing (pET-P) clone and the negative control, although a small (approx. 10  $\mu$ M) decrease in RDX was seen in the first hour of incubation, no further decrease in the level of RDX was seen throughout the remaining incubation time.

#### **4.3.4.2 XplA activity in cell free extracts**

XplA activity in cell free extracts of XplA expressing (pET-A) and XplA co-expressed with permease (pET-AP) clones was measured described in Chapter 3 (3.2.1). Cell free extracts (0.01 g/ mL) were incubated in minimal medium with 100  $\mu$ M of RDX. After 90 min of incubation, 95 % of the RDX had been removed from the medium when using the cell free extracts obtained from XplA expressing (pET-A) clone, whereas just 50 % of the RDX was removed when using the extracts from XplA co-expressed with permease (pET-AP) clone (Fig. 4.6). Additionally, the SDS-PAGE analysis also revealed a more abundant band for XplA in cell free extract from the pET-A clone than pET-AP clone, where similar amounts of total protein were analysed (data not shown).

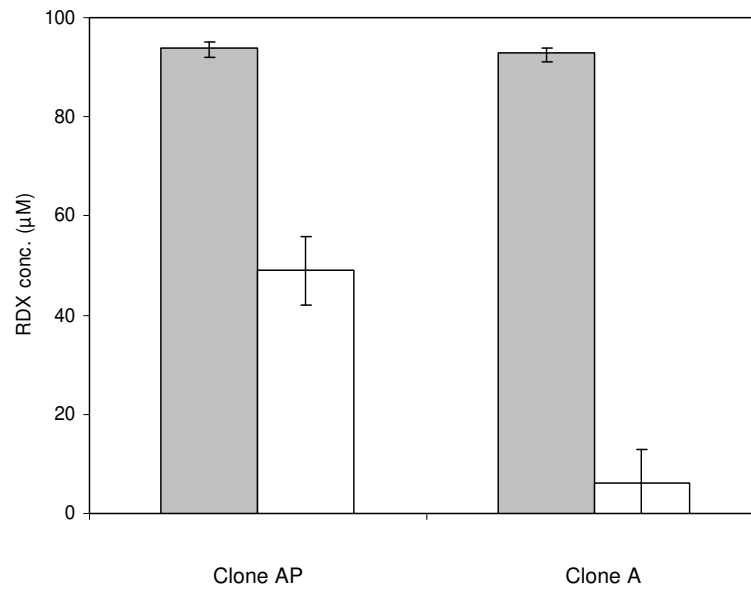


**Figure 4.6. RDX removal using cell free extracts of XpIA co-expressed with the permease (clone AP) compared to the XpIA expressing control (clone A).** Grey and white bars represent RDX concentration at 0 and 90 min of incubation, respectively. Error bars show one standard deviation for triplicate samples.



#### 4.3.4.3 RDX uptake assays

To compare the RDX uptake in cells of the permease expressing (pET-P) clone and Rosetta 2 (empty vector), induced cells (0.25 g/ mL) were incubated in potassium phosphate buffer (pH 7.4) with 80  $\mu$ M of RDX. Samples were centrifuged at 14,000 x g for 5 min and supernatants directly used for HPLC analysis.

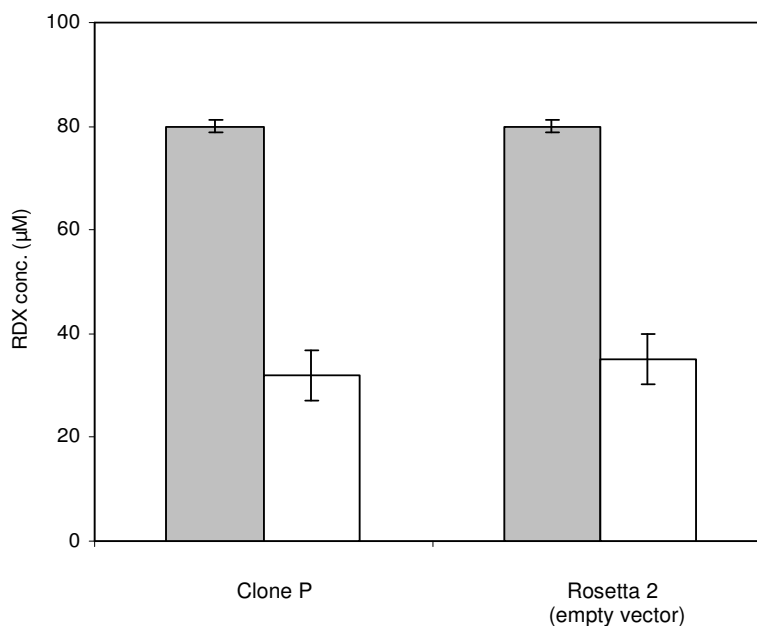


**Figure 4.7. RDX uptake in cells of the permease expressing clone (clone P) and Rosetta 2 (empty vector).** Grey and white bars represent RDX concentration at 0 and 30 min of incubation, respectively. Error bars show one standard deviation for triplicate samples.

Cells of *E. coli* expressing the permease showed the same RDX uptake compared to the negative control (Rosetta 2 with empty vector) after 30 min of incubation (Fig. 4.7). Recombinant cells of *E. coli* did not remove more RDX than the control and SDS-PAGE analysis did not reveal any significant expression of the permease (data not shown). Since no antibody against this permease was available, the expression of permease in permease expressing (pET-P) clone could not be monitored. Thus, no further analysis with this construct was performed.

In order to monitor expression of the permease and study the uptake of RDX, the permease from strain 11Y was cloned into the N-terminal His-Tag expressing vector,

pET-YSBLIC3C and the permease sequence verified. The permease expressing clone was designated as Rosetta 2 pLICP2.

#### 4.3.4.4 Growth of induced and uninduced Rosetta 2 pLICP2

It was reported that the expression of membrane proteins slows down the growth of host cells after induction (Miroux and Walker, 1996). To study the effect of induction on the growth of Rosetta 2 pLICP2, growth of induced and uninduced cells was compared. Rosetta 2 pLICP2 was grown in LB until  $OD_{600}$  approximately 0.5 and induction was performed. Another batch of cells was left to continue to grow without addition of IPTG.

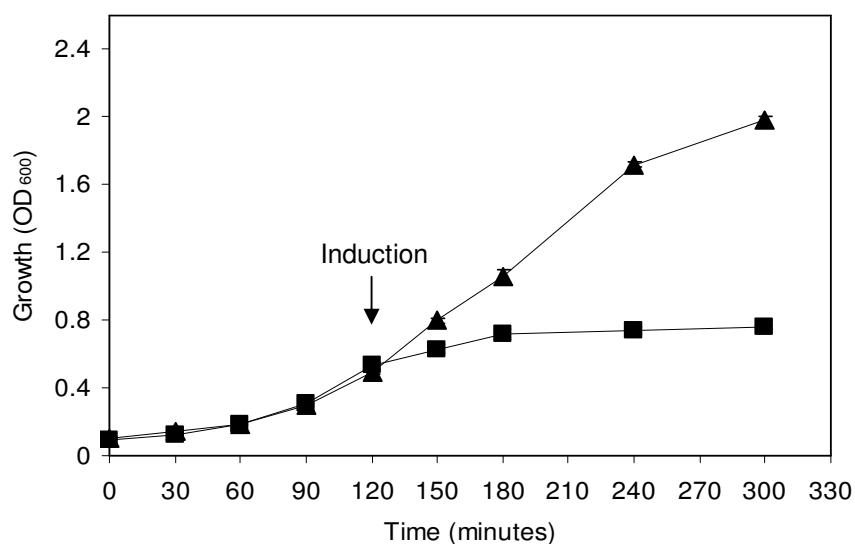


**Figure 4.8. Effect of IPTG induction on growth of Rosetta 2 pLICP2.** Uninduced cells (triangles) and induced cells (squares). Error bars show one standard deviation for triplicate samples.

In Figure 4.8, it was clearly seen that the induced cells grew far slower than the uninduced cells.

#### 4.3.4.5 Permease detection in the total protein fraction

To detect the permease in the total protein fraction of Rosetta 2 containing pLICP2, western blot analysis was conducted. In the first expression trial, cells were harvested after 3 hours of IPTG induction. This time point was based on previously studies that found membrane proteins accumulated at high levels when cells were harvested at this time point (Miroux and Walker, 1996, Mulligan et al., 2009). However, no immunoreactive protein was detected in the total protein fraction of Rosetta 2 pLICP2 (Fig. 4.9a-b) using anti-His antibodies. In the second expression trial, the incubation time was prolonged to 18 hours after the induction. The same result was observed; no band representing the permease was shown on the western blot (Fig. 4.9c).

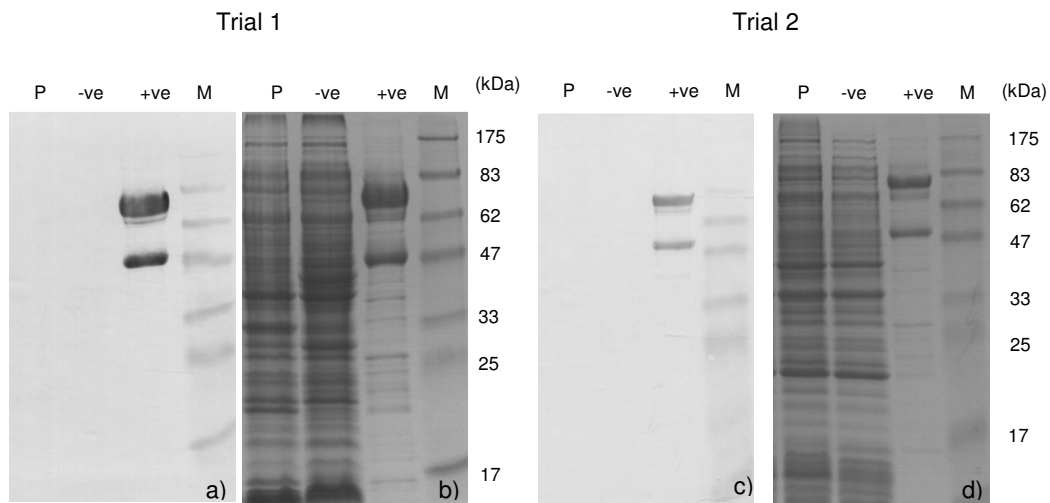


**Figure 4.9. SDS-PAGE and western blots of total proteins of Rosetta 2 pLICP2.** Rosetta 2 pLICP2 was incubated at 37 °C and grown until OD<sub>600</sub> 0.5. The cultures were then induced by IPTG (1 mM) followed by incubation at 25 °C for 3 h (Trial 1) or 18 h (Trial 2). After cells were harvested, protein solubilisation buffer was added to the pellets to obtain the total soluble protein fraction. Samples were heated at 100 °C for 15 min prior to running onto the SDS-PAGE gels. (a) Western blot analysis (Trial 1), (b) 12 % SDS-PAGE (Trial 1), (c) Western blot analysis (Trial 2), (d) 12 % SDS-PAGE (Trial 2), (M) Protein marker, (P) Total protein of Rosetta 2 pLICP2, (-ve) Rosetta 2 with empty vector, (+ve) positive control (partial purified His-Tagged Not 10 obtained from Marie Delenne).

Thus to improve the limits of detection, it was decided to concentrate the permease by isolating the membrane protein fraction.

#### 4.3.4.6 Permease detection in the membrane protein fraction

The membrane proteins were firstly isolated from the Rosetta 2 pLICP2, which were grown at 25 °C degree for 3 hours after induction. Once the membrane proteins of Rosetta 2 pLICP2 were obtained, this fraction was run on SDS-PAGE gel followed by western blotting. No heating was applied to the samples before loading on the SDS-PAGE gels as membrane proteins in the SDS loading buffer tend to form aggregates during the 100 °C heating process (personal communication, Christopher Mulligan).

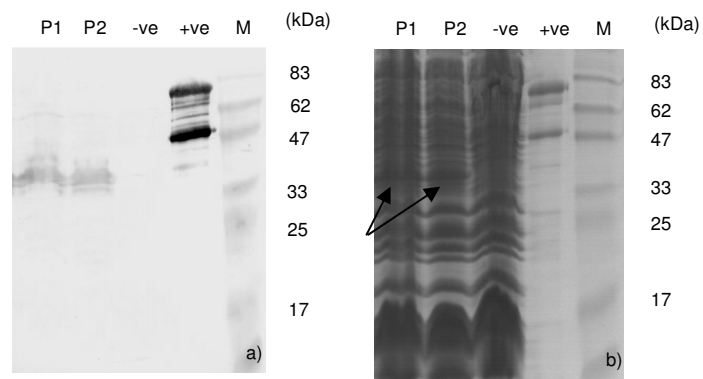


**Figure 4.10. Detection of His-tagged permease.** (a) Western blot analysis, (b) 12 % SDS-PAGE, (M) Protein marker, (P1 and P2) Membrane proteins fraction of two batches of Rosetta 2 pLICP2, (-ve) Rosetta 2 with empty vector, (+ve) positive control (partial purified His-Tag Not 10).

A band of approximately 40 kDa of immunoreactive species was present in the membrane fraction of both of the tested batches of Rosetta 2 pLICP2 (Fig. 4.10a), representing the molecular weight of the permease. The expressed permease was also seen on an SDS-PAGE gel (arrows). This immunoreactive species was not detected in membrane fraction of Rosetta 2 with empty vector (negative control). This indicates that the permease was successfully expressed in the membrane protein fraction. The molecular weight is slightly smaller than the predicted molecular weight (49 kDa); however, it is a common phenomenon that membrane proteins migrate faster in SDS-PAGE gels (Mulligan, 2008).

#### 4.3.4.7 Effect of temperature on the expression of the permease

To assess the effect of temperature on the expression of the permease, Rosetta 2 pLICP2 was incubated at 25 °C and 37 °C for 3 hours after the addition of IPTG.

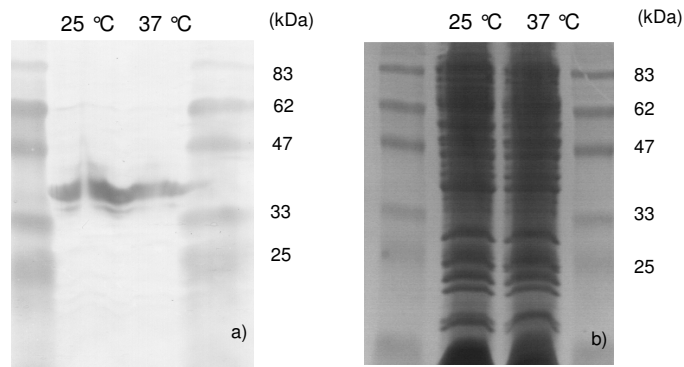


**Figure 4.11. Permease expression at different induction temperature.** (a) Western blot analysis, (b) 12 % SDS-PAGE. Cultures were grown in LB until  $OD_{600} \sim 0.5$  and induced with IPTG. Cultures were incubated at 25 °C and 37 °C over a period of 3 h after the induction.

The western blot analysis revealed that both batches of cells that were induced at different temperature (25 °C or 37 °C) produced a positive signal after incubating with His-tag antibody conjugated with peroxidase. This suggested the permease was expressed at both temperatures. However, expression was slightly higher at 25 °C (Fig. 4.11a). Thus, the expression of the permease was performed at this temperature.

#### 4.3.4.8 Effect of IPTG concentration on permease expression

To investigate the effect of varying IPTG concentrations on the expression of the permease, Rosetta 2 pLICP2 was grown at 25 °C for 3 hours and induced at OD<sub>600</sub> 0.5 with different IPTG concentration of 0, 0.1, 0.25, 0.5, 0.75 and 1 mM.

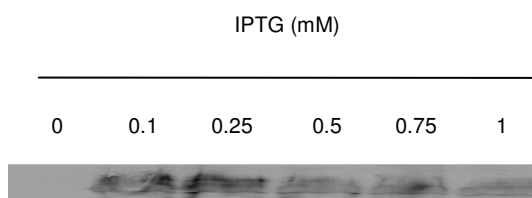


**Figure 4.12. Effect of IPTG concentration in permease expression.** Western blot with anti His-tag antibody of the induced Rosetta 2 pLICP2 in various concentration of IPTG (0-1 mM). Cells were harvested after 3 h of IPTG induction.

A positive signal with a molecular mass of approximately 40 kDa was detected in all Rosetta 2 cells induced with IPTG by western blot analysis. When cells were induced with 0.25 mM of IPTG the strongest signal was obtained (Fig. 4.12). Similar amounts of permease were detected when cells were induced with 0.5, 0.75 or 1 mM of IPTG. The optimal concentration of 0.25 mM was used to induce Rosetta 2 pLICP2 in consecutive experiments.

#### 4.3.4.9 Purification of permease and peptide mass fingerprinting

To identify if the protein species with a molecular mass of ~40 kDa on the SDS-PAGE gel was the rhodococcal permease, it was purified and peptide mass fingerprint was performed.

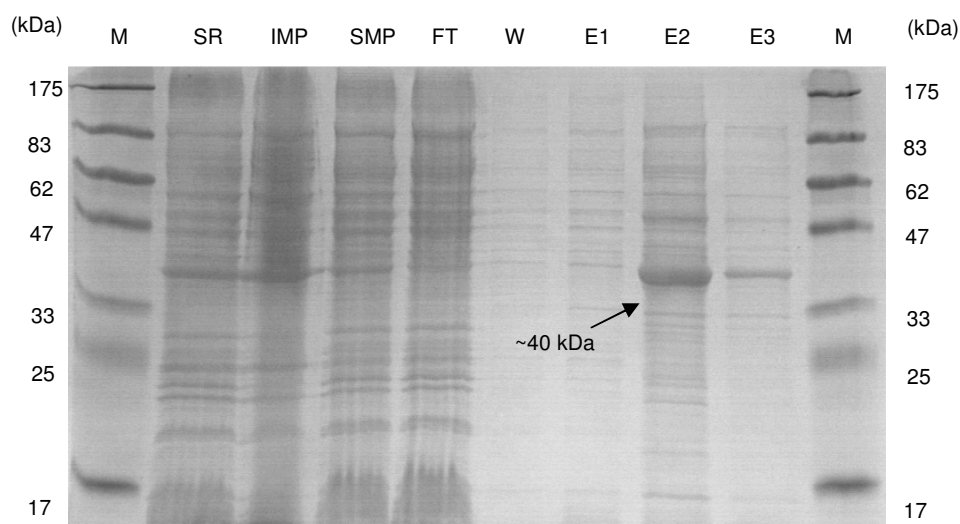


**Figure 4.13. Purification of permease using Nickel column.** Rosetta 2 pLICP2 were grown under the optimum conditions. The membrane proteins were harvested and were solubilised using 0.5 % of n-dodecyl- $\beta$ ,D-maltoside (Lemuh et al., 2009). The soluble membrane proteins were incubated with resin (nickel column) for 1.5 hours. Elution was carried out after a single washing step. The eluates were analysed using SDS-PAGE gel. (M) Protein marker, (SR) solubilisation reaction, (IMP) insoluble membrane proteins, (SMP) soluble membrane proteins, (FT) flow through, (W) washing step, (E1-E3) elutions of permease.

The permease was successfully purified using the nickel resins. Figure 4.13 shows a strong band in the eluted sample (E2) with a molecular weight of ~40 kDa. This band was cut from the gel and sent for peptide mass fingerprint analysis (performed by Technology Facility at the University of York), which confirmed that this band contained protein matched to the strain 11Y permease, thus confirming the immunoreactive species observed in the western blot analysis was the permease.

#### 4.3.4.10 Whole cell RDX uptake assays

To functionally characterise the rhodococcal permease, RDX uptake assays were carried out using whole cells of Rosetta 2 pLICP2 (method adapted from Mulligan, 2008).

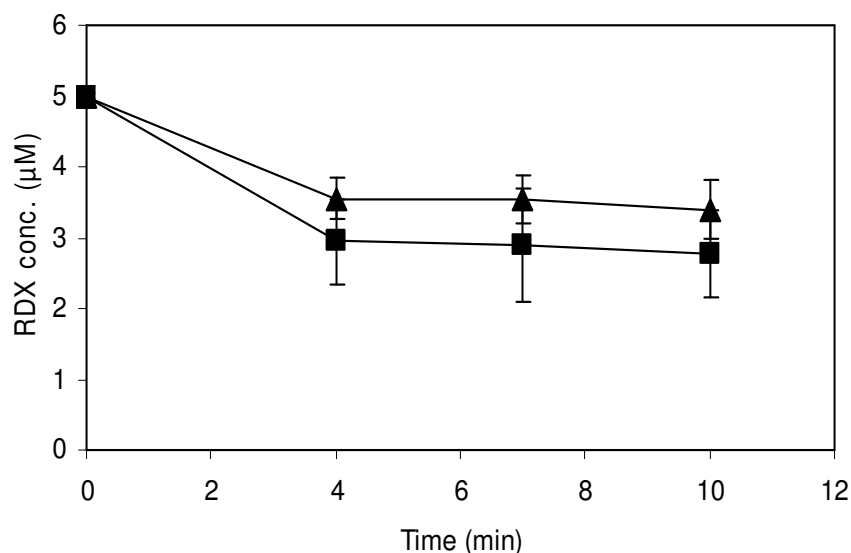


**Figure 4.14. Uptake of RDX by induced and uninduced Rosetta 2 pLICP2.** The induced and uninduced cells (final concentration: 0.05 g/mL) were suspended in potassium phosphate buffer. RDX was added and samples were taken at 0, 4, 7 and 10 minutes with continuous stirring. Samples were centrifuged and supernatants were taken for RDX measurement by HPLC. Induced cells (squares), Uninduced cells (triangles).

Six uptake assays from three batches of cells were carried out individually. Whilst on average the induced cells gave a slightly higher rate of RDX uptake, this difference was not significant (Fig. 4.14). Additionally, uptake assays at higher RDX concentration (90 µM) also showed no difference in the RDX uptake rates between the induced and uninduced cells (data not shown). This indicates that the presence of permease in Rosetta 2 pLICP2 did not significantly enhance the RDX uptake.



## 4.4 Discussion

The transcription of the putative *permease* and *xplA* in strain 11Y were upregulated significantly when RDX was used as the sole nitrogen source compared to when cells were grown in the absence of RDX. Interestingly, when ammonium chloride was supplied together with RDX, both genes were downregulated compared to when RDX was the only nitrogen supply. The similar trend of expression in both *permease* and *xplA* suggests that both of these genes are under the same regulation and the putative transporter could be involved in RDX transport.

The architecture of cell walls in Gram-positive and Gram-negative bacteria is different. Gram-positive bacteria possess a cell membrane which is bordered by a thick peptidoglycan layer. Cell walls of Gram-negative bacteria comprise of an inner cell membrane, followed by a thin peptidoglycan layer and an additional outer membrane. Due to these differences, expressing a Gram-positive transporter in *E. coli* could be challenging. However, reports in the literature describe that transporters from Gram-positive bacteria including a rhodococcal transporter were successfully expressed and functionally characterised in *E. coli* (Degen et al., 1999, Komeda et al., 1997, Zolotarev et al., 2008). Therefore, the 11Y permease was expressed in *E. coli* for characterisation.

Assuming that the 11Y permease is a RDX transporter, it was expected that XplA co-expressed with the permease, would increase RDX degradation compared to when XplA was expressed alone. To investigate this, both *permease* and *xplA* were cloned individually and together into a vector to produce three clones: *E. coli* expressing XplA, *E. coli* expressing the permease and *E. coli* co-expressing both XplA and the permease. Cell free extract assays showed that the clones expressing XplA produce higher levels of XplA compared to clones expressing both proteins. This is perhaps not surprising as the total amount of recombinant protein expressed is often reduced by the number of expressed genes (Johnston et al., 2000, French et al., 1995). The different levels of XplA activity in XplA expressing and XplA co-expressed with permease cells when expressed under the same condition, coupled with the lack of a permease antibody meant that these studies were inconclusive in determining involvement of the permease in RDX degradation.

The co-expression strategy in this study used two genes on a single vector under the control of a single promoter. There are alternative co-expression compatible vectors that could have been used such as pETDuet-1 (Novagen) and pRSFDuet-1 (Novagen). However, these alternative vectors have the same limitation in that the amount of protein produced will generally be reduced when two genes are expressed in the *E. coli* host compared to when one gene is expressed.

Following use of pET-YSBLIC3C as the expression system for the permease and xplA, both resting cell and cell free extract assays confirmed that the XplA was successfully expressed when co-expressed with the permease. Since the permease was cloned upstream of the actively expressed XplA, it is likely that the *permease* was transcribed. However, without a permease-specific antibody, it was not possible to determine whether this rhodococcal permease was successfully integrated as a membrane protein in *E. coli*. Therefore, a His-tagged permease construct was produced to monitor the expression of this membrane protein.

As described in section 4.3.4.4, the growth of the permease expressing clone was slowed down after IPTG induction (Fig. 4.8). This phenomenon is commonly observed in bacteria recombinantly expressing membrane proteins under the control of the T7 promoter (Miroux and Walker, 1996, Mulligan, 2008). The bacteriophage T7 RNA polymerase is approximately seven times more efficient than the *E. coli* RNA polymerase. This high activity of T7 RNA polymerase can result in uncoupling of transcription and translation (Miroux and Walker, 1996), whereby more mRNAs are produced, but fewer proteins are translated. The effect of uncoupling of transcription and translation causes cells grows slowly after the IPTG induction.

The *E. coli* strains C41 (DE3) and C43 (DE3), which are derived from the commercial strain BL21 (DE3) have better growth rate than BL21 (DE3) after IPTG induction during membrane protein expression (Miroux and Walker, 1996). The expression of membrane proteins in C41 (DE3) and C43 (DE3) was found to be higher than in the parent strain BL21 (DE3). Therefore, these strains have been widely used to express membrane proteins by various research groups (Masi et al., 2003, Mohanty and Wiener, 2004, Mokhonov et al., 2005, Quick and Wright, 2002, Lucet et al., 1999, Mulligan, 2008).

Since BL 21(DE3) does not have additional copies of specific tRNA genes that are rare in *E.coli*, both C41 (DE3) and C43 (DE3) derived from BL 21 (DE3) are unlikely to supply tRNAs for rare codons. There are rare codons present in *xplA* and *permease*, it was thus decided not to use C41 (DE3) and C43 (DE3) as hosts for expression in the expression studies. Instead, Rosetta 2 (DE3) was employed to express *permease* and *xplA* as this strain supply tRNAs rare codons. Successful *permease* and *XplA* expression were achieved as reported in result sections of this chapter.

Initial trials of His-tagged *permease* expression failed to detect the putative transporter in the total proteins by western blot, as shown in Figure 4.9. By isolating the membrane protein fraction, a band with the molecular mass of approximately 40 kDa was detected. Variation of the IPTG concentration resulted in altered *permease* expression levels in this study (section 4.3.4.8). The maximum yield was achieved when 0.25 mM IPTG was used for induction.

Expression could be further increased by inducing the Rosetta 2 pLICP2 at 25 °C compared to 37 °C as shown by the western blot analysis (section 4.3.4.7). Different optimal temperatures for the expression of membrane proteins have been reported (Lucet et al., 1999, Quick and Wright, 2002, Drew et al., 2006, Mokhonov et al., 2005, Mulligan, 2008, Eriksson et al., 2009). In general, the optimum temperature for membrane protein expression ranges between 20 °C and 25 °C, it has been suggested that this temperature range is the preferred temperature for optimum membrane proteins expression (Eriksson et al., 2009). Examples of membrane proteins that were successfully expressed at this range of temperature were a membrane glycosyltransferase (Eriksson et al., 2009), the integral membrane protein SpoIIIE (Lucet et al., 1999), a TRAP transporter YiaN (Mulligan, 2008) and a putative amino acid transporter YbaT (Drew et al., 2006). However, another study reports that a formate-nitrite transporter TpNirC was expressed optimally at 37 °C (Beckham et al., 2010).

Whole cell RDX uptake assays (section 4.3.4.10) demonstrated that the *permease* expressing clone (Rosetta 2 pLICP2) did not show higher RDX uptake over the incubation time compared to the control. It would be interesting to purify the *permease* in high yield and reconstitute this transporter into liposomes. In vitro RDX uptake assays could be performed using the constructed proteoliposomes. However, as radio

labelled RDX, required for this method, was not available in the UK, the proteoliposome approach was not attempted.

Alternately, it was decided to delete the permease in strain 11Y by using an unmarked gene deletion system (van der Geize et al., 2001). The next chapter reports the construction and characterisation of a permease knockout strain derived from strain 11Y.

# Chapter 5

## Construction and characterisation of rhodococcal knockout strains

### 5.1 Introduction

Two distinct, plasmid encoded, gene clusters flanking *xplA* were isolated as described in Section 1.10 (Ander et al., 2009, Indest et al., 2010). One characterised gene cluster, from *Gordonia* sp. strain KTR9, contains four open reading frames (Figure 1.11) (Indest et al., 2010). The second gene cluster is from *Rhodococcus rhodochrous* strain 11Y (Fig. 5.1), which is highly conserved amongst the RDX degrading bacteria including the *Microbacterium* sp. MA1 (North America), *Rhodococcus* DN22 (Australia), *Rhodococcus* spp. (Belgium and UK), and has not been characterised yet. Because this gene cluster is highly conserved amongst strains from geographically distinct regions, it was considered that further characterisation of these genes with respect to RDX metabolism was warranted.

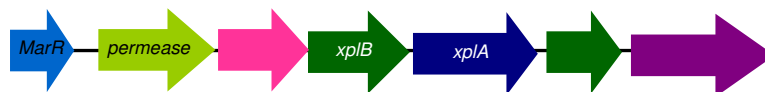
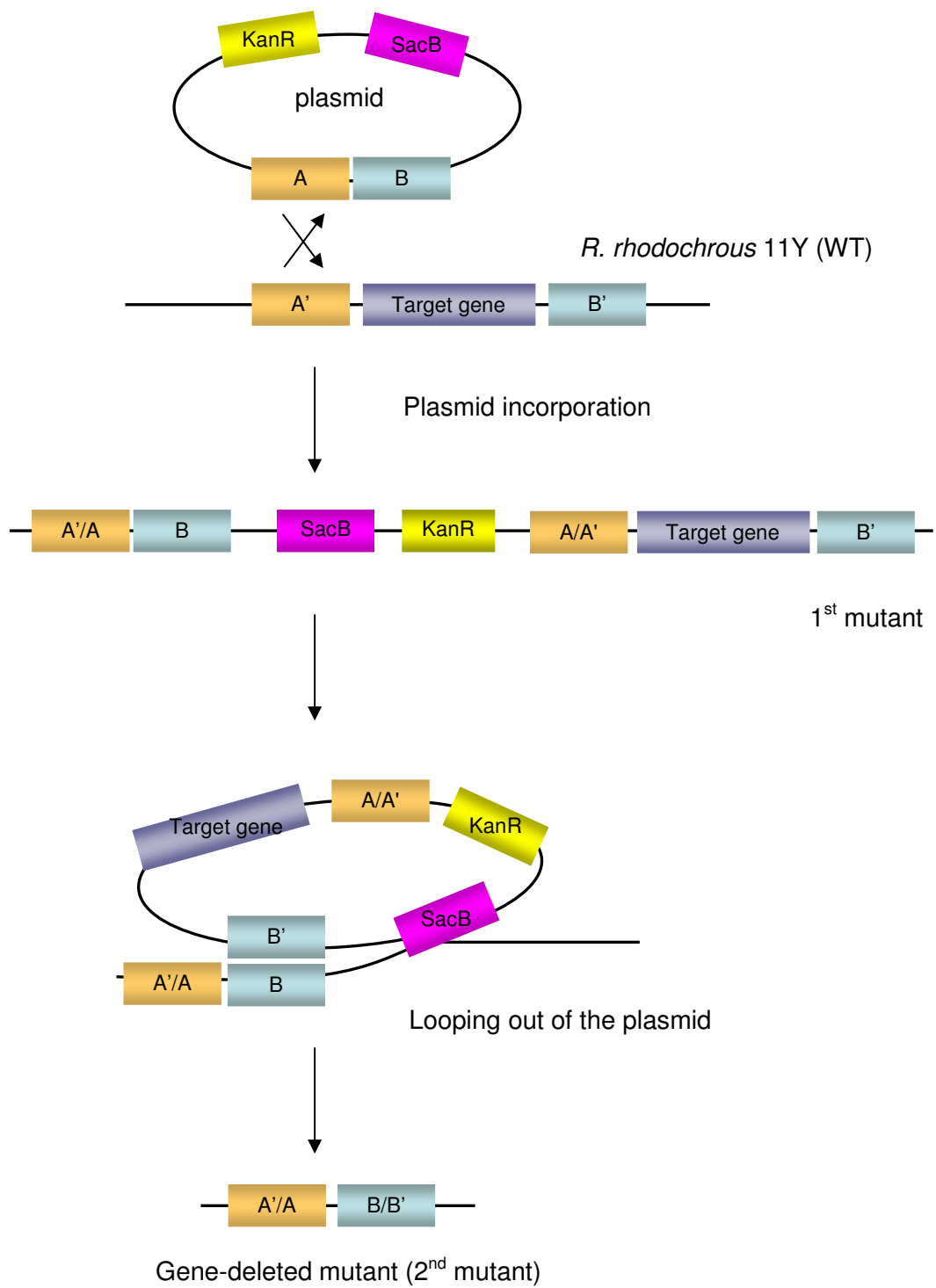


Figure 5.1. Organisation of the RDX degradation gene cluster in *R. rhodochrous* 11Y.

To characterise the *xplA* gene cluster in strain 11Y, an unmarked gene deletion system was employed to generate four knockout strains: MarR, permease, *xplB* and *xplA* knockouts (van der Geize et al., 2001). This method involves the use of a mutagenic plasmid (pK18mobsacB) and a donor strain *E. coli* S17-1. The pK18mobsacB was previously derived from a small plasmid pK18 isolated from *E. coli*, with modifications to have a broad-host-range transfer machinery of plasmid RP4 (oriT), multiple cloning

site, kanamycin resistance and sucrose sensitive *sacB* genes (Schäfer et al., 1994). The presence of RP4 allows the plasmid to be transferred into a wide range of Gram-positive and Gram-negative bacteria via conjugation. This feature is crucial as DNA manipulation in Gram-positive bacteria is often hindered by the lack of highly efficient transfer systems. This mutagenic plasmid has previously been successfully used to construct a marker-free gene deletion in variety of strains (van der Geize et al., 2001, Yang et al., 2007, Rosloniec et al., 2009, Okamoto et al., 2010). In short, the mutagenic plasmid is firstly transferred from the donor strain (*E. coli* S17-1) into the recipient strain (strain 11Y wild-type). The first homologous recombination occurs resulting in incorporation of the mutagenic plasmid into the genome of strain 11Y, producing a kanamycin resistant and sucrose sensitive strain (1<sup>st</sup> mutant). At this stage, the gene to be deleted (the target gene) is still present in the genome. Following a second cross-over event, the mutagenic plasmid, together with the target gene, is removed creating a gene deleted mutant (2<sup>nd</sup> mutant) (Figure 5.2).



**Figure 5.2. The principle of the construction of a gene-deleted strain using the unmarked gene deletion system (van der Geize et al., 2001).**

## 5.2 Materials and methods

### 5.2.1 Inserts preparation

To construct the mutagenic plasmids, inserts were generated (Fig. 5.3) using the primers listed in Table 2.1 (Chapter 2). The upstream sequence (Insert 1) of the regulator, permease, *xplB* and *xplA* were all individually amplified to produce PCR products with *EcoRI* and *NdeI* restriction sites at the 5' and 3' end. The downstream regions (Insert 2) of four of the individual genes were amplified to produce PCR products with the *NdeI* and *HindIII* restriction sites at the 5' and 3' end. The PCR products were purified and the DNA concentration determined.

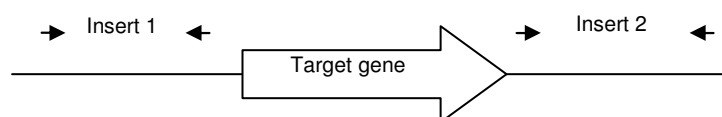


**Figure 5.3. Generation of inserts (upstream and downstream sequences of target gene) using primers listed in Table 2.1 (Chapter 2).**

### 5.2.2 Plasmids construction

Digestions were carried out as described in Chapter 4 (Section 4.2.1) with some modifications. The *EcoRI* and *NdeI* restriction enzymes were used to digest Insert 1 and *HindIII* and *NdeI* were used to digest Insert 2 (Figure 5.3). The plasmid (Fig. 5.4) was digested with *EcoRI* and *HindIII* and digested products separated on an agarose gel, purified and then plasmid dephosphorylated before ligation. Ligation and transformation was carried out as described in previous chapters (Section 2.6.6 and 4.2.1).



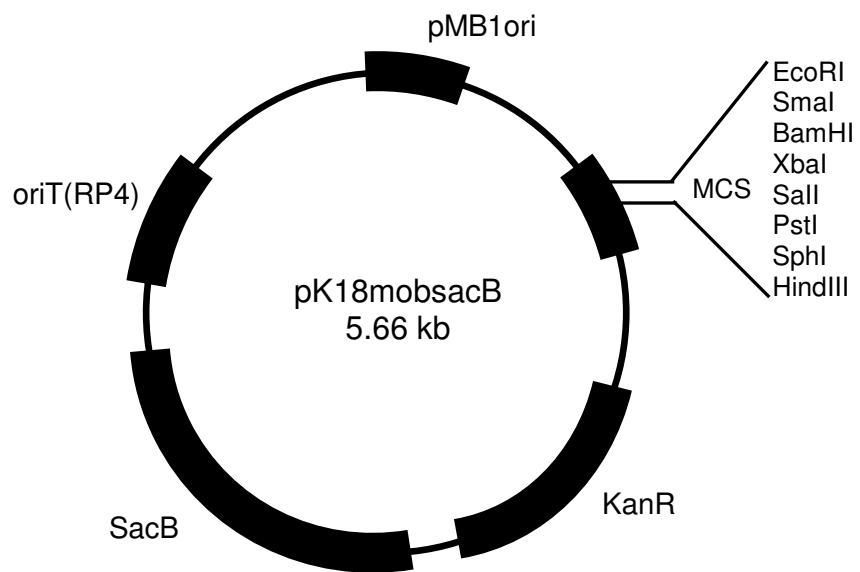


**Figure 5.4. Plasmid map of pK18mobsacB.**

### 5.2.3 Screening, selection and validation of positive clones

To check whether the clones carried the correct inserts, colony PCR were performed using primers as shown in Table 5.1. Clones that carried the correct size of PCR product were selected. To validate the positive constructs, they were checked after digesting with restriction enzymes. Once the plasmids (constructs with correct inserts) were made, they were maintained in *E. coli* (Novablue).

**Table 5.1. Primers used to check inserts size.** Colony PCR using an annealing temperature of 58 °C, yielded PCR products with predicted size. For further details of primers see Chapter 2 (Table 2.1).

Mutagenic plasmid for gene deletion	Primers	Size of product
regulator (ORF 27)	UpF861(rp)+EcoRI and DwnR852(rp) +HindIII	1.7 kb
permease (ORF 29)	UpF822(perm)+EcoRI and DwnR975(perm)+HindIII	1.8 kb
<i>xplB</i> (ORF 31)	UpF1083( <i>xplB</i> )+EcoRI and DwnR849( <i>xplB</i> )+HindIII	1.9 kb
<i>xplA</i> (ORF 32)	UpF816( <i>xplA</i> )+EcoRI and DwnR975( <i>xplA</i> )+HindIII	1.8 kb

### **5.2.4 Transconjugation**

The recipient strain, *R. rhodochorous* 11Y was spread onto LBP agar supplemented with nalidixic acid (30 µg/mL) and incubated at 30 °C for 5 days. Each mutagenic plasmid (pK18mabsacB-xplA, pK18mabsacB-xplB, pK18mabsacB-permease, and pK18mabsacB-MarR) was transformed into *E. coli* S17-1 (donor strain). After 24 hours of incubation, about 1000 transformants were obtained on a LBP agar supplemented with kanamycin (25 µg/mL). The plate was incubated for another 24 hours at room temperature then 2 mL of LBP medium was added onto both the recipient and donor strain agar. Cells were harvested and transferred into an Ependoff tube. Aliquots of 750 µL of both strains were gently mixed together and followed by centrifugation at 8,000 x g for one minute. Cells were resuspended in 1 mL of LBP and 200 µL aliquots were spread onto non-selective agar. All plates were incubated at 30 °C overnight. After the incubation, 2 mL LBP was added to the plates and cells were harvested. Cells were diluted into 2 and 4-fold and aliquots (100 µL) were spread on LBP agar supplemented with nalidixic acid (30 µg/mL) and kanamycin (50 µg/mL). Transconjugants appeared after 3-4 days incubation and colonies that were kanamycin resistant and sucrose sensitive were selected. Colony PCR using primers specific to *sacB* was performed to further confirm the presence of the mutagenic plasmid in the recipient strain.

### **5.2.5 Second cross-over**

Sucrose sensitive derivatives of strain 11Y (1<sup>st</sup> mutant) were grown in 10 mL of non-selective LBP medium at 30 °C, 120 rpm overnight. Cells were diluted into 2, 4 and 10-folds and aliquots (100 µL) spread on LBP agar supplemented with nalidixic acid (30 µg/mL) and sucrose (10 % w/v). Sucrose resistant colonies grew after 2-3 days incubation at 30 °C and colonies that were sucrose resistant and kanamycin sensitive were selected for screening for the gene deletion in the strain.

### **5.2.6 Screening and selection of gene deleted strain**

Gene deletion was confirmed by PCR using gene specific primers (Table 5.1) amplifying from the external region of the deleted genes. The gene deleted mutants produced shorter PCR products than the wild-type.

## 5.3 Results

### 5.3.1 Construction of knockout strains

#### 5.3.1.1 Empty plasmid validation

After receipt of the plasmid pK18mobsacB, the sample was reconstituted into nuclease-free water and transformed into *E. coli* (Novablue). Two colonies that grew on kanamycin selective agar were selected. These colonies were streaked onto agar plates containing sucrose (10 % w/v). None of the colonies were able to grow on agar plates containing sucrose indicating that the *sacB* was expressed and active.

To check the size of the plasmid, purified plasmid was digested with *EcoRI* or *HindIII*, as restriction sites of these enzymes were located on multiple cloning sites of the plasmid. Plasmid digestion showed the size of linearized plasmid was about 5.6 kb (Fig. 5.5), which is within range of the size of pK18mobsacB (Fig. 5.3).

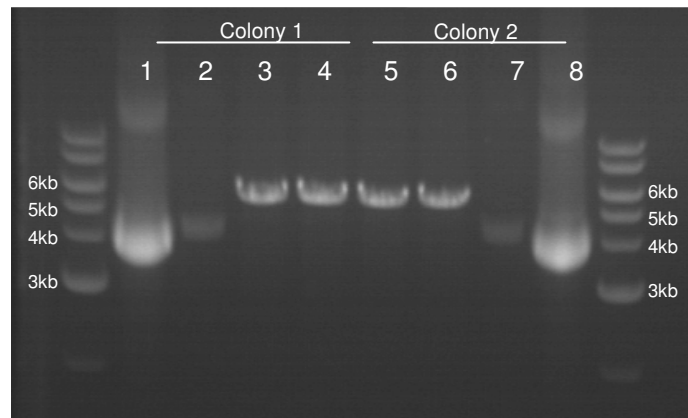


**Figure 5.5. Undigested and digested plasmid of pK18mobsacB from two selected colonies.** Lane 1 and 8: Undigested plasmid with no dilution. Lane 2 and 7: Undigested plasmid with 20x dilution. Lane 3 and 5: *EcoRI*-digested plasmid. Lane 4 and 6: *HindIII*-digested plasmid.

### 5.3.1.2 Construct validation

To validate the gene knockout plasmids for the regulator, permease, *xplB* and *xplA*, the DNA was digested with restriction enzymes (*EcoRI*, *NdeI* and/or *HindIII*). A typical result of the plasmid digestions is shown in Figure 5.6. All of the digestions produced the expected sized products. Thus, these mutagenic plasmids were used for the following experiments.

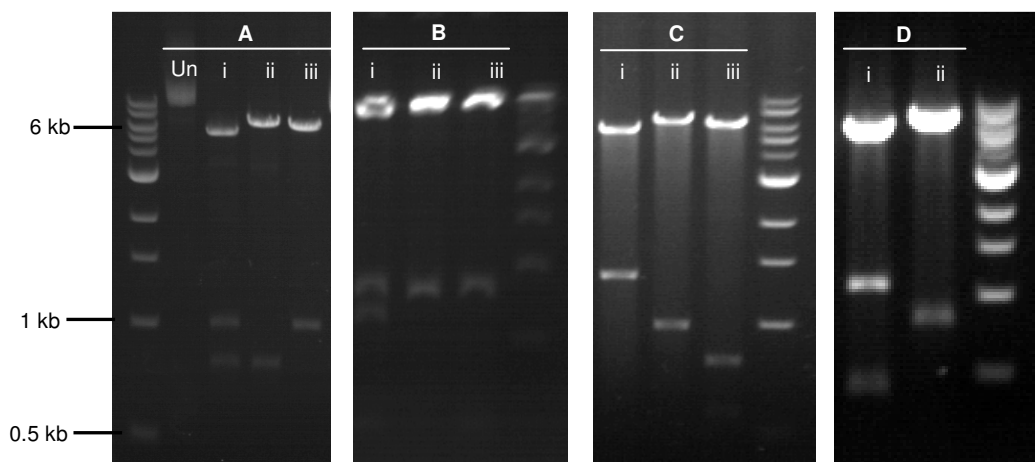


**Figure 5.6. Plasmid digestions.** A-D were the typical digestions of mutagenic plasmid that used for gene deletion of permease, regulator, *xplA* and *xplB*, respectively. Lane Un: undigested plasmid. Lane Ai and Bi: plasmid digested with *EcoRI*, *NdeI* and *HindIII*. Lane Aii, Bii and Ciii: plasmid digested with *EcoRI* and *NdeI*. Lane Aiii, Biii, Cii and Dii: plasmid digested with *NdeI* and *HindIII*. Lane Ci: plasmid digested with *EcoRI* and *HindIII*. Lane Di: plasmid digested with *EcoRI*. All of the digestions showed correct size of the predicted products.

### 5.3.1.3 Transconjugation

After the transconjugation process for all sets of gene deletion experiments, 100 kanamycin resistant colonies (Fig. 5.7) derived from *R. rhodochrous* 11Y were grown on sucrose (10 % w/v) containing agar and sucrose sensitive colonies were selected (Fig. 5.8).

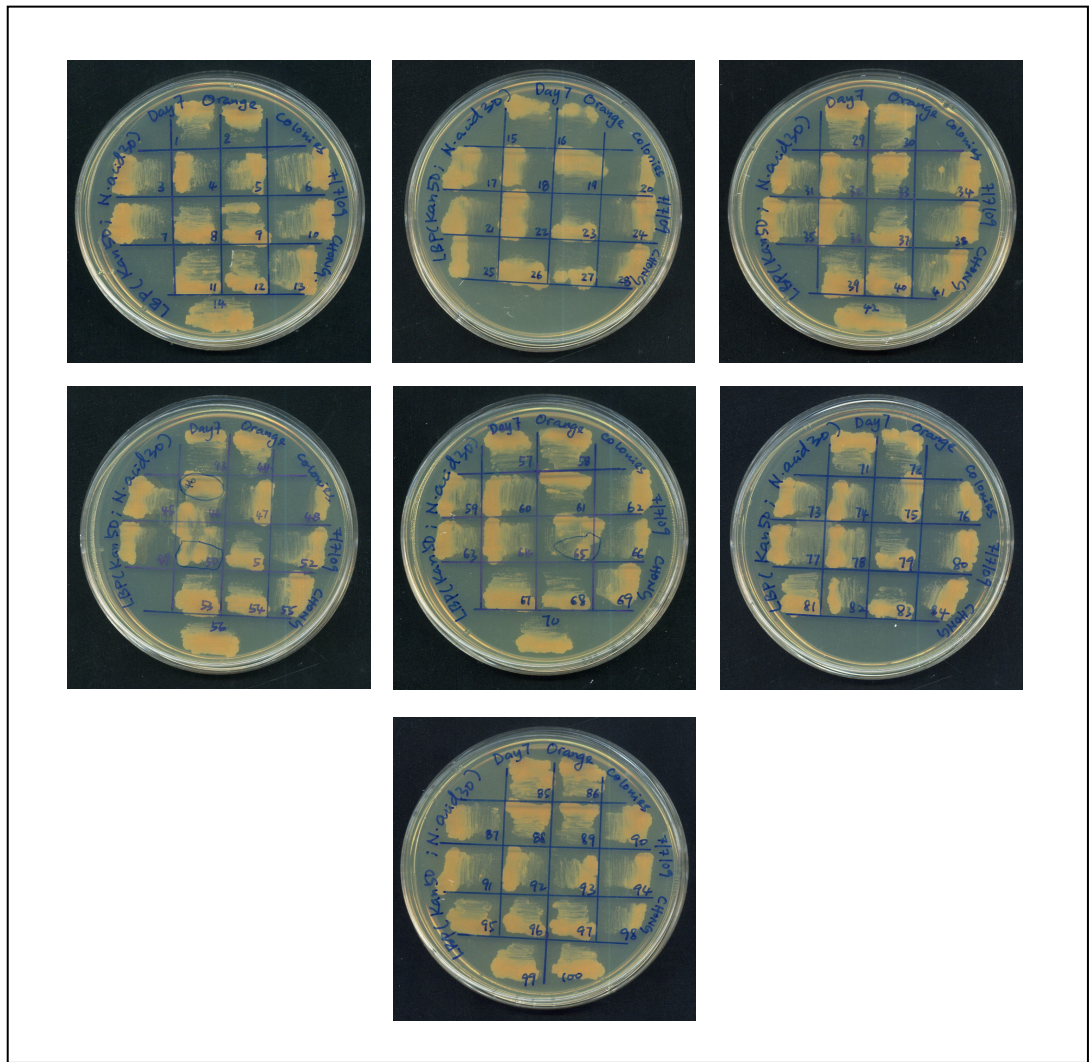


**Figure 5.7.** The 100 selected colonies growing on kanamycin containing agar. Colonies were incubated at 37 °C for 2 days.

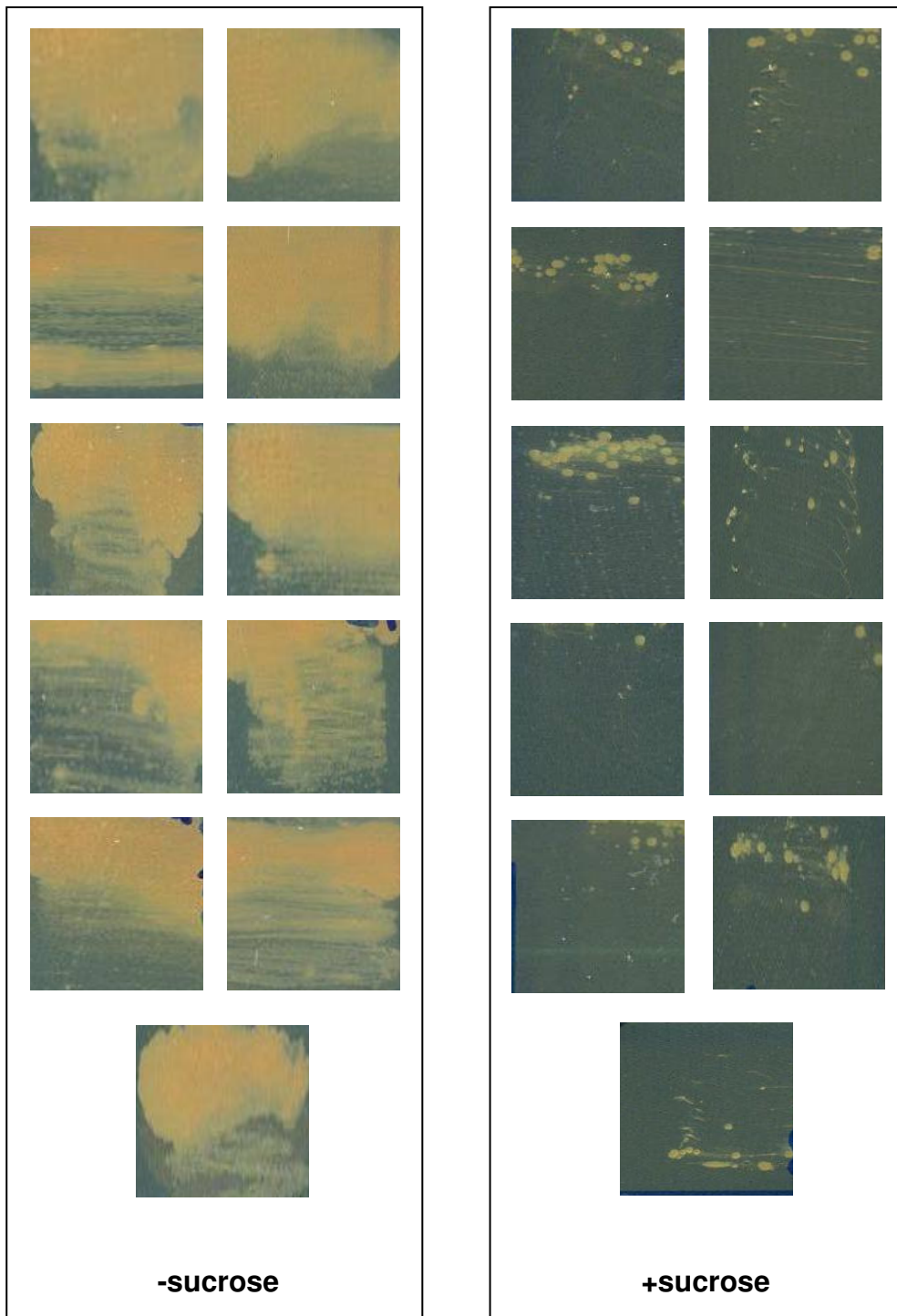


**Figure 5.8. Sucrose sensitive colonies after transconjugation process.** A 100 of the selected colonies were grown on to kanamycin (50  $\mu\text{g}/\text{mL}$ ) and sucrose (10 % w/v) containing LBP agar. As positive control, all colonies were grown on LBP agar without sucrose. They were incubated at 37  $^{\circ}\text{C}$  for 2 days.

Figure 5.9 shows that the *sacB* gene was amplified from all of the colonies that carried the mutagenic plasmid confirming that the mutagenic plasmid has been transferred into *R. rhodochorous* 11Y.

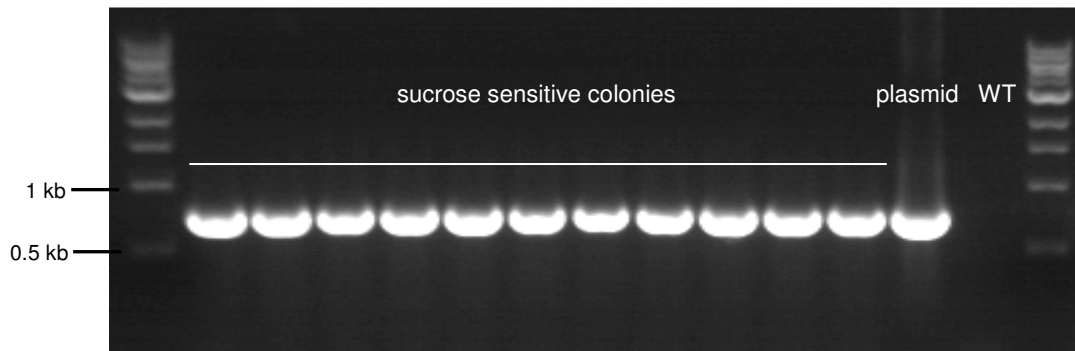


**Figure 5.9. Detection of *sacB*.** All of the PCR reaction produced the expected size (770 bp) using primers specific to *sacB*. Positive control: pK18mobsacB. Negative control: strain 11Y wild-type.



### 5.3.1.4 Gene-deleted strains

To generate the gene-deleted strains, one of the sucrose sensitive colonies was grown on non-selective medium (LBP medium without kanamycin and sucrose) for 24 h. Cells were spread onto sucrose containing agar and the sucrose resistant mutant left to grow (Fig. 5.10).

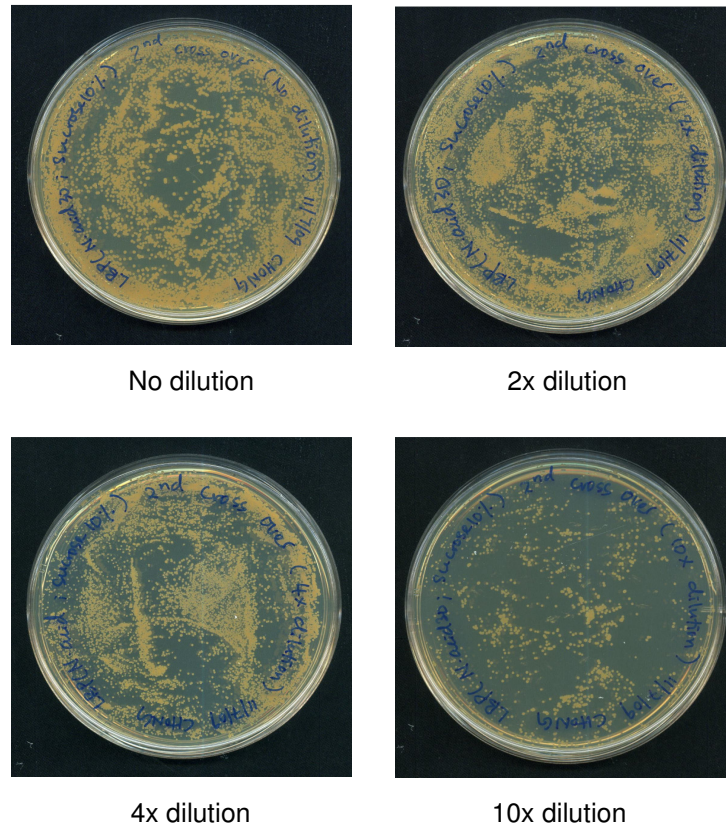


**Figure 5.10. Sucrose resistant colonies on sucrose containing agar**

Of the 100 sucrose resistant colonies that were randomly selected and grown on kanamycin containing agar, more than 80 % of the colonies were unable to grow (data not shown). This indicates that the mutagenic plasmid was likely removed from these colonies. To further confirm the removal of plasmid from the colonies, a total of 26 of these colonies were selected for PCR amplification using primers specific to *sacB*. The result (Fig. 5.11) reveals that PCR products were not amplified indicating that the mutagenic plasmid has been removed from sucrose resistant colonies.



**Figure 5.11. Detection of *sacB*.** No PCR product was generated using primers specific to *sacB* in the selected colonies. Positive control: pK18mobsacB. Negative control: strain 11Y wild-type.

To identify the gene-deleted strains, the external primers (see caption of Figure 5.12) were used to amplify the external region (upstream and downstream) of the deleted gene. As a result, a shorter PCR product (about 1.8 kb) was amplified from the gene-deleted colonies compared to that amplified from the wild-type of *R. rhodochrous* 11Y (Fig. 5.12A-D). The *xplA*, *xplB*, permease or MarR gene sequence was deleted in all four selected gene-deleted strains, confirmed by sequencing.

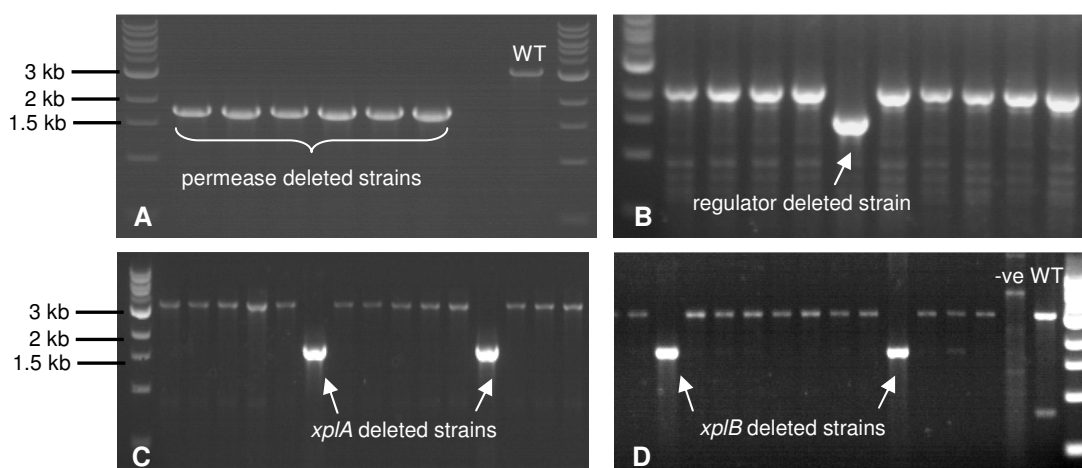


**Figure 5.12. Identification of the gene-deleted strains.** Primers used in PCR amplification in reaction (A): UpF822(perm) and DwnR975(perm); (B): UpF861(rp) and DwnR852(rp); (C): UpF816(*xplA*) and DwnR975(*xplA*); (D): UpF1083(*xplB*) and DwnR849(*xplB*). The expected product for the gene-deleted strain is about 1.8 kb. A shorter PCR product was amplified in the gene deleted strains.

## 5.3.2 Characterisation of the knockout strains

### 5.3.2.1 Characterisation of the *xplA* knockout strain

It is known that there is more than one polychlorinated biphenyl (PCB) degrading system in *Rhodococcus* sp. (Seto et al., 1995). To investigate whether there are any additional RDX degrading gene(s) present in strain 11Y, the *xplA* knockout strain was constructed.

The *xplA* knockout and wild-type strains were incubated in minimal medium, with RDX as a sole nitrogen source at a concentration of 150  $\mu\text{M}$ , over 48 h of incubation. Growth of the strains and RDX elimination throughout the incubation time were monitored. HPLC analysis revealed that whilst the wild-type strain 11Y removed all of the RDX in the minimal medium within 8 h, no RDX removal was observed with the knockout strain over 48 h of incubation (Fig. 5.13). The growth of the *xplA* knockout strain reached and  $\text{OD}_{600}$  of 0.6 after 48 h of incubation which is probably due to the carry-over of nitrogen source from inoculum (LB-grown cells) or the knockout strain utilised nitrogen from dead cells for growth.

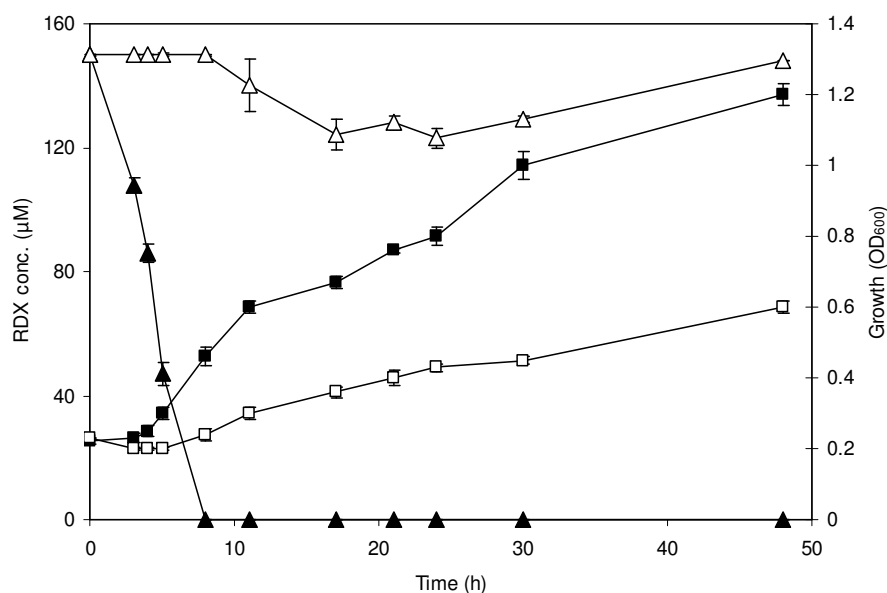


**Figure 5.13. Growth of the *xplA* knockout strain and wild-type on RDX minimal medium.** RDX concentration for wild-type (closed triangles) and *xplA* knockout strain (open triangles).  $\text{OD}_{600}$  for wild-type (closed squares) and *xplA* knockout strain (open squares). Error bars show one standard deviation for triplicate samples.

### 5.3.2.2 Western blot analysis

To check that XplA was absent in the knockout strain, western blot analysis was carried out; no XplA was detected in the knockout cell free extract (Fig. 5.14) while the positive control (11Y wild-type) showed a band of correct molecular weight (60 kDa).

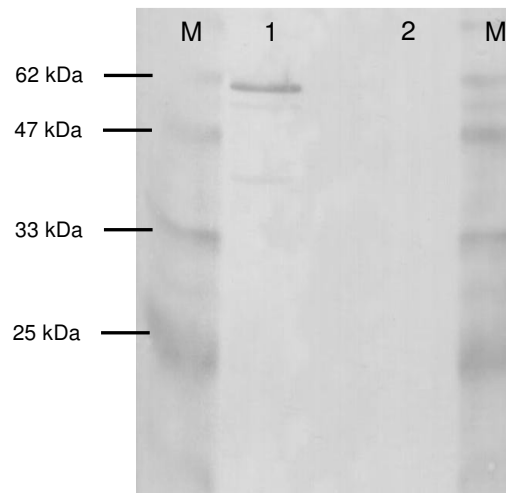


**Figure 5.14. Western blot analysis of cell free extracts of *xplA* knockout and wild-type strains.** (M): Protein marker. (1): WT cell free extracts (0.1 g/mL). (2): *xplA* knockout cell free extracts (0.1 g/mL).

### 5.3.2.3 Resting cell assays of the *xpIA* knockout strain

Resting cell incubations of the *xpIA* knockout and wild-type strains of 11Y were performed in minimal medium containing 90  $\mu\text{M}$  of RDX, at room temperature (approximately 20  $^{\circ}\text{C}$ ) over 60 minutes. Wild-type cells removed all of the RDX in the medium within 30 minutes. No RDX removal by the knockout strain was observed over the incubation time (Fig. 5.15).

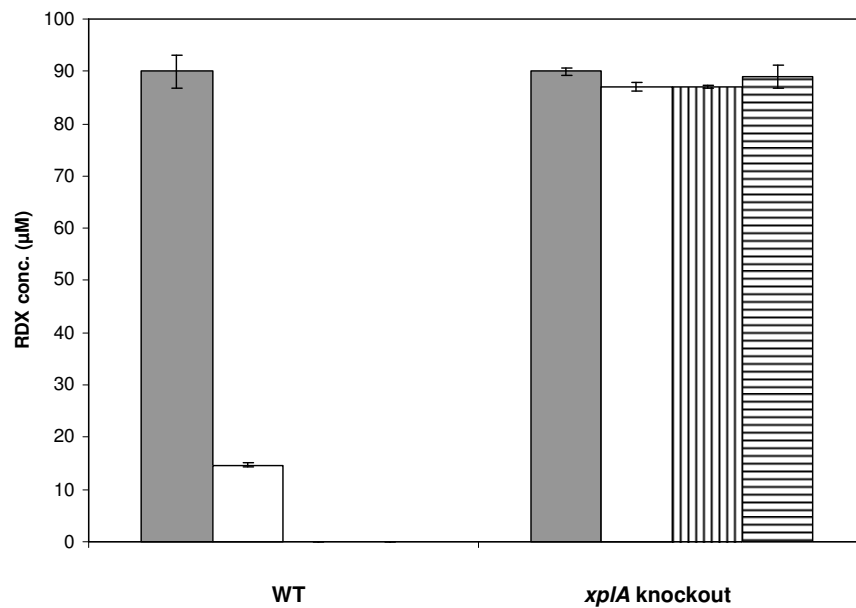


**Figure 5.15. Resting cell assays for wild-type and the *xpIA* knockout strains of *R. rhodochrous* 11Y.** The data show RDX concentration at incubation time of 0 min (grey bars), 10 min (white bars), 30 min (vertical bars) and 60 min (horizontal bars). Error bars indicate one standard deviation for triplicate samples.

#### 5.3.2.4. Growth of the *xplA* knockout strain on RDX dispersion agar

RDX dispersion agar is a minimal medium, agarose-grade agar containing 5 mM RDX as the sole source of nitrogen. The agar has a white, opaque appearance due to insoluble RDX crystals. All of the RDX degrading bacteria isolated so far produce a zone of clearance, where the opacity disappears, around the edge of the colony. The mechanism behind the zone of clearance still remains unknown and to investigate this, the *xplA* knockout strain was grown on RDX dispersion agar supplemented with an additional nitrogen source ( $\text{NH}_4\text{Cl}$ ,  $\text{KNO}_3$  or  $\text{NaNO}_2$ ). The results demonstrated that there was no zone of clearance formed by the *xplA* knockout strain in the RDX dispersion agar supplemented with another nitrogen source ( $\text{NH}_4\text{Cl}$ ,  $\text{KNO}_3$  or  $\text{NaNO}_2$ ) (Fig. 5.16). This shows that the formation of a zone of clearance by the wild-type strain has a direct relationship to XplA activity.

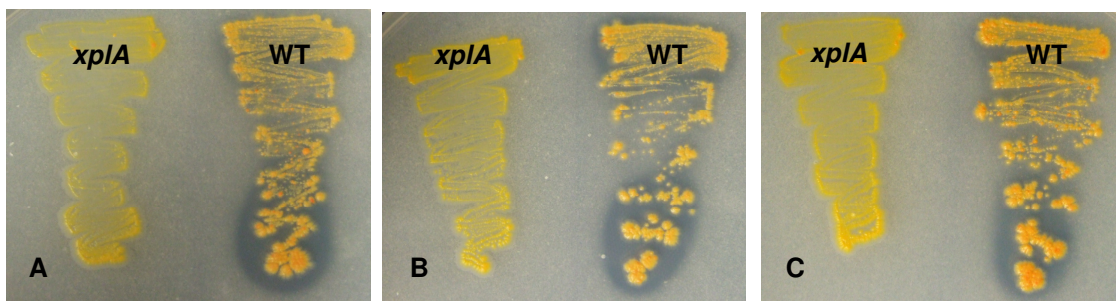


**Figure 5.16. The *xplA* knockout and wild-type strains on RDX dispersion agar.** These agar were supplemented with 5 mM of RDX and 250 μM of (A)  $\text{NH}_4\text{Cl}$ ; (B)  $\text{KNO}_3$  and (C)  $\text{NaNO}_2$ . Strains were allowed to grow at 30 °C for 2 weeks.

### 5.3.2.5 Characterisation of the *xplB* knockout strain

To determine whether XplB is the sole reductase partner for XplA, an *xplB* knockout strain was constructed. Sequencing analysis confirmed that *xplB* had been removed and that the coding sequence of the neighbouring *xplA* gene was unaltered. To compare the RDX-degrading ability of the *xplB* knockout strain with that of the wild-type, both strains were grown in minimal medium containing 150  $\mu\text{M}$  RDX as the sole nitrogen source. The growth ( $\text{OD}_{600}$ ) and RDX removal were monitored over the 48 h of incubation time (Fig. 5.17). The *xplB* knockout strain removed RDX at a rate of 3.1  $\mu\text{M}/\text{h}$  and removed all the RDX within 48 h with the  $\text{OD}_{600}$  reaching 1.0 after 48 h. The wild-type removed RDX at the faster rate of 18.8  $\mu\text{M}/\text{h}$ .

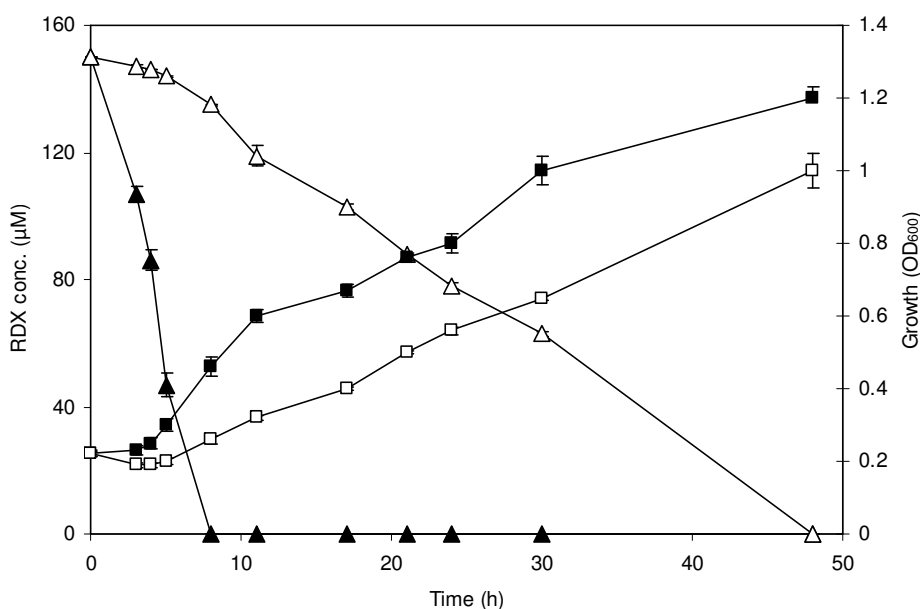


**Figure 5.17. Growth of the *xplB* knockout strain and wild-type strains on RDX as a sole nitrogen source.** RDX concentration for wild-type (closed triangles) and *xplB* knockout strain (open triangles).  $\text{OD}_{600}$  for wild-type (closed squares) and *xplB* knockout strain (open squares). Error bars show one standard deviation for triplicate samples.

### 5.3.2.6 Resting cell assays for the *xp/B* knockout strain

A comparison of RDX removal by resting cells of the *xp/B* knockout and wild-type strains was carried out. The pattern of RDX removal was consistent with the growth experiments described above (5.3.2.5). When resting cells were incubated in RDX minimal medium, approximately 83 % of the RDX was removed by the wild-type strain and 12 % by the knockout strain during the 10 min incubation time (Fig. 5.18).

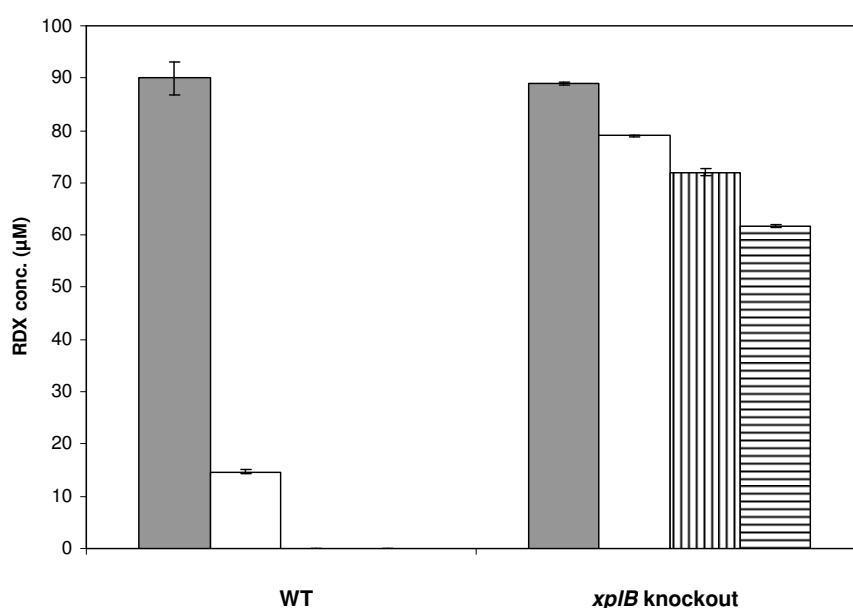


**Figure 5.18. Resting cell assays for wild-type of *R. rhodochrous* 11Y and the *xp/B* knockout strains.** The data show RDX concentration at incubation time of 0 min (grey bars), 10 min (white bars), 30 min (vertical bars) and 60 min (horizontal bars). Error bars indicate one standard deviation for triplicate samples.



### 5.3.2.7 Quantitative RT-PCR and western blot analysis for the *xpIB* knockout strain

The reduced rate of RDX removal in the *xpIB* knockout strain compared to wild-type could be due to a lower level of *xpIA* transcript or protein. To investigate this, real time PCR and western blots were performed. Cell free extracts of wild-type and the knockout cells grown in RDX minimal medium were prepared and RNA and protein extracted.

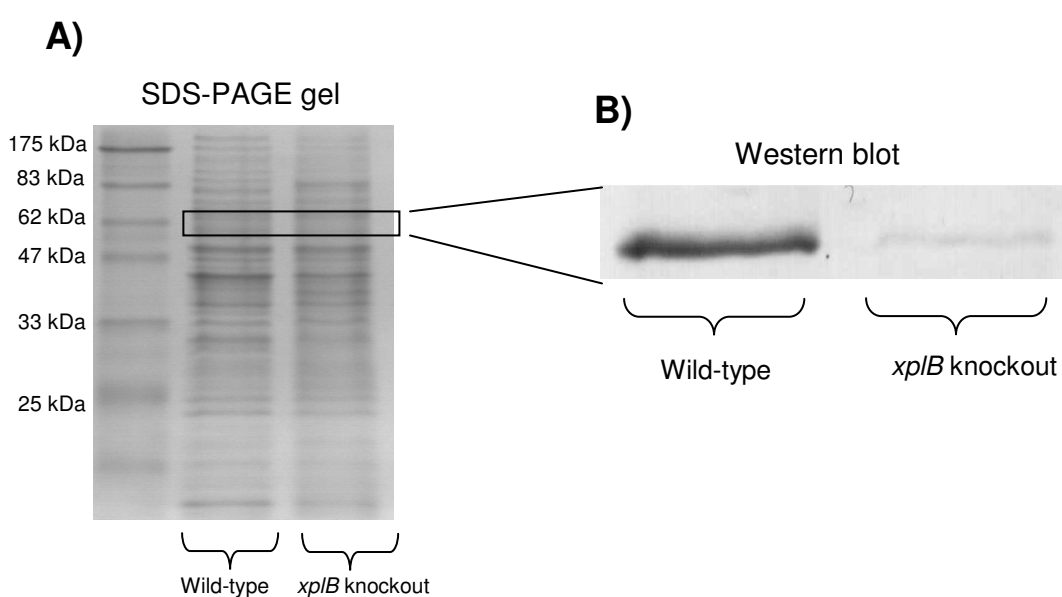


**Figure 5.19. SDS-PAGE and western blot of cell free extracts of strain 11Y wild-type and the *xpIB* knockout strains.** (A) 12 % SDS-PAGE (B) Western blot analysis for XpIA.

Transcriptional analysis revealed that the *xpIB* knockout and wild-type strain had similar levels of *xpIA* expression (data not shown). Nevertheless, western blot analysis demonstrated that XpIA expression was lower in the *xpIB* knockout strain compared to the wild-type strain (Fig. 5.19).

### 5.3.2.8 Characterisation of the permease knockout strain

Real time PCR analysis of the *permease* and *xplA* genes in wild-type 11Y demonstrated that both genes were up-regulated in the presence of RDX (Section 4.3.2). This finding indicated that the permease could be involved in RDX uptake in strain 11Y. Thus, a permease knockout strain was constructed (Fig. 5.12). Growth experiments revealed that RDX degradation and growth rates for the knockout and wild-type strains were nearly identical (Fig. 5.20). Additionally, resting cell assays showed no difference in the RDX removal rates between the permease knockout and wild-type strains (data not shown).

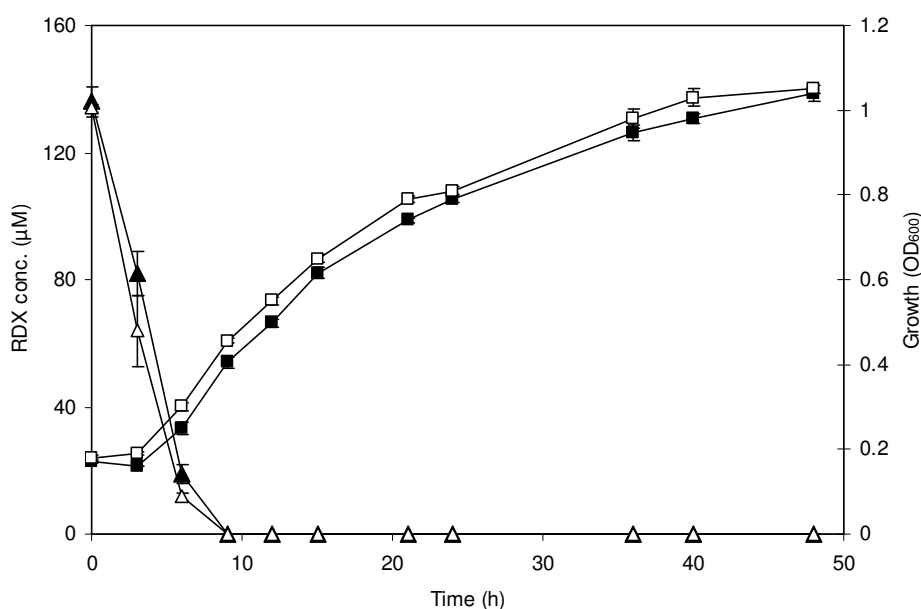


**Figure 5.20. Growth of the permease knockout strain and WT on RDX as a sole nitrogen source.** RDX concentration for WT (closed triangles) and permease knockout strain (open triangles). OD<sub>600</sub> for WT (closed squares) and permease knockout strain (open squares). Error bars show one standard deviation for triplicate samples.

To investigate whether the putative permease has higher affinity toward RDX at a lower RDX concentration, the knockout and wild-type strains were incubated in minimal medium containing 40 μM RDX over 8 hours of incubation time.

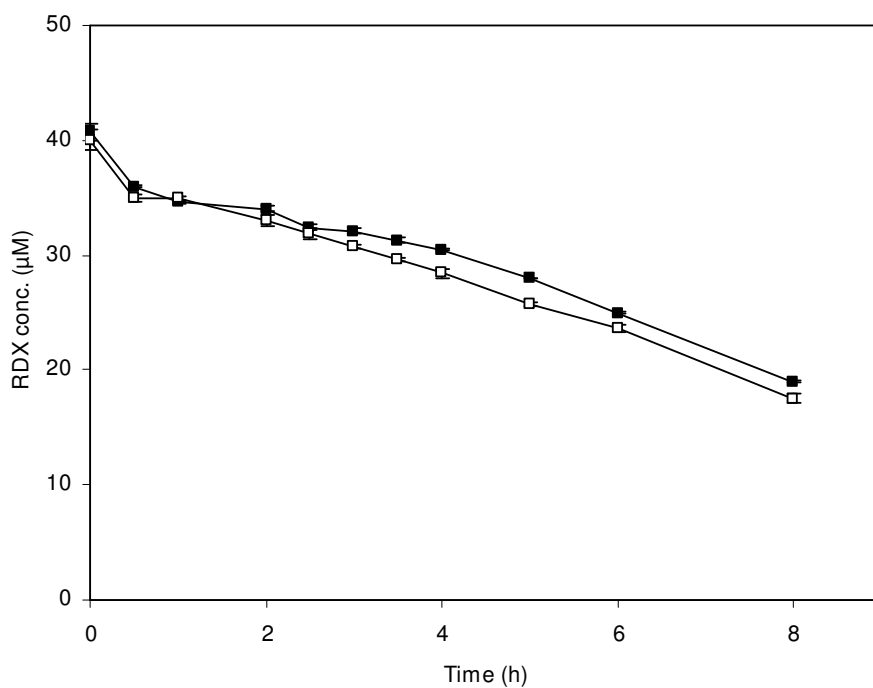


**Figure 5.21. RDX removal by the permease knockout and wild-type strains at a lower RDX concentration.** RDX concentration for WT (closed squares) and *permease* knockout strain (open squares). Error bars show one standard deviation for duplicate samples.

No significant differences in RDX degradation were observed in either of the strains (Fig. 5.21).

### 5.3.3 Initial investigation of *xplA* regulation in strain 11Y

#### 5.3.3.1 Studies under nitrogen-limiting conditions and RDX

Earlier studies suggested that RDX degrading activity in strain 11Y is induced by RDX (Seth-Smith, 2002). To investigate whether expression of *XplA* in strain 11Y is induced when cells are exposed under nitrogen-limiting/starving conditions or to RDX as sole nitrogen source, cells were grown under a range of nitrogen conditions. Cells were grown overnight (17 h) in medium containing the nitrogen sources described below (Table 5.2), after which time, the cells were harvested and transferred into new medium for a further 3 hour incubation.

**Table 5.2. Growth and the treatment media.** Cells (0.1 mg/mL) were inoculated into the growth medium (700 mL) and incubated at 30 °C with shaking (180 rpm) for 17 hours. After the harvesting of cells, same amount of cells (2 mg/mL) were transferred into the treatment medium (250 mL) for 3 hours incubation.

<u>Growth medium</u>		<u>3 hours treatment</u>
(a) 750 $\mu$ M $\text{KNO}_2$	→	450 $\mu$ M $\text{KNO}_2$
(b) 5 mM $\text{KNO}_3$	→	5 mM $\text{KNO}_3$
(c) 750 $\mu$ M $\text{KNO}_3$	→	450 $\mu$ M $\text{KNO}_3$
(d) 750 $\mu$ M $\text{KNO}_3$	→	No nitrogen (starving)
(e) 750 $\mu$ M $\text{KNO}_3$	→	150 $\mu$ M RDX
(f) 250 $\mu$ M RDX	→	150 $\mu$ M RDX

After 3 hours of treatments, cells were used for subsequent experiments: resting cell assays, western blot analysis, cell free extract activity assays and quantitative real time PCR.

Resting cell incubations were performed in minimal medium with 100  $\mu\text{M}$  of RDX at 30  $^{\circ}\text{C}$  over 60 minutes (Figure 5.22). Cells treated with (b) 5 mM  $\text{KNO}_3$  (closed squares) had the lowest RDX removal rates. Cells treated in (a and c) nitrogen-limiting (open triangles and closed circles) and (d) starving (open diamonds) conditions were able to take up RDX more quickly than cells grown in (b) unlimited nitrogen conditions (5 mM  $\text{KNO}_3$ ). Interestingly, the RDX uptake rates were further increased in (e and f); cells grown overnight and/or treated for 3 h in RDX (closed triangles and open squares). The cells with the longest pre-incubation exposure to RDX (f) (closed triangles) demonstrated the highest RDX uptake of all the treatments.

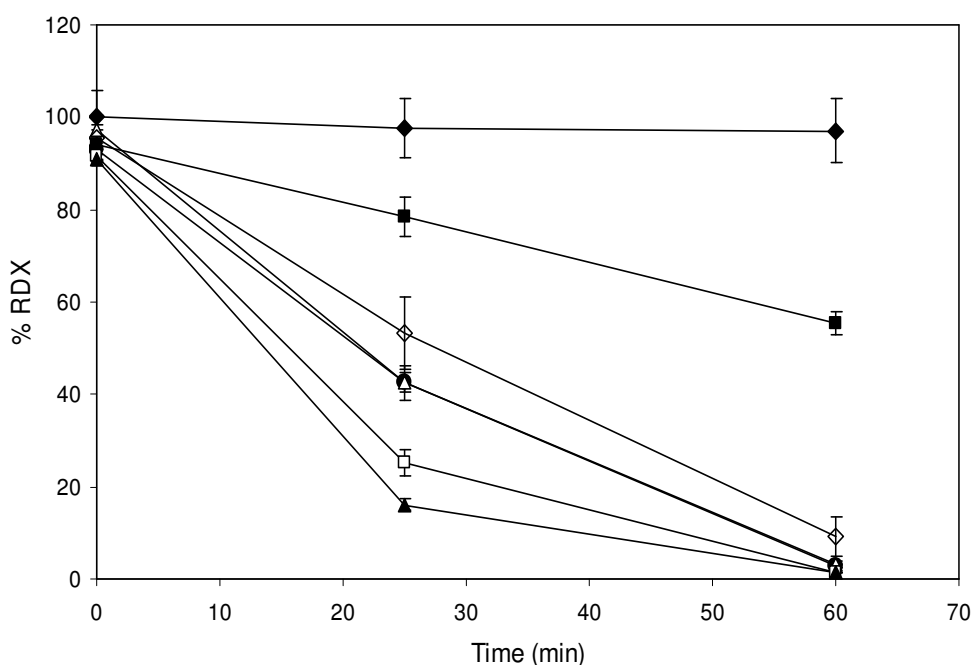


**Figure 5.22. RDX degradation by whole cells of *R. rhodochrous* 11Y under different nitrogen conditions.** RDX-grown cells treated with 150  $\mu\text{M}$  RDX (closed triangles),  $\text{KNO}_3$ -grown cells treated with 150  $\mu\text{M}$  RDX (open squares),  $\text{KNO}_3$ -grown cells treated with 450  $\mu\text{M}$   $\text{KNO}_3$  (open triangles),  $\text{KNO}_2$ -grown cells treated with 450  $\mu\text{M}$   $\text{KNO}_2$  (closed circles),  $\text{KNO}_3$ -grown cells treated with no nitrogen medium (open diamonds),  $\text{KNO}_3$ -grown cells treated with 5 mM  $\text{KNO}_3$  (closed squares), no cells control (closed diamonds) Error bars show one standard deviation for duplicate samples.

To monitor the XplA expression when cells of *R. rhodochrous* 11Y were exposed to different nitrogen conditions, western blot analysis was performed. The analysis revealed that the expression of XplA was higher in cells which were grown overnight and then treated for 3 h to RDX (condition (f) in Table 5.2) compared to cells treated with the other nitrogen sources ( $\text{KNO}_2$ ,  $\text{KNO}_3$ ) or no nitrogen (Figure 5.23).

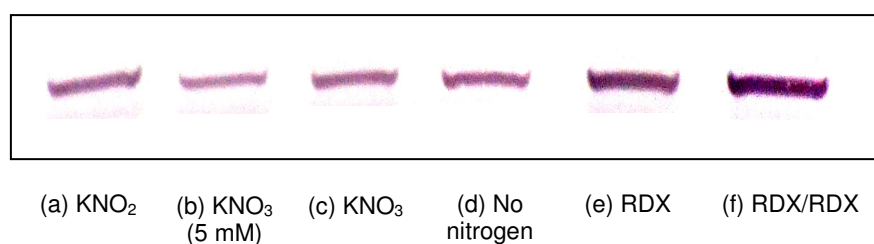


**Figure 5.23. Western blot analysis of cell free extracts of strains 11Y from different nitrogen treatments.** (a)  $\text{KNO}_2$ -grown cells treated with  $\text{KNO}_2$  ( $450 \mu\text{M}$ ); (b)  $\text{KNO}_3$ -grown cells treated with  $\text{KNO}_3$  ( $5 \text{ mM}$ ); (c)  $\text{KNO}_3$ -grown cells treated with  $\text{KNO}_3$  ( $450 \mu\text{M}$ ); (d)  $\text{KNO}_3$ -grown cells treated with no nitrogen; (e)  $\text{KNO}_3$ -grown cells treated with RDX ( $150 \mu\text{M}$ ); (f) RDX-grown cells treated with RDX ( $150 \mu\text{M}$ ). Same amount of proteins ( $14 \mu\text{g}$ ) were loaded onto the SDS-PAGE gel.

Activity assays in cell free extracts were also performed. These were carried out by monitoring the depletion of NADPH at 340 nm. The results demonstrated that the specific activity of XplA could be measured in cells treated with RDX. RDX-grown cells treated with RDX (condition (f) in Table 5.2) showed higher specific XplA activity than nitrate-grown cells treated with RDX (condition (e) in Table 5.2). No activity was detected in cells exposed to  $\text{KNO}_3$ ,  $\text{KNO}_2$  or no nitrogen (Figure 5.24) (condition (a), (b), (c) and (d) in Table 5.2). This result was in agreement with data obtained from the resting cell assays and western blot analysis that higher XplA activity and amount of XplA was detected in the RDX-exposed cells (Figure 5.22 and 5.23).

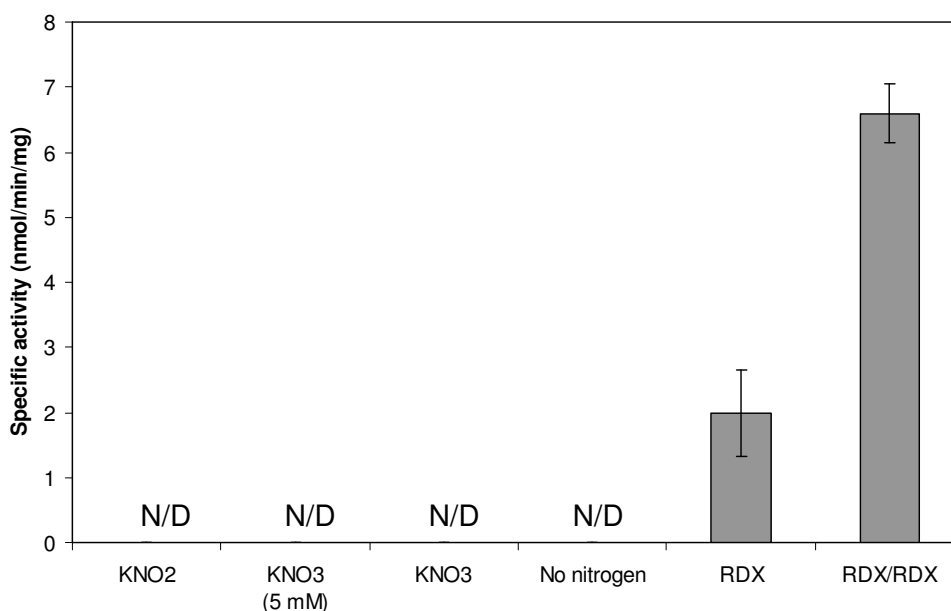


**Figure 5.24. Specific XplA activity in cells treated with different nitrogen sources. RDX (condition (e) in Table 5.2); RDX/RDX (condition (f) in Table 5.2).** Results are mean of three technical replicates of two biological measurements. N/D: Not detected.

The transcript levels of *xpIA* in cells treated under different nitrogen conditions throughout the 3 hours incubations were monitored (Fig. 5.25). The *xpIA* transcript levels of cells treated with high nitrogen source (5 mM KNO<sub>3</sub>) were generally low throughout the incubation time (closed squares). Cells treated with low nitrite/nitrate, no nitrogen or RDX had higher XpIA transcript levels than high-nitrogen treated cells. No increase in transcription was seen either of the RDX treatments compared to low nitrogen-treated and nitrogen-starving cells.

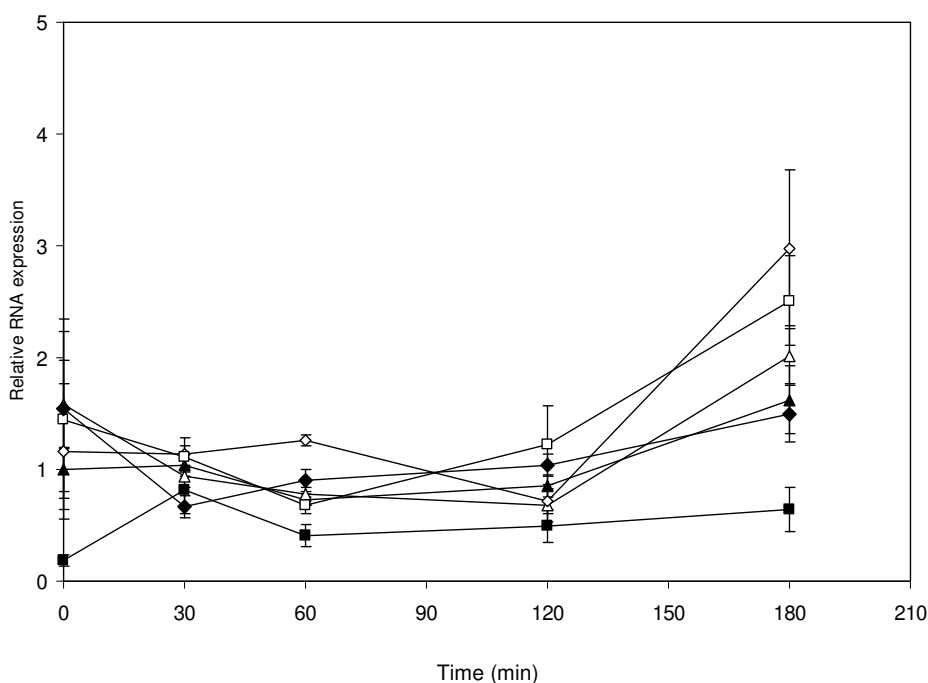


**Figure 5.25. Transcript levels of *xpIA* at different time points of the whole cell studies.** KNO<sub>2</sub>-grown cells treated with 450 μM KNO<sub>2</sub> (closed triangles), KNO<sub>3</sub>-grown cells treated with 5 mM KNO<sub>3</sub> (closed squares), KNO<sub>3</sub>-grown cells treated with 450 μM KNO<sub>3</sub> (open triangles), KNO<sub>3</sub>-grown cells treated with no nitrogen medium (open diamonds), KNO<sub>3</sub>-grown cells treated with 150 μM RDX (open squares), RDX-grown cells treated with 150 μM RDX (closed diamonds). Expression level of *gyrB* (endogenous control) was the same in all of the conditions. Error bars show one standard deviation for four samples.



### 5.3.3.2 Putative promoter prediction of the *xplA* operon

To investigate the presence of putative promoter regions in the gene cluster, sequence from ORF 27 to ORF 32 (Figure 5.26) was analysed by softberry-BPROM, a bacterial promoter prediction software programme (<http://linux1.softberry.com/berry.phtml?topic=bprom&group=programs&subgroup=gfin>). Two putative promoter regions were predicted. These putative promoters are located upstream of the putative permease (ORF 29) and upstream of *xplB* (Figure 5.26). The exact locations of these two putative promoters on the gene cluster are shown in Figure 5.27 and 5.28.

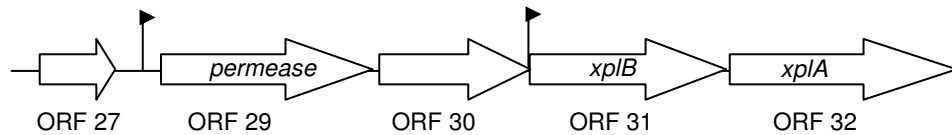


**Figure 5.26.** The RDX degrading gene cluster in strain 11Y. The predicted putative promoter regions were present upstream of the putative permease (ORF 29) and the *xplB* (ORF 31).

**(ORF 27)**

**gtg**acgaacgacgatctggtgcaccggctgcggttcgctgaccgtcgaactcgatgtcttc  
M T N D D L V H R L R S L T V E L D V F

ggggccggcttcgcccccgaacgggttgcacgccaccgatgtacgtgccctgatcgct  
G A G F A A R N G L H A T D V R A L I A

cttctggaccgggatcgggcccggcgcctctcctgggtggctggcggggcatctc  
L L D R D R A G A V A S P G W L A G H L

ggactcaacagtgcgtcgaccaccgcgctcatcgatcgactggaatcgaagggtctggtg  
G L N S A S T T A L I D R L E S K G L V

gaccgcagggcgcgacgactcggatcgctgccgggttgcgctgcacgtcaccgacgcggcc  
D R R R D D S D R R R V A L H V T D A A

caggagatgggctggaccttcttcgggcccgttgatcgaccaggtgatcgcggtggccgac  
Q E M G W T F F G P L I D Q V I A V A D

ggtttctccgacgacgaactgaccacgatccgcacatttctggaccaggtcaccgctgcg  
G F S D D E L T T I R T F L D Q V T A A

gtggcgggagtcggaccgcg**tg**agtgtcctgggtccgcagccgctgaccctgtccgcac  
V A G V R T R -

accgctcacctcagggtcgaaccggagccgtccgcccgatggttaccggaacatgaccat

tgttaattctgcg<sup>-35 P<sub>1</sub></sup>ctccggcctggcgtcaaaaaa<sup>-10 P<sub>1</sub></sup>ccctatgttgtagtatTTGGCGAAA

tccgtttggcgtcaggagattcaggcatggccacgacgaatgtgtatccgacagacgagg

gggtcccggaccgggacgcccagatgctggccgaactcgggttatacgtccgaattcaaac

**(ORF 29)**

gggag**atg**agtccgtgggcgaaacttcgccctcggcttcacctacctgtcgcccgtcgctc  
M S P W A N F A L G F T Y L S P V V

gggatctacacggctcttcgcctatgcatggcacaggccggcccgcgatgatctggagc  
G I Y T V F A Y A M A Q A G P P M I W S

ctcgtcatcggtgggectcgggcagttcctgggtggcgtgatcttcagcgaggtcgtcgcc  
L V I V G L G Q F L V A L I F S E V V A

cagttcccggtcgcggggggcgtgtatccgtggacacgcccgactctggggccggaagtac  
Q F P V A G G V Y P W T R R L W G R K Y

**Figure 5.27. Nucleotide and amino acid sequence of MarR-like regulator (ORF 27) and initial part of the putative permease (ORF 29). Start (gtg or atg) and stop (tga) codons are shown in bold. The first putative promoter regions (-10 and -35) in upstream of the putative permease is shown in boxes.**

(ORF 30)

**atg**acgaacatcagagctgtcgtgtacggcgtcggagcgatgaactccgtgatcaccg  
M T N I R A V V Y G V G A M N S V I T R  
tatctgctcgacaaggacgtcgagatcgtaggcggccatctcgcgcagtcgacgacaaggtg  
Y L L D K D V E I V G A I S R S P D K V  
ggcaaggacctcggcggaggtcaccggactcgaccgtcgactcggagtgatcgatcagcgac  
G K D L G E V T G L D R R L G V S I S D  
gaccgacgaggtgttcacgaggacgagtcggacatcgcggtcgtcgcgatcaccagc  
D P H E V F T R T S P D I A V V A I T S  
tatctcgtggacgcccgggagcacttcggtatcgactgtcgcacgggggtcaacgtgatc  
Y L V D A A E H F R I A L S H G V N V I  
acgctgtccgaggaagcgtctatccctggaacaccgcccgaactgaccgcccgaactc  
T L S E E A L Y P W N T A P E L T A E L  
gatgcactcgccaaggagcatggcgtgaccatcacggggcgggggtttccaggacagcttc  
D A L A K E H G V T I T G G G F Q D S F  
tgggtgaacgcggtcggccagctgatgggcacggcacaccgcatcgactcggtcaccggg  
W V N A V A Q L M G T A H R I D S V T G  
acgagttcgtggaacgtcgacgagtacggcccgaactggccgagctgcagcaggtcggc  
T S S W N V D E Y G P E L A E L Q Q V G  
gcgacgatcgaggagttcgacgctggtgcccgagaagccgtgcgtccgcccacattcggc  
A T I E E F D A W C R E A V R P P T F G  
cggatcgctctcgatgcgctggtcgccggagcggggctgacgcccgaagcagatcctgacg  
R I A L D A L V A G A G L T P K Q I L T  
cgcaccgaaccggaactggcacacgagactctgactgtgctgccctggggatcgacgtc  
R T E P E L A H E T L H C A A L G I D V  
ccgcccggaaagtgcacggttcaccgacatcgacgagatccgcacggaagagggcccg  
P P G K C I G F T D I D E I R T E E G P  
gtcttcgtcttccggatgtccggccggtgtacggccccgacgacagcgatgtcaacgaa  
V F V F R M S G R L Y G P D D S D V N E  
tggacgatccacggcgaaccgatctggtgatgtccaacggcaccgcccggacgatggcc  
W T I H G E P D L V M S N G T P P T M A  
accacctgcaccaattggtgaaccgtatccccgacgtgctcgacgcccgaccgggattc  
T T C T Q L V N R I P D V L D A D P G F  
gtgaccgtcgtcgatctgccaggtgcgctaccggcacggtcggctgcacgaccacctg  
V T V V D L P R L R Y R H G R L H D H L  
agcaggtggtcatcggatcgttacatcgtgcgcgaagaadtgtaacaatag**atg**gacatc  
S R W S S D R Y I V R E E L - M D I

```
atgagtgaagtggacgtggcaccgcgcgtggcgggtggtcgggcgcccggaccgtcggggtgt
M S E V D V A P R V A V V G A G P S G C

ttcaccgcacagcaactccgcaagcagtgcccgagggtggaggtcaccgtcttcgaccgg
F T A Q Q L R K Q W P E V E V T V F D R

ctaccaccccgttcgggctccttcgctacggcgtggctcccgaccatcagggcacgaag
L P T P F G L L R Y G V A P D H Q G T K
```

**Figure 5.28. Nucleotide and amino acid sequence of the putative dihydrodipicolinate reductase (ORF 30) and initial part of the *xp/B* (ORF 31).** Start (atg) and stop (taa) codons are shown in bold. The second putative promoter regions (-10 and -35) in upstream of the *xp/B* is shown in boxes.

### 5.3.3.3 Sequence analysis of the MarR-like regulator in 11Y

A multiple alignment of the 11Y putative MarR-like regulator and its homologues is shown in Figure 5.29. The 11Y regulator was found to share 100 % amino acid identity with the *Microbacterium* sp. MA1 regulator and 62 % amino acid identity with a putative regulator from *Gordonia bronchialis* DSM 43247. The other *Rhodococcal* regulator described in Fig. 5.29 shared more than 50 % amino acid identity with the MarR regulator from strain 11Y. A conserved (helix-turn-helix) domain was detected in the amino acid sequence of the putative 11Y regulator (amino acid residues 52 to 127) by two sequence analytical programmes: blastp (<http://blast.ncbi.nlm.nih.gov/Blast.cgi>) and Interprot scan (<http://www.ebi.ac.uk/Tools/pfa/iprscan/>).

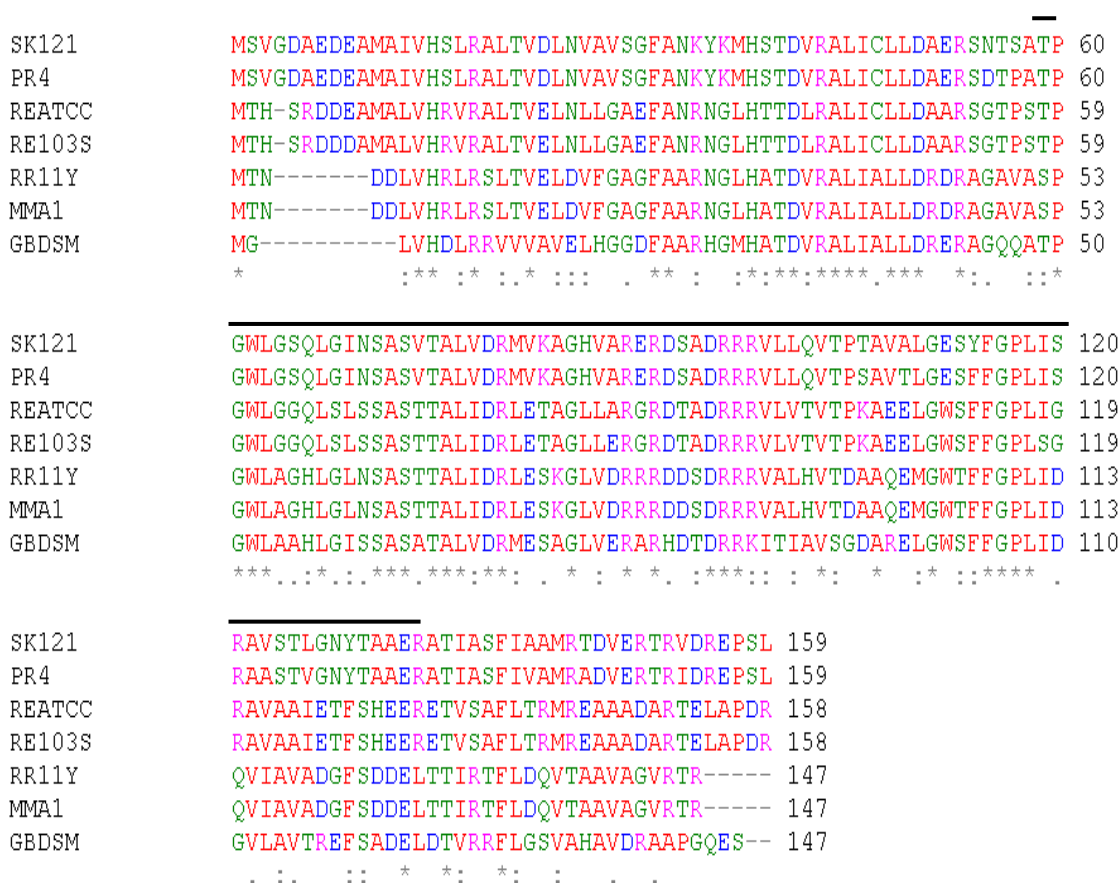


**Figure 5.29. The alignment of MarR-like regulator of 11Y with its homologues.** Abbreviations: (SK121) *Rhodococcus erythropolis* SK121, (PR2) *Rhodococcus erythropolis* PR2, (REATTC) *Rhodococcus equi* ATCC 33707, (RE103S) *Rhodococcus equi* 103S, (RR11Y) *Rhodococcus rhodochrous* 11Y, (MMA1) *Microbacterium* sp. MA1, (GBDSM) *Gordonia bronchialis* DSM 43247. The helix-turn-helix domain is indicated with bar. The identical amino acid residues are indicated with \*.

The organisation of the *XplA* gene cluster in strain 11Y suggests that the genes on the cluster are regulated by the MarR-like transcriptional regulator (ORF 27). To investigate whether the putative regulator is controlling *xplA* expression, the putative regulator was deleted. Characterisation of the putative transcriptional regulator knockout is described in the following sections.

### 5.3.3.4 RDX removal by whole cells of RDX-grown regulator knockout strain

Early ( $OD_{600} \sim 0.3$ ) and late ( $OD_{600} \sim 0.8$ ) log stages of regulator knockout and wild-type cells were used in resting cell assays to monitor RDX degradation over the incubation time. Cells were incubated in RDX minimal medium at room temperature for 1 hour. Results (Table 5.3) showed similar amount of RDX removal in the knockout and WT strains.

**Table 5.3. Resting cell assays for regulator knockout and wild-type strains.** Cells (0.02 g/mL) were incubated in minimal medium containing 150  $\mu$ M RDX as a sole nitrogen source. Samples were taken at interval time of 10 min and 20 min. Results represent the averages of percentage RDX removal (standard deviation) of triplicate samples.

Strains	Percentage of RDX removal			
	Early log stage cells		Late log stage cells	
	10 min	20 min	10 min	20 min
WT	26.9 (0.6)	37.8 (0.4)	35.6 (1.1)	57.4 (2.3)
Regulator KO	26.7 (0.4)	37.9 (0.5)	32.7 (0.9)	63.6 (1.3)

### 5.3.3.5 RDX removal by the regulator knockout strain exposed to different nitrogen sources

As described in section 5.3.3.1, the wild-type strain of 11Y exposed to nitrogen-limiting and nitrogen-starving conditions resulted in increased of RDX degrading activity compared to that found in cells grown in a range of alternative nitrogen sources. To investigate whether the regulator knockout has a similarly enhanced level of RDX degradation when exposed to these conditions, the knockout and wild-type strains were treated under following conditions (Table 5.4).

**Table 5.4. Growth and treatment media.** Cells (0.1 mg/mL) were inoculated into the growth medium (700 mL) and incubated at 30 °C with shaking (180 rpm) for 17 hours. After the harvesting of cells, same amount of cells (2 mg/mL) were transferred into the treatment medium (250 mL) for 3 hours incubation. After the treatment, cells were used for resting cell experiments.

<u>Growth medium</u>		<u>3 hours treatment</u>
(a) 750 $\mu\text{M}$ $\text{KNO}_2$	→	450 $\mu\text{M}$ $\text{KNO}_2$
(b) 5 mM $\text{KNO}_3$	→	5 mM $\text{KNO}_3$
(c) 750 $\mu\text{M}$ $\text{KNO}_3$	→	No nitrogen (starving)

Resting cell assays demonstrated that the RDX removal rates in the regulator knockout were lower than wild-type when treated with nitrite (450  $\mu\text{M}$ ) and nitrate (5 mM). There was no difference in the degradation rates when both wild-type and the regulator knockout strains were treated with medium that contained no nitrogen source (Fig. 5.30).

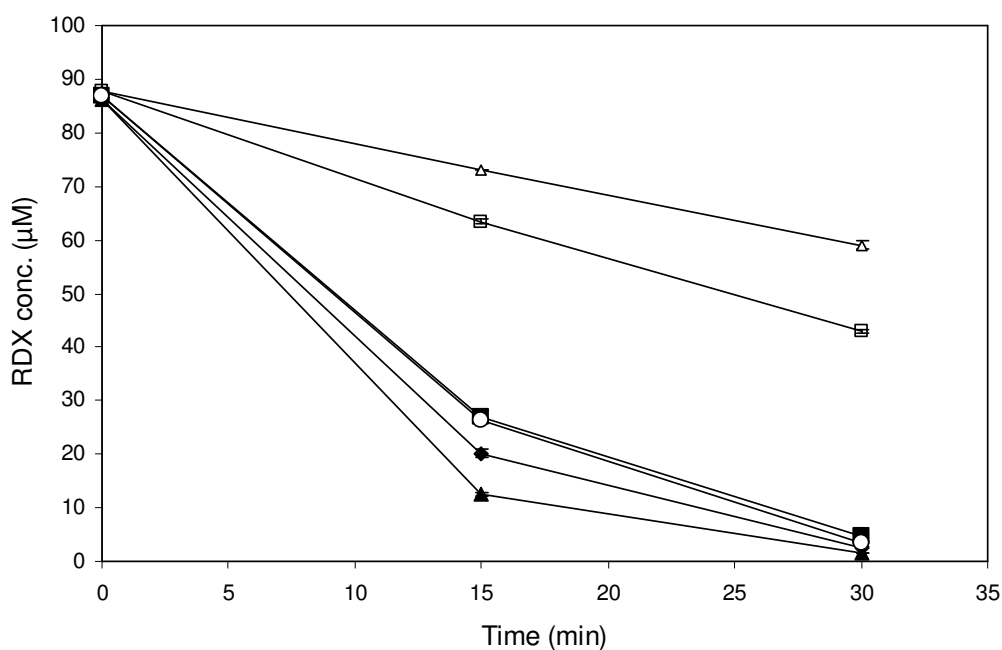


**Figure 5.30. RDX removal by the regulator knockout and wild-type strains.**  $\text{KNO}_2$ -grown cells treated with 450  $\mu\text{M}$   $\text{KNO}_2$  (WT-closed triangles; knockout-closed diamonds).  $\text{KNO}_3$ -grown cells treated with no nitrogen medium (WT-open circles; knockout-closed squares).  $\text{KNO}_3$ -grown cells treated with 5 mM  $\text{KNO}_3$  (WT-open squares; knockout-open triangles). Error bars show one standard deviation for duplicate samples.



### 5.3.3.6 A comparison of RDX degradation and growth of the wild-type and regulator knockout strains in the presence of alternative nitrogen sources

Studies have shown that RDX degradation by whole cells was delayed in the presence of alternative nitrogen sources (Nejidat et al., 2008, Jung et al., 2011). To investigate whether the RDX degradation in the wild-type and regulator knockout strains is also affected by the presence of alternative nitrogen sources, growth experiments were performed with different nitrogen sources.

Cells were grown in minimal medium contained RDX only or RDX with additional nitrogen sources (nitrite/nitrate) and RDX degradation was monitored over the incubation time. For the wild-type strain, RDX was degraded at the fastest rate when no alternative nitrogen source was supplemented in the medium, with 91 % of RDX removal after 12 h of incubation (Fig. 5.31). The presence of alternative nitrogen sources delayed the RDX degradation in wild-type. In the presence of  $\text{KNO}_3$  or  $\text{NaNO}_2$ , approximately 59 % and 49 % of the RDX was degraded, respectively, within 12 hours after inoculation.

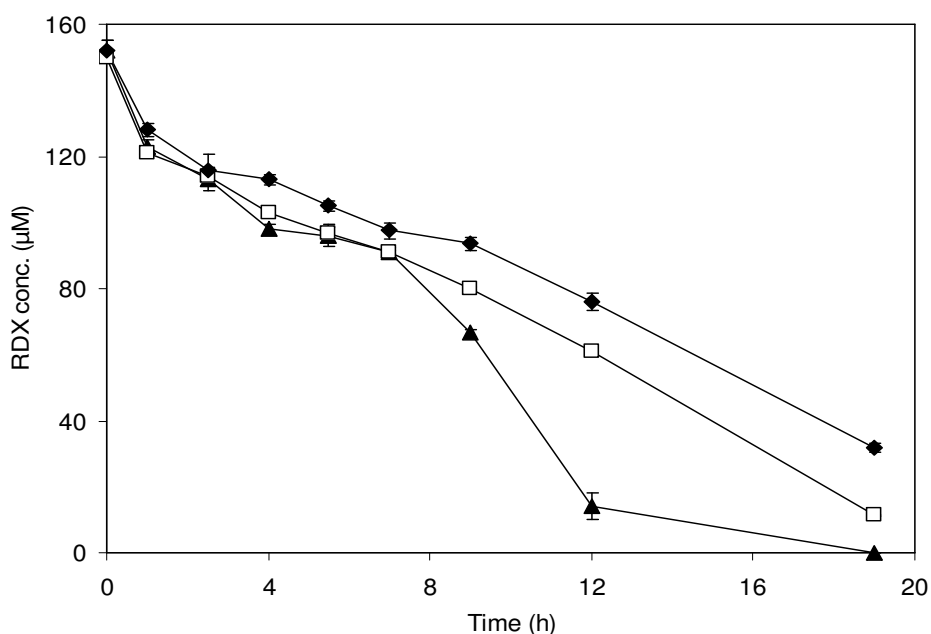


**Figure 5.31. Effect of nitrogen on RDX degradation in strain 11Y wild-type.** RDX alone (closed triangles), supplemented with 5 mM of  $\text{KNO}_3$  (open squares) and  $\text{NaNO}_2$  (closed diamonds). Error bars show one standard deviation for duplicate samples.

The growth of wild-type cells was monitored by measuring the optical density (OD) at 600 nm. While cells in medium containing RDX-only and RDX supplemented with nitrite grew at a similar rate, cells in medium containing RDX supplemented with nitrate grew faster (Figure 5.32).

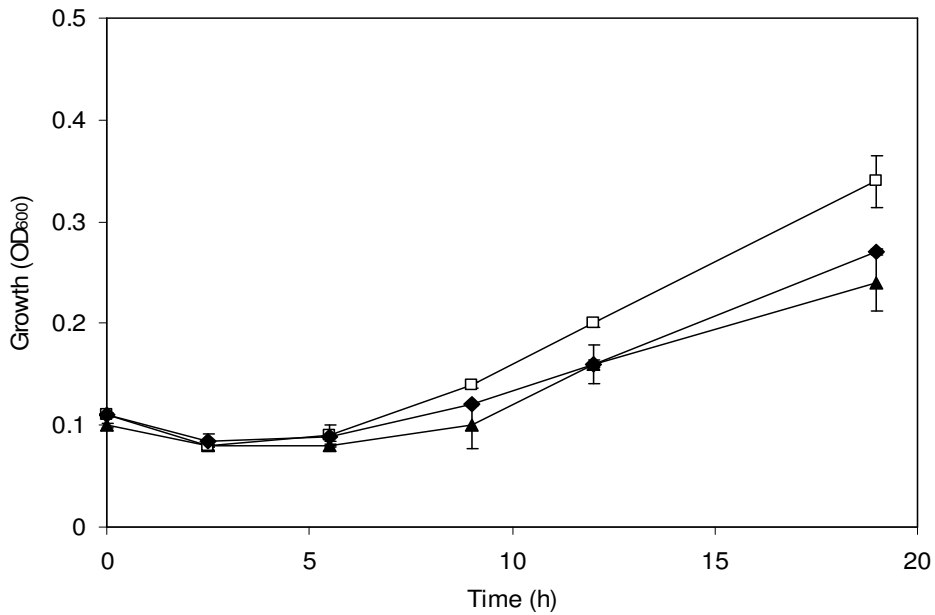


**Figure 5.32. Growth profile of strain 11Y wild-type.** RDX alone (closed triangles), supplemented with 5 mM of KNO<sub>3</sub> (open squares) and NaNO<sub>2</sub> (closed diamonds). Error bars show one standard deviation for duplicate samples.

The effect of nitrite and nitrate on RDX degradation by the regulator knockout strain was found to be similar to wild-type (Fig. 5.33).

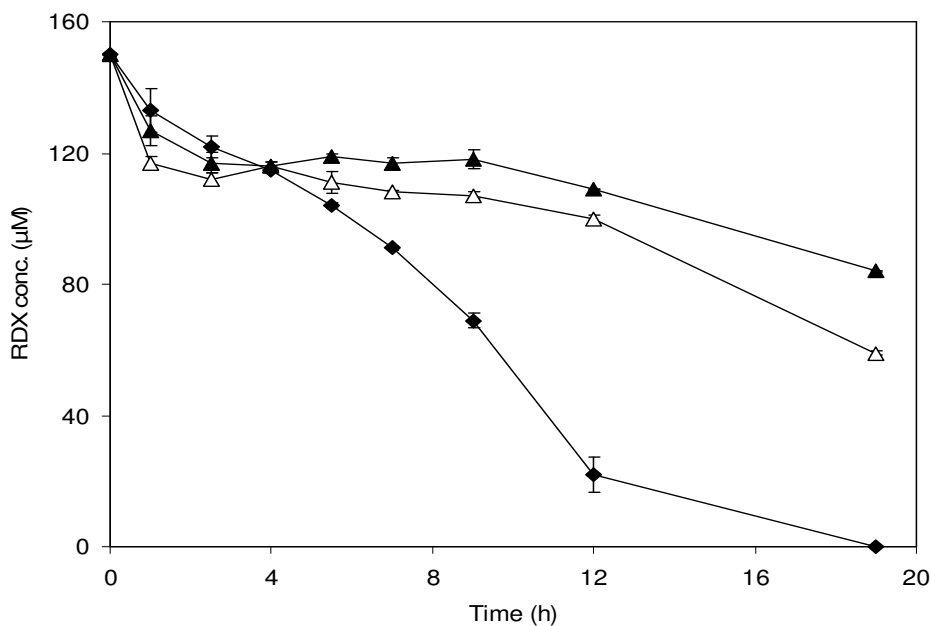


**Figure 5.33. Effect of nitrogen on RDX degradation by growing cells of the regulator knockout strain.** RDX-alone (closed diamonds), supplemented with 5 mM of KNO<sub>3</sub> (open triangles) and NaNO<sub>2</sub> (closed triangles). Error bars show one standard deviation for duplicate samples.

While the regulator knockout in medium containing RDX-only and RDX supplemented with nitrite grew at similar rates, cells in medium containing RDX supplemented with nitrate grew slightly faster (Figure 5.34).

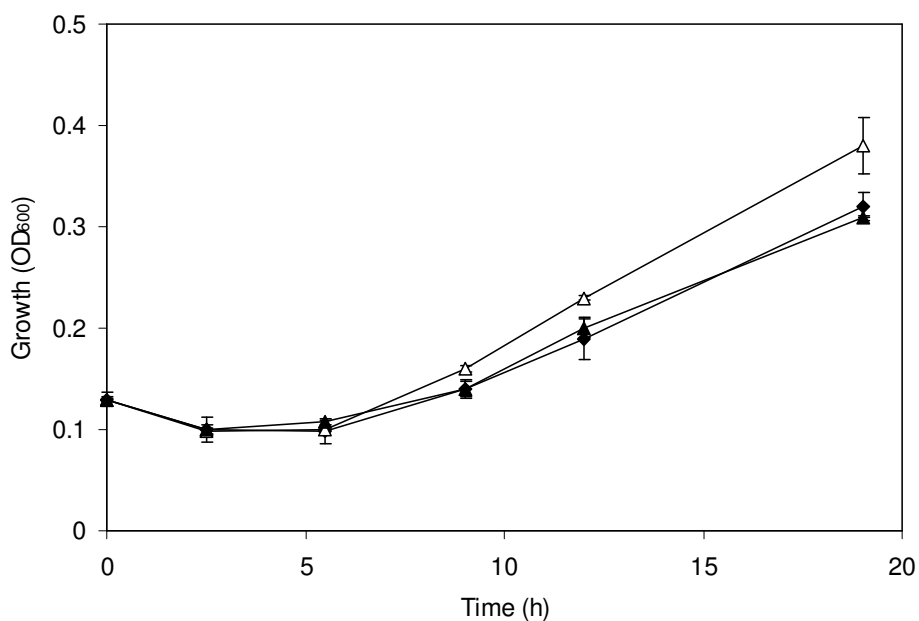


**Figure 5.34. Growth profile of the regulator knockout.** RDX alone (closed diamonds), supplemented with 5 mM of KNO<sub>3</sub> (open triangles) and NaNO<sub>2</sub> (closed triangles). Error bars show one standard deviation for duplicate samples.

When the RDX degradation rates of both wild-type and putative regulator knockout strains, grown in medium containing the same nitrogen sources (RDX-only, RDX + KNO<sub>3</sub> or RDX + NaNO<sub>2</sub>), were compared, a similar RDX degradation rate was observed to that grown in medium contained RDX-only (Fig. 5.35A). However, in medium containing RDX + KNO<sub>3</sub> and RDX + NaNO<sub>2</sub>, the RDX degradation rate for the knockout strain was slower than wild-type (Fig 5.35B and C).

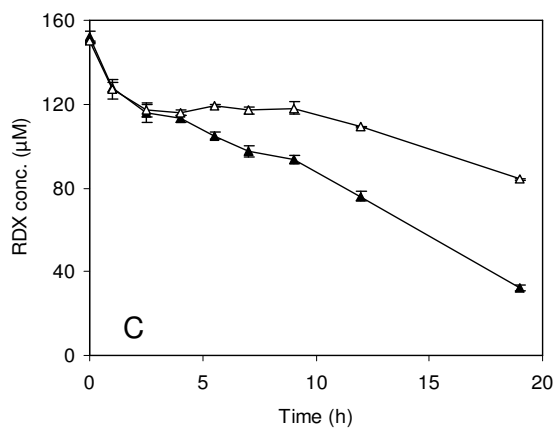
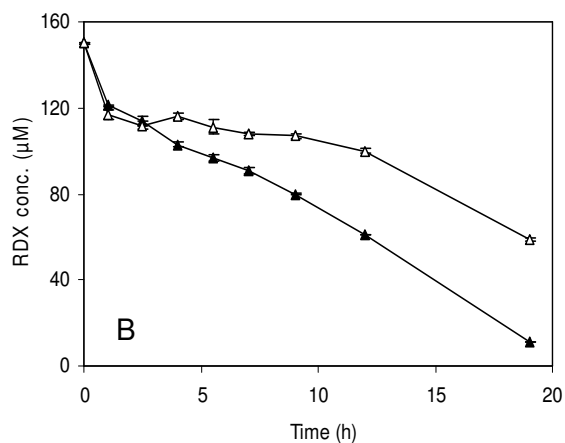
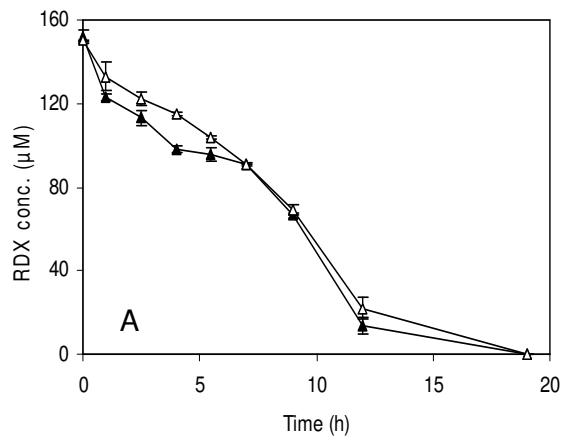


**Figure 5.35. Comparison of RDX degradation between regulator knockout and wild-type strains.** Strains 11Y WT (closed triangles) and regulator knockout (open triangles) were incubated in minimal medium contained different nitrogen source: (A) RDX-alone, (B) RDX and  $\text{KNO}_3$ , (C) RDX and  $\text{NaNO}_2$ . Initial concentration for RDX and other nitrogen sources ( $\text{KNO}_3$  or  $\text{NaNO}_2$ ) was 150  $\mu\text{M}$  and 5 mM, respectively. Error bars show one standard deviation for duplicate samples.

## 5.4 Discussion

A total of four gene knockouts of *R. rhodochrous* 11Y (MarR-like regulator, permease, *xplB* and *xplA*) were successfully constructed using an unmarked gene deletion system (van der Geize 2001). The mutagenic plasmids were transferred into the genome of strain 11Y by conjugation, and following selection stages, gene deleted strains were obtained. There are fewer tools available to manipulate the DNA in Gram-positive bacteria compared to *E. coli*. This unmarked gene deletion system is one of the most efficient systems to delete a gene from the genome of Gram-positive bacteria and successful cases of the gene deletion using the same approach in *Rhodococcus* spp. have been reported (Yang et al., 2007, Rosloniec et al., 2009, Okamoto et al., 2010, Wilbrink et al., 2011).

The genus *Rhodococcus* is well known to have the ability to metabolise broad range of organic compound, such as naphthalene (Kulakov et al., 2005), polychlorinated biphenyl (Seto et al., 1995), atrazine (Behki et al., 1993, Shao et al., 1995) and RDX (Fournier et al., 2002, Seth-Smith et al., 2008). Multiple transformation systems for PCB degradation in *Rhodococcus* strain RHA1 have been reported (Seto et al., 1995). Besides this, multiple homologues of alkane hydrolase and extradiol dioxygenase have also been identified in *Rhodococcus* strain Q15 and *Rhodococcus* sp YK2, respectively (Whyte et al., 2002, Iida et al., 2002). To investigate whether *xplA* is the sole RDX degrading gene in *Rhodococcus* strain 11Y, this gene was deleted, and the resulting *xplA* knockout characterised. The *xplA* deleted strain was unable to degrade RDX in liquid medium in growth and resting cell experiments showing that XplA is the only RDX degrading gene presence in strain 11Y.

When grown on RDX dispersion agar, a defined zone of clearance was observed around colonies of the wild-type strain and these were not seen when the *xplA* knockout strain was grown on similar medium (Figure 5.16). This shows that XplA activity is directly linked to the zone of clearance formation mechanism. While RDX is being degraded by XplA within 11Y, a gradient diffusion of RDX through the surrounding agar occurs. This leads to solubilisation of insoluble RDX and thus a zone of clearance around the colonies develops.

Recombinant XplB has been shown to transfer electrons from NADPH to XplA for RDX degradation (Jackson et al., 2007). It was therefore not surprising that the *xplB*

knockout strain showed reduced RDX activity when compared to the wild-type in growth and resting cell experiments. But, that some XplA activity is retained in the *xplB* knockout suggests that XplA is able to obtain reducing equivalents from another source. Heterologous and homologous expressions of *xplA* without *xplB*, into non-RDX degraders (*E.coli*, *R. rhodochrous* CW25 and *R. jostii* RHA1) are able to degrade RDX *in vivo* (Seth-Smith et al., 2002, Jackson et al., 2007, Indest et al., 2010). This indicates that one or more surrogate reductases, that can partner XplA for RDX activity, are present in the non-RDX degraders. Importantly, this also demonstrates that the transfer of *xplA* alone from donor to recipient naturally in the microbial environment is sufficient for the recipient to acquire the ability to degrade RDX.

In bacteria, genes encoding related functions are frequently situated close to each other (Williamson et al., 2006, Yu et al., 2007). The putative *permease* (ORF 29) located upstream of the *xplA/B* genes cluster in strain 11Y was speculated to be involved in the transport of RDX. Characterisation of the permease knockout strain showed no differences in RDX removal in both growth experiments and resting cell assays when compared with the wild-type, implying that there might be more than one transporter involved in the uptake of RDX. It is reported that L-lactate permease (LldP) and glycolate permease (GlcA) in *E. coli* are able to take up the 2-hydroxymonocarboxylic acid substrates (Nunez et al., 2002). A second example is the succinate transport system in *Rhizobium tropici* CIAT899 (Batista et al., 2009). An insertion mutant of the first succinate transporter (DctA permease) was unexpectedly able to use succinate as a sole carbon source (Batista et al., 2001). The second succinate transporter (KgtP permease) was uncovered by Tn5 mutagenesis of *dctA* mutant.

Sequence analysis indicates that ORF 29 encodes a putative transporter with homology to the amino acid permease from *Mycobacterium vanbaalenii* PYR-1, with 76 % sequence identity. (<http://blast.ncbi.nlm.nih.gov/Blast.cgi>). Transmembrane helix prediction using software TMHMM Server version 2.0 (<http://www.cbs.dtu.dk/services/TMHMM/>) showed twelve transmembrane helices present in this putative transporter. Based on sequence analysis, the permease in 11Y might be involved amino acid transport. Uncharacterised ORF 30 (Fig. 5.26), which located in between the putative permease (ORF 29) and *xplB* (ORF 31) of the strain 11Y RDX gene cluster, encodes a putative dihydrodipicolinate reductase. This

reductase has been shown to be involved in the L-lysine biosynthesis pathway and the initial substrate of the pathway is L-aspartate (Rodionov et al., 2003). Therefore, it would be interesting to investigate the role of the putative permease in transport of L-lysine and L-aspartate in strain 11Y. Due to time limitations, studies investigating the putative permease as L-lysine and L-aspartate transporter were not carried out.

An investigation into the regulation of *xplA* demonstrated that a basal level of XplA was produced when cells were grown in medium containing excess nitrogen (5 mM KNO<sub>3</sub>). The XplA activity was further induced by nitrogen-limiting (450 μM KNO<sub>2</sub> or KNO<sub>3</sub>) and starving (no nitrogen) conditions. So far, there is no record in the literature reporting that XplA activity could be induced by low nitrogen availability in the medium. The presence of RDX (conditions (e) and (f) in Table 5.2) further induced the XplA activity. The XplA activity assays in cell free extracts and western blot analysis are in agreement with the result of the resting cell experiments. Collectively, these findings confirmed RDX is able to act as an inducer for XplA expression in strain 11Y.

Palindromic sequences have been found in the upstream of haloalkane dehalogenase (*dhaA*) and an ATPase (*ParA*) genes in *Rhodococcus* spp. (Kulakova et al., 1997, De Mot et al., 1997). Generally, the presence of palindromic sequence could lead to the hairpin formation of the DNA and allow regulator to interact with the DNA, resulting in the repression or activation of the transcription (Perera and Grove, 2010). Sequence analysis of the promoter regions in 11Y failed to identify any palindromic sequences ([http://www.biophp.org/minitools/find\\_palindromes/demo.php](http://www.biophp.org/minitools/find_palindromes/demo.php)). Two putative promoter regions were located within the RDX degrading gene cluster in strain 11Y (Fig. 5.26) which implies that more than one type of regulation mechanisms could be involved in controlling XplA expression. In resting cell assays (Figure 5.22), two types of XplA induction were observed, one in which the XplA expression is induced by the low nitrogen availability conditions and RDX. Bioinformatic analysis of the *Gordonia* sp. RDX degrading gene cluster revealed only one putative promoter (Indest et al., 2010).

In the presence of high concentrations of nitrite or nitrate (5 mM), RDX degradation in 11Y wild-type was reduced when compared to when RDX only was present in the medium (Section 5.3.3.6). Similar results were observed in *Rhodococcus* strain YH1 (Nejidat et al., 2008) and *Gordonia* strain KTR9 (Indest et al., 2010), suggesting a similar RDX regulation system is present in these RDX degrading bacteria.



Sequence analysis suggests that the putative transcriptional regulator (ORF 27) in the 11Y gene cluster is a MarR-like regulatory protein, a multiple antibiotic resistance regulator in *Gordonia bronchialis* DSM 43247 (protein ID: 62 %). MarR, probably amongst the best characterised regulator protein from MarR family, is a repressor that controls the gene expression of multiple antibiotic resistant *marAB* operon in *E. coli* (Alekhshun and Levy, 1997). Structural studies have revealed that salicylate is able to complex with MarR (Alekhshun et al., 2001), which is unable to bind to the operator region of *marAB* and allows transcription. Many other MarR-type regulators are also reported to be negative regulators (Park and Kim, 2001, Fuangthong et al., 2001, Providenti and Wyndham, 2001, Wilkinson and Grove, 2005). Few of them are found to be activators. BadR from *Rhodopseudomonas palustris* is one example (Egland and Harwood, 1999). It is interesting to observe that the RDX removal rates of the regulator knockout were slower than wild-type whether they were treated with a low (450  $\mu$ M) or high concentration of nitrate (5 mM) (Fig. 5.30). Additionally, section 5.3.3.6 demonstrated that the presence of nitrate or nitrite in the medium delayed the RDX degradation in the regulator knockout compared to wild-type (Figure 5.35). These hint that the MarR-like regulator in 11Y could be acting as a positive regulator in controlling the *xpIA* expression in 11Y. Since these are preliminary studies, further characterisation of this regulator is necessary to understand in more detail how it controls the gene cluster and is integrated in the regulation of central nitrogen metabolism in 11Y. The future works of this regulator are discussed in final discussion chapter.

# Chapter 6

## 6.1 Final discussion

The members of the genus *Rhodococcus* are able to degrade a broad range of organic compounds (Behki et al., 1993, Seto et al., 1995, Seth-Smith et al., 2002, Whyte et al., 2002, Larkin et al., 2005, Kulakov et al., 2005, Bernstein et al., 2011). To date, *Rhodococcus* spp. appear to be the majority of RDX degrading bacteria. The goal of this study was to gain a better understanding on the biodegradation of RDX in *Rhodococcus* spp., specifically exploring the RDX degradation in *Rhodococcus erythropolis* strain HS4 and analysis of the RDX degrading gene cluster in *Rhodococcus rhodochrous* strain 11Y.

The *Rhodococcus erythropolis* strain HS4 was previously found to be able to degrade RDX and its RDX degrading system was characterised as cytochrome P450 system by metyrapone, a P450 inhibitor. However, no *xplA* and *xplB* homologues were detected by both Southern blot analysis (Seth-Smith et al., 2008) and PCR (using primers specific to these genes described in Chapter 3), suggesting this strain could potentially possess an alternative RDX degrading P450. An attempt to purify the protein of interest in HS4 using affinity purification was not successful. Although earlier western blot analysis using XplA antibody revealed a band at the molecular weight of 58 kDa, the band was later confirmed to be an artefact and was also detected in cell free extracts of *Rhodococcus* CW25, a non-RDX degrading bacterium. The most recent studies on HS4 have revealed that it has lost its ability to degrade RDX, possibly encoded on a similar plasmid to that known to contain *xplA/B* in other strains of Rhodococci. Due to the loss of RDX degrading activity in HS4, the investigation on this strain was not continued. The isolation of new RDX degrading gene(s) is an area of particular interest as other RDX strains are likely to exist. *Stenotrophomonas maltophilia* PB1 was the only reported Gram-negative RDX degrading bacterium (Binks et al., 1995). When PB1 cell free extracts was incubated with RDX in phosphate buffer, RDX degrading activity was detected. Unlike strain 11Y, reductase and cofactor recycling system were not required to detect RDX degrading activity in PB1 cell free extracts. This suggests that the RDX degrading system in strain PB1 could be different from XplA/B system in strain 11Y.

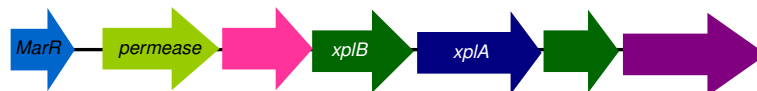


**Figure 6.1. XplA/B gene cluster in *R. rhodochrous* 11Y.**

At present, two distinct plasmid-encoded gene clusters flanking with the *xplA* and *xplB* have been successfully found (Adeer et al., 2009, Indest et al., 2010). The gene cluster from *Microbacterium* sp. MA1 contains nine open reading frames (ORF) including two transposases (Figure 1.11). The other gene cluster is from *Gordonia* sp., which has four open reading frames (Figure 1.12). Bioinformatics revealed that the RDX degrading gene cluster in strain 11Y is nearly identical (>99.8 % amino acid identity) to the gene cluster from *Microbacterium* sp. MA1, with the exception of the transposases (ORF 28 and 35), which were absent in the 11Y gene cluster (Figure 6.1). Interestingly, recent sequence comparisons of the RDX degrading clusters in RDX degrading *Rhodococcus* spp. that were isolated from geographically distinct location (Belgium, UK and Australia) revealed more than 99.8 % amino acid sequence identity to the 11Y gene cluster (Dana Sabir, personal communication). The finding suggests the gene cluster may have been transferred via the horizontal gene transfer prior to its global distribution. Recently studies demonstrated the pGKT2 containing *xplA/B* gene cluster could be transferred by conjugation (Jung et al., 2011). Of 26 recipients, pGKT2 was successfully transferred from *Gordonia* sp. KTR9 to *Gordonia polyisoprenivorans*, *Rhodococcus jostii* RHA1 and *Nocardia* sp. TW2, conferring the recipients the ability to degrade RDX and to utilise RDX as a sole source of nitrogen.

Heterologous expression of the rhodococcal permease in *E. coli* successfully resulted in this protein being incorporated in the membrane, which was confirmed by peptide mass fingerprinting. Cells of *E. coli* Rosetta 2 were found to be able to express the permease; however, whole cell uptake assays did not show higher RDX uptake in the permease-expressing clone compared to the control (non-expressing clone). A

permease deleted strain derived from *Rhodococcus* strain 11Y was constructed using the unmarked gene deletion system. Characterisation of this knockout strain including growth experiments, resting cell assays and western blot analysis revealed no significant difference in comparison to the wild-type. More than one type of transporters can be involved in uptake of the same substrate in bacteria (Batista et al., 2001, Nunez et al., 2002, Batista et al., 2009). However, to prove if the 11Y permease is the RDX transporter, the *in vitro* RDX uptake assays would need be performed using the constructed proteoliposomes. Although the transporter of RDX in strain 11Y remains unknown, by using a Tn5-based random mutagenesis approach may help to identify the RDX transporter (Fernandes et al., 2001).

The *xplA* knockout lost its ability to degrade RDX suggesting XplA is the only enzyme that degrades RDX in 11Y. The *xplB* knockout confirmed XplA could obtain reducing equivalents from another source. Perhaps this is not surprising as a total of three reductases were found in the genome of *Rhodococcus* sp. RHA1 (McLeod et al., 2006). Also, expression of XplA in non-RDX degrading bacteria (*E. coli* and *Rhodococcus* spp.) and plants (*Arabidopsis*) demonstrated RDX degrading activity, indicating the flexibility of XplA to partner other reductase(s) for RDX activity (Rylott et al., 2006, Indest et al., 2010).

An investigation into the regulation of *xplA* in strain 11Y was performed. Resting cell experiments using the wild-type strain revealed that the basal XplA activity was detected in excess nitrogen medium. XplA activity found to be induced in nitrogen-limiting or no nitrogen medium, and the activity further enhanced by RDX. Growth experiments of the wild-type cells also showed that RDX degradation in medium containing excess nitrogen was delayed when compared to cells were growing in RDX only medium. These findings imply that *xplA* expression in 11Y is regulated and the regulation is linked to the central nitrogen metabolism in 11Y. Nitrogen control in *Rhodococcus* spp. has not been well studied to date; however, the general patterns of nitrogen metabolism and regulation in Gram-positive bacteria has been reviewed by Amon and co-workers (2010). The regulatory network of nitrogen metabolism in *Corynebacterium* sp., a close related bacterium to *Rhodococcus* strain 11Y, revealed the involvement of a global nitrogen regulator (AmtR).

AmtR-DNA binding studies demonstrated 35 nitrogen genes are directly regulated by AmtR in *Corynebacterium glutamicum* (Jakoby et al., 2000, Beckers et al., 2005, Buchinger et al., 2009, Amon et al., 2010). Some examples of these genes are *glnK*, encoding nitrogen regulatory protein PII, *gltB*, encoding glutamate synthase, *ureC*, urease alpha subunit and *amtA*, encoding an ammonium transporter. Based on the AmtR consensus motif of *Corynebacterium* sp. (ATCTATAGN<sub>1-4</sub>ATAG) (Burkovski, 2003), homologues of putative AmtR binding sites on 11Y gene cluster were found. These putative binding sites were located on -10 boxes of the putative promoter regions of the gene cluster: AaCccTAtN<sub>4</sub>gTAG (upstream of permease) and AaCTgTAaN<sub>2</sub>ATAG (upstream of *xplB*), with 3-5 nucleotides differences compared to the AmtR consensus motif of *Corynebacterium* sp (nucleotides differences marked with lower case + underline).

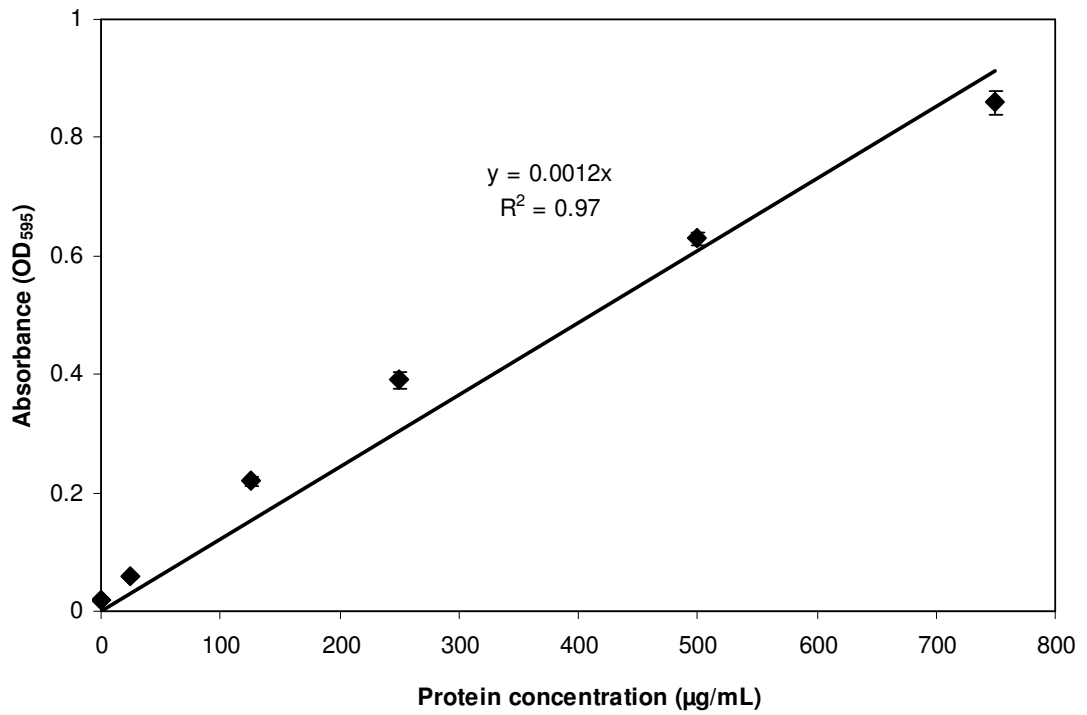
The MarR-like knockout strain when previously exposed to nitrogen-excess or limiting conditions degraded RDX more slowly than the wild-type cells in whole cell experiments. Also, growth experiments performed in medium containing RDX plus nitrite/nitrate demonstrated the RDX degradation in the MarR-like knockout strain was slower compared to wild-type. These findings imply that the putative 11Y regulator could be positively regulating the *xplA* expression in 11Y. Although the majority of the MarR-like regulators are repressors, there have been a few reports where these proteins have been shown to be activators. RosR, a MarR-like regulator controls multiple genes in *Corynebacterium* sp. (Bussmann et al., 2010), as a repressor for genes encoding monooxygenase and glutathione S-transferases and, as an activator for genes encoding the putative nitrate/nitrite transporter and nitrate reductase. Since two putative promoter regions were identified on the RDX degrading cluster in 11Y, electrophoretic mobility shift assay (EMSA) could be carried out to identify if these regions are able to interact with the 11Y MarR. The role of MarR in regulating genes in 11Y can be further investigated by comparing the global gene expression between the MarR knockout and wild-type by DNA microarray experiments. Genes that are up or down-regulated can be identified and EMSA will confirm the role of MarR in controlling these genes in 11Y.

The regulation of herbicide atrazine - degradative genes (*atrR-atrDEF*) in *Pseudomonas* sp. strain ADP (Govantes et al., 2010) was found to be similar to the regulation of RDX degrading genes in *Rhodococcus* strain 11Y. The *Pseudomonas* sp.

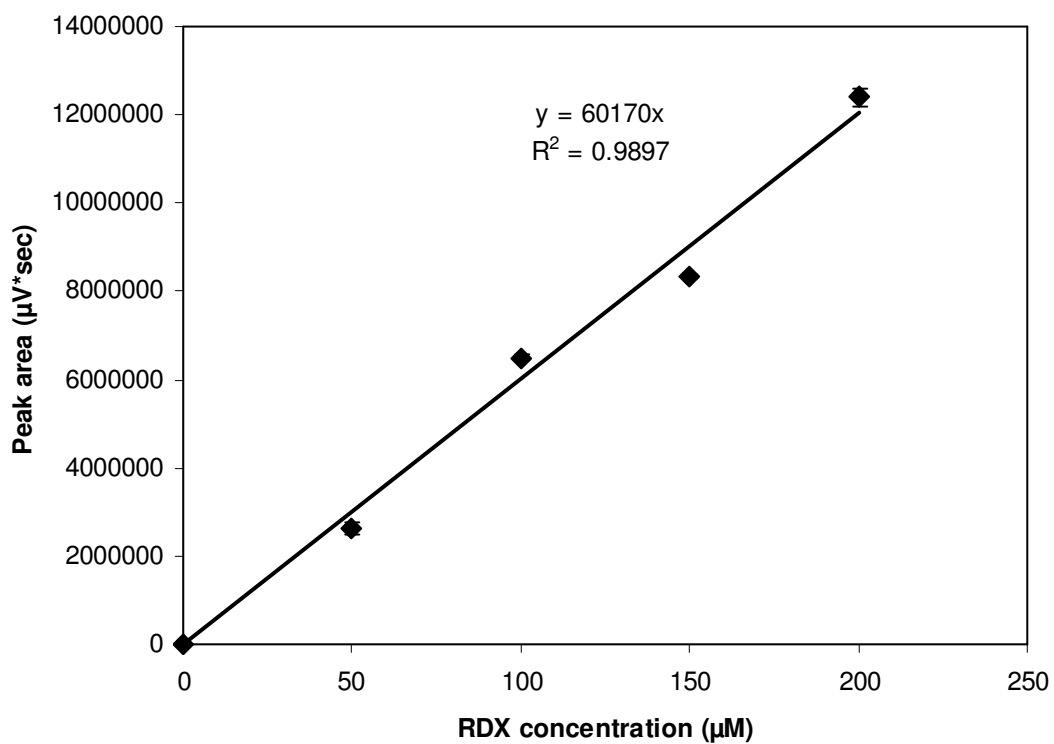
strain ADP is able to use atrazine as the sole nitrogen source (Garcia-Gonzalez et al., 2003). The atrazine degradation using whole cells, which was previously grown in rich nitrogen medium, was inhibited. Efficient atrazine degradation in the strain was observed when using cells previously grown under nitrogen-limiting conditions, on atrazine or on an intermediate product of atrazine degradation cyanuric acid. The regulatory network of atrazine degradation that integrates to the central nitrogen metabolism in *Pseudomonas* sp. has recently been described (Hervas et al., 2008, Govantes et al., 2010). The transcription of *atzR*, encoding a regulator that controls the atrazine gene cluster (*atrDEF*), is activated by a global nitrogen regulator NtrC. AtzR activates *atrDEF* transcription when two type of signals are sensed: cyanuric acid and nitrogen limitation, by a PII signal transduction protein (GlnK), resulting in expression of genes on the cluster (*atrDEF*). Based on the similar induction pattern between atrazine and RDX activities in the whole cell assays, it is possible that the regulation of RDX degradation in 11Y is similar to the regulation of atrazine degradation. It would be interesting to investigate the regulatory network for RDX degradation that links this to the central nitrogen metabolism in strain 11Y. The genes involved in the regulatory network for example a global nitrogen regulator and PII signal transduction protein could be identified and their role in *xpIA* regulation in 11Y investigated.

The key finding in this study was that the RDX degrading activity in whole cells was induced by nitrogen-limiting conditions and further induced by RDX. This information is particularly useful for the remediation of RDX contaminated areas. Efficient biological treatment of RDX contaminated sites could be achieved by optimising the treatment parameters, which one of them is the nitrogen levels at the treatment site (e.g. adjusting the nitrogen levels at the treatment site). Isolation of RDX degrading strains that are able to metabolise RDX efficiently under rich and low nitrogen conditions would be an area of particular interest as this strain could degrade RDX efficiently without being affected by the level of nitrogen.

## Appendix A: Typical protein assay standard curve

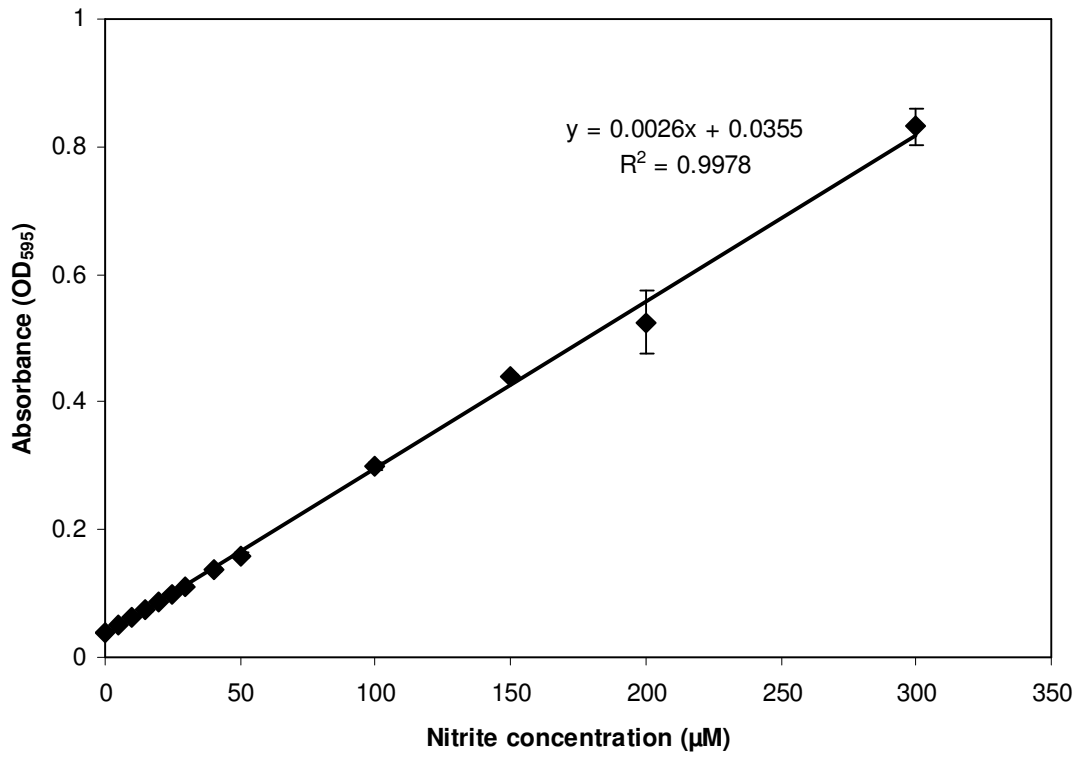


## Appendix B: Typical RDX standard curve





## Appendix C: Typical nitrite standard curve



## Appendix D: Sequencing analysis for knockouts

A shorter PCR product was amplified in the gene-deleted strains. Sequencing analysis revealed that the gene (permease, regulator, *xp/A* or *xp/B*) in the knockout was deleted. The gene deleted sequence was indicated with dash (-).

### a) permease knockout

```
TCTCGATTATCGAGAGACTAGATCATCGAGCGAAGTCGCGTACGGTGAACCTCGTGACGAACGAC
GATCTGGTGCACCGGCTGCGTTCGCTGACCGTCAACTCGATGTCTTCGGGGCCGGCTTCGCCG
CCCGAAACGGGTTCACGCCACCGATGTACGTGCCCTGATCGCTCTTCTGGACCGGGATCGGGC
CGGCGCCGTCGCCTCTCCTGGGTGGCTGGCGGGGCATCTCGGACTCAACAGTGCCTCGACCACC
GCGCTCATCGATCGACTGGAATCGAAGGGTCTGGTGGACCGCAGGCGCGACGACTCGGATCGTC
GCCGGTTCGCGTGCACGTCACCGACGCGGCCAGGAGATGGGCTGGACCTTCTTCGGGCCGTT
GATCGACCAGGTGATCGCGGTGGCCGACGGTTTCTCCGACGACGAACTGACCACGATCCGCACA
TTTCTGGACCAGGTCACCGCTGCGGTGGCGGGAGTCCGGACCCGCTGAGTGTCTGGGTCCGCA
GCCGCTGACCCTGTCCGCACACCGCTCACCTCAGGGTTCGAAACCGGAGCCGTCCGCCCGATGGTT
ACCGGAACATGACCATTGTTAATTCTGCGTTCCGGCCCTGGCGTCAAAAAACCCTATGTTTGTAG
TATTTGGCGAAATCCGTTTGGCGTCAGGAGATTTCAGGCATGGCCACGACGAATGTGTATCCGAC
AGACGAGGGGGTCCCGGACCGGACGCGCCAGATGCTGGCCGAACTCGGTTATACGTCC-----
```

Stop codon of MarR regulator (ORF 27)

Permease gene (ORF 29) was deleted

Start codon of dihydrodipicolinate reductase (ORF 30)

```
TAGCGACCATGACGAACATCAGAGCTGTCTGTACGGCGTCGGAGCGATGAACTCCGTGATCAC
CCGCTATCTGCTCGACAAGGACGTCGAGATCGTAGGCCCATCTCGCGCAGTCCGGACAAGGTG
GGCAAGGACCTCGGCGAGGTCACCGACTCGACCGTTCGACTCGGAGTGTGATCAGCGACGACC
CGCACGAGGTGTTACGCGGACGAGTCCCGACATCGCGGTCGTCGCGATCACCAGCTATCTCGT
GGACGCCGCGGAGCACTTCCGTATCGCACTGTGCGACGGGGTCAACGTGATCACGCTGTCCGAG
GAAGCGCTCTATCCCTGGAACACCGCGCCC GAACTGACCGCGGAACTCGATGCACTCGCCAAGG
AGCATGGCGTGACCATCACGGGCGGGGGTTTCCAGGACAGCTTCTGGGTGAACCGGTCGCCCA
GCTGATGGGCACGGCACACCGCATCGACTCGGTCACCGGGACGAGTTTCGTGGAACGTGACGAG
TACGGCCC GAACTGGCCGAGCTGCAGCAGGTCGGCGCGACGATCGAGGAGTTCGACGCCTGGT
GCCGAGAAGCCGTGCGTCCGCCACATTCGGCCGGATCGCTCTCGATGCGCTGGTCGCCGGAGC
GGGGCTGACGCCCAAGCAGATCCTGACGCGCACCGAACCCGAACTGGCACACGAGACTCTGCAC
TGTGCTGCCCTGGGGATCGACGTCCCGCCGGAAAGTGCATCGGCTTACCGACATCGACGAGA
TCCGCACGGAAGAGGGCCCGGTCTTCGTCTTCCGGATGTCCGGCCGGCTGTACGGCCCCGACGA
```

CAGCGATGTCAACGAATGGACGATCCACGGCGAACCCGATCTGGTGATGTCCAACGGCACCCCG  
CCGACGATGGCCACCACCTGCACCCAATTGGTGAACCGTATCCCCGACGTGCTCGA

## b) MarR regulator knockout

GAGAGAGCGCGGCCCGTCGGGGCCGCTTCGGTACGATCGTCCGAGTCTTCGGGAAACCGGCTCC  
TGCGCAATACATCTGGGTCCACAGCGTTCCGGGTCGGTCCCACGTGTCTCCCACGAGAGAAAC  
CGTCGCAGACGCGGGGGAGTGGGCGCGATGAGCGTCGGGATGGCGTGCTGCAGATAGGCGATAC  
GGAGTCCTGCGAAACACGATGTGCGGTTCGAGCAGTGCCAGGTTGCGTACGCGAGCACCGTGTTG  
CCCGGTCGCGAAGCCCAGCGCGATCATCGCGCCGTACGAGTGGCCGACGACGTCGACCGTGTCG  
GTGGCCGCGGGATGGACGGCGATGTGGGCGCTGCTGATTGCGTCGGGGATCCGGTCGAGAACGG  
CTGCGAGCCAGTCGAATAGCTCGGCGGGAGCTCGTGGGCTCGCAGCGCCGGGACGGGACCGTCC  
GGCGTCGCCGAGGAGGTCGACGGCGATGACGTGGCGACCGGTCGCCAGGTGTTCCATGACGTTT  
ACATACGACATCGACGTGGCTCCGCCGCCCGCAAAGGACCAGCGGCACGGCGTCGAGGGGCA  
CGGCGTCGGGGGTGTCCGGGCGCGCCCGATGATCGTGACCCGGGTGATGCCGTGCGCCGTCTC  
GACATCGATCGGATGCCCTCCCGAGCGTGCAGGAGCGCGTCTAGGCGTCGAAAAACGCGATG  
CCCTGCGGCGTGGCGGCGAAGACGTCGAGTGTGGGC---

MarR gene (ORF 27) was deleted

Start codon of *permease* (ORF 29)

AGTATTTGGCGAAATCCGTTTGGCGTCAGGAGATTCAGGCATGGCCACGACGAATGTGTATCCG  
ACAGACGAGGGGGTCCCGACCGGGACGCCAGATGCTGGCCGAACTCGGTTATACGTCCGAAT  
TCAAACGGGAGATGAGTCCGTGGGCGAACTTCGCCCTCGGCTTACCTACCTGTGCCCCGTCGT  
CGGGATCTACACGGTCTTCGCCTATGCGATGGCACAGGCCGGCCCGCCGATGATCTGGAGCCTC  
GTCATCGTGGGCTCGGGCAGTTCCTGGTGGCGCTGATCTCAGCGAGGTCGTCGCCAGTTCC  
CGGTCGCGGGGGCGTGTATCCGTGGACACGCCACTCTGGGGCCGGAAGTACGCGTGGATGAC  
GGGCTGGGTGTATCTGATCGCGCTGCTCGTCACCATCGGTTCCGGTCGCCCTACGGATCGGGGCCG  
TTCATCGCGTCGCTCTTCGGCTACGAGGCGACCGCCTGGACCATCGCCCTGTGTGGTGTGGTGA  
TGGTCGCCATCGCGACCGCCATCAACTTCCTCGGCACCAGGTTGGTCTCGGCGGGCCCGTCTT  
CGGTTTCGCCCGGAGCTGATCGGCGCCCTCGTGGTGGCGTGTATCTGATCGCCACACACCGG  
CAGGTCGATCTGAGTGCCCTCTTCGACTCGTTCGGCGCCT

c) *xpI*A knockout

GTGCGCTCCACGCCACCGACGCCAAGTTTCGACCCGGTGATGATGCGTGAACCTGGCGCACCTGG  
CGTCGACGGAGTTCCGCCTCGCCGATGCGGGGGTGCTCGCCACGGCAGAGTCCTCCGACCCGCG  
GAGTGGCGCCCTGGCCCACGTCGTCGAACGCGAGAGCCCCGGCGGCACCGGCCACGACGGTGGTG  
TTCCACTTCGGATCGACCCCGGTTCGAGGTGATCGGCACCGACCGCGCGGAGGCCGTCAAGGTGC  
GCACCGGCGTGCACACCACGACTCTCGCGTGCACACCGTCATCACCGCAATCGGTTTCGAGTC  
GGCCGTAAACGACGACCTCGACCTGACGCTGTACCGCGACGCCGATCCGGGAGAGGATTTTCTT  
GCTCCGGGCCTGTACCGCACCGGGTGGCTGCACAGTTCCACCGGAGCGCTTCCCGAGATGCGGG  
CCCGTGGCCGGCGTTGGCGGCCGAATCCGCCGCGATCATGCCGGTCACCATCCGGCCCGTCC  
GGGTCTGGTGGCAATCCCTTACGAAGTGATCGACCGGACAGTCGATTTTCGACGGCTGGATGCGG  
ATCGACGAGGCGGAGGTCGCCTCGGCCTCGCCGGCCGCATCCGGCAGAAGGTCCGCGAGGTCG  
ACGCGATGCTGGCGTTGGCCCCGACCGTGCCGGCCGAATCGGTCTGCTGAGACGGCAGGCCTGC  
AGTGAACCC-----ATCCGATCTCACCTGCCCGCGACCCGCGGGCAGCTCGATCCACCCGAGA

← *xpI*A (ORF 32) was deleted      Stop codon of *xpI*B (ORF 31) →

GGAATCATCATGTCCGACACGCTCGCGTCCGCTGCCGCGGTCTTCAGAAGTTCTCCCTGGACA  
CCTTCGACGGCCTGGAGTGGGAGGTGATGGGTGTGCGGGAAGGCGGCCGAGGGGCTGCTCGCCC  
AGGTGCGCGACGCGGTGCACAGGGGTGCGACCTGCACGTCGGTGGAGAGCTCGCCGAGCACGG  
ATGGTTCACCCCGGCAGTCCTGACCGGGGTACCCCGGACATGCGCGCTTACCGTGAGGAGCTG  
TTCGGCCCCGGTCCCGTCTATTTCGGTGTCCGACGACGACGAGGCGGTGCTCTCGCGAACG  
ACGTCCCGTTCGGGCTCGGGGGTGCTGTCTTCTCGAGCGACGAGCAGCGGGCGATCGCGGTGCG  
GTCGCGACTCGAGGTGGGTATGGCCAATGTGAACACCTCGGCCGGCGAAGGCGCCGACGTGCCG  
TTCGGCGGAACCAAGCGTTCGGGCTTCGGGCGGGAACCTCGGACCGCTCGGCATCGGCGAATTCG  
TCAACCGGCGCGTCTTCTACGTGCAGCGGTGACCTTCCCGCGGGCCCGCGCGTCGACGCAGCGG  
GGTCTGCGCCCGCTCGCCGCACGACGGTGACCGTTCGGCGCGCGGCCCGCGGAACAGGTGTGCT  
GTCGATCGTCACATGACTAACCTCTAACCGGGACACGGCACATCCGATGATGTGCCGCCCGAGG  
ACGACGGCGTCAGGGCGAAGGGCGGATCAGCGATGGGACGATACGACGAGGCGTTACACGGGC  
GACCGAGGACCGTGAGGGTTTCTGGCTCGACGCGCGTCCGCGATCGACTGGACGGTCACTCCG  
ACGCGGGCGCTCGACGACTCCGCCGCCCGTTCTACCGGTG

d) *xp/B* knockout

GCGCGACGATCGAGGAGTTCGACGCCTGGTGCCGAGAAGCCGTGCGTCCGCCACATTTCGGCCG  
GATCGCTCTCGATGCGCTGGTCGCCGGAGCGGGGCTGACGCCAAGCAGATCCTGACGCGCACC  
GAACCCGAACCTGGCACACGAGACTCTGCACTGTGCTGCCCTGGGGATCGACGTCCCGCCGGGAA  
AGTGCATCGGCTTCACCGACATCGACGAGATCCGCACGGAAGAGGGCCCGGTCTTCGTCTTCCG  
GATGTCCGGCCGGCTGTACGGCCCCGACGACAGCGATGTCAACGAATGGACGATCCACGGCGAA  
CCCGATCTGGTGATGTCCAACGGCACCCCGCCGACGATGGCCACCACCTGCACCCAATTGGTGA  
ACCGTATCCCCGACGTGC-----CCCGAGATGGAGTGTGGAGAATCATGACCGACGTAACTG

*xp/B* (ORF 31) was deleted

Start codon of *xp/A* (ORF 32)

TCCTGTTTCGGAACCGAGACCGGCAACGCCGAGATGGTCGCCGACGACATCGTTTCTGCCCTGGG  
GGAATTCGATATCGAGGCCACCGTGGTGGGGATGGAGGACTTCGACGTCGACAGATCTGGCCGCC  
TCCGGCACGGTCGTGCTCGTCACCTCCACCTACGGAGAGGGTGAAGTCCCGGCGACGACCCAGC  
CCTTCTTCGATGCGATGAAGGCGGCCGAGCCTGACCTCACGGGTCTGCGGTTTCGGGGCCTTCGG  
CCTCGGCGACAGCACCTACGACACCTACAACAACGCGATCGACATCCTCGTCGGTTCGGGTGACA  
GACGCAGGAGCGACACAGGTTCGGCGCAACGGGCGGCACGATGCCGCGTCCTTCCAGCCGGCGG  
ACGGACCCGTGGCCGAGTGGGCCAAACAGTTCGCCGAAGCCCTCTCTGATCGAACTCGACGAGG  
AGGACATGAGATGACCGCTGCGTCCATCGATCGCGAGCTCGTGCCGTGGTTCGGATCCCGAATTC  
AGGAACAACCCCTATCCCTGGTATAGGCGACTGCAACAGGACCATCCGGTGCACAAGCTGGAGG  
ACGGCACCTACCTGGTGTCCCGGTACGCCGACGTGAGTCATTTTCGCGAAACTGCCCATCATGAG  
CGTCGAACCCGGATGGGCCGACGCCGGGCCCTGGGCGGTTCGCGAGCGACAC

# References

- AHMAD, F., SCHNITKER, S. P. & NEWELL, C. J. (2007) Remediation of RDX- and HMX-contaminated groundwater using organic mulch permeable reactive barriers. *Journal of Contaminant Hydrology*, 90, 1-20.
- AKHAVAN, J. (2004) Chemistry of Explosives (2nd edition). Royal Society of Chemistry, Great Britain.
- ALEKSHUN, M. N. & LEVY, S. B. (1997) Regulation of chromosomally mediated multiple antibiotic resistance: the mar regulon. *Antimicrobial Agents and Chemotherapy*, 41, 2067-2075.
- ALEKSHUN, M. N., LEVY, S. B., MEALY, T. R., SEATON, B. A. & HEAD, J. F. (2001) The crystal structure of MarR, a regulator of multiple antibiotic resistance, at 2.3 Å resolution. *Nat Struct Mol Biol*, 8, 710-714.
- AMON, J., TITGEMEYER, F. & BURKOVSKI, A. (2010) Common patterns – unique features: nitrogen metabolism and regulation in Gram-positive bacteria. *Fems Microbiology Reviews*, 34, 588-605.
- ANDEER, P. F., STAHL, D. A., BRUCE, N. C. & STRAND, S. E. (2009) Lateral transfer of genes for hexahydro-1,3,5-trinitro-1,3,5-triazine (RDX) degradation. *Applied and Environmental Microbiology*, 75, 3258-3262.
- ANNAMARIA, H., MANNO, D., STRAND, S. E., BRUCE, N. C. & HAWARI, J. (2010) Biodegradation of RDX and MNX with *Rhodococcus* sp. Strain DN22: New Insights into the Degradation Pathway. *Environmental Science & Technology*, 44, 9330-9336.
- BAILEY, A. & MURRAY, S. G. (2000) Explosives, propellants and pyrotechnics. Redwoods Books, Wiltshire.
- BATISTA, S., CATALAN, A. I., HERNANDEZ-LUCAS, I., MARTINEZ-ROMERO, E., AGUILAR, O. M. & MARTINEZ-DRETS, G. (2001) Identification of a system that allows a *Rhizobium tropici* *dctA* mutant to grow on succinate, but not on other C-4-dicarboxylates. *Canadian Journal of Microbiology*, 47, 509-518.
- BATISTA, S., PATRIARCA, E. J., TATE, R., MARTINEZ-DRETS, G. & GILL, P. R. (2009) An alternative succinate (2-Oxoglutarate) transport system in *Rhizobium tropici* is induced in nodules of *Phaseolus vulgaris*. *Journal of Bacteriology*, 191, 5057-5067.
- BECKERS, G., STROSSER, J., HILDEBRANDT, U., KALINOWSKI, J., FARWICK, M., KRAMER, R. & BURKOVSKI, A. (2005) Regulation of AmtR-controlled gene expression in *Corynebacterium glutamicum*: mechanism and characterization of the AmtR regulon. *Molecular Microbiology*, 58, 580-595.
- BECKHAM, K. S. H., POTTER, J. A. & UNKLES, S. E. (2010) Formate-nitrite transporters: Optimisation of expression, purification and analysis of prokaryotic

- and eukaryotic representatives. *Protein Expression and Purification*, 71, 184-189.
- BEHKI, R., TOPP, E., DICK, W. & GERMON, P. (1993) Metabolism of the herbicide atrazine by *Rhodococcus* strains. *Appl. Environ. Microbiol.*, 59, 1955-1959.
- BERNSTEIN, A., ADAR, E., NEJIDAT, A. & RONEN, Z. (2011) Isolation and characterization of RDX-degrading *Rhodococcus* species from a contaminated aquifer. *Biodegradation*, 1-9.
- BERTHE-CORTI, L., JACOBI, H., KLEIHAUER, S. & WITTE, I. (1998) Cytotoxicity and mutagenicity of a 2,4,6-trinitrotoluene (TNT) and hexogen contaminated soil in *S*-typhimurium and mammalian cells. *Chemosphere*, 37, 209-218.
- BEYCHOK, M. (1987) A data base of dioxin and furan emissions from municipal refuse incinerators. *Atmospheric Environment (1967)*, 21, 29-36.
- BHUSHAN, B., HALASZ, A., SPAIN, J., THIBOUTOT, S., AMPLEMAN, G. & HAWARI, J. (2002) Biotransformation of hexahydro-1,3,5-trinitro-1,3,5-triazine catalyzed by a NAD(P)H: Nitrate oxidoreductase from *Aspergillus niger*. *Environmental Science & Technology*, 36, 3104-3108.
- BHUSHAN, B., TROTT, S., SPAIN, J. C., HALASZ, A., PAQUET, L. & HAWARI, M. (2003) Biotransformation of hexahydro-1,3,5-trinitro-1,3,5-triazine (RDX) by a rabbit liver cytochrome p450: insight into the mechanism of RDX biodegradation by *Rhodococcus* sp strain DN22. *Applied and Environmental Microbiology*, 69, 1347-1351.
- BINKS, P. R., NICKLIN, S. & BRUCE, N. C. (1995) Degradation of hexahydro-1,3,5-trinitro-1,3,5-triazine (RDX) by *Stenotrophomonas maltophilia* PB1. *Applied and Environmental Microbiology*, 61, 1318-1322.
- BONSOR, D., BUTZ, S. F., SOLOMONS, J., GRANT, S., FAIRLAMB, I. J. S., FOGG, M. J. & GROGAN, G. (2006) Ligation independent cloning (LIC) as a rapid route to families of recombinant biocatalysts from sequenced prokaryotic genomes. *Organic & Biomolecular Chemistry*, 4, 1252-1260.
- BRYANT, C. & DELUCA, M. (1991) Purification and characterization of an oxygen-insensitive NAD(P)H nitroreductase from *Enterobacter cloacae*. *Journal of Biological Chemistry*, 266, 4119-4125.
- BUCHINGER, S., STRÖSSER, J., REHM, N., HÄNBLE, E., HANS, S., BATHE, B., SCHOMBURG, D., KRÄMER, R. & BURKOVSKI, A. (2009) A combination of metabolome and transcriptome analyses reveals new targets of the *Corynebacterium glutamicum* nitrogen regulator AmtR. *Journal of Biotechnology*, 140, 68-74.
- BUSSMANN, M., BAUMGART, M. & BOTT, M. (2010) RosR (Cg1324), a hydrogen peroxide-sensitive MarR-type transcriptional regulator of *Corynebacterium glutamicum*. *Journal of Biological Chemistry*, 285, 29305-29318.

- CLAUSEN, J., ROBB, J., CURRY, D. & KORTE, N. (2004) A case study of contaminants on military ranges: Camp Edwards, Massachusetts, USA. *Environmental Pollution*, 129, 13-21.
- COLEMAN, N. V., SPAIN, J. C. & DUXBURY, T. (2002) Evidence that RDX biodegradation by *Rhodococcus* strain DN22 is plasmid-borne and involves a cytochrome p-450. *Journal of Applied Microbiology*, 93, 463-472.
- CRAIG, H. D., SISK, W. E., NELSON, M. D. & DANA, W. H. (1995) Bioremediation of explosive-contaminated soils: A status review *Proceedings of the 10th Annual Conference on Hazardous Waste Research*, 164-179.
- CROCKER, F., INDEST, K. & FREDRICKSON, H. (2006) Biodegradation of the cyclic nitramine explosives RDX, HMX, and CL-20. *Applied Microbiology and Biotechnology*, 73, 274-290.
- DAVIS, J. L., WANI, A. H., O'NEAL, B. R. & HANSEN, L. D. (2004) RDX biodegradation column study: comparison of electron donors for biologically induced reductive transformation in groundwater. *Journal of Hazardous Materials*, 112, 45-54.
- DE MOT, R., NAGY, I. N., DE SCHRIJVER, A., PATTANAPIITPAISAL, P., SCHOOF, G. & VANDERLEYDEN, J. (1997) Structural analysis of the 6 kb cryptic plasmid pFAJ2600 from *Rhodococcus erythropolis* NI86/21 and construction of *Escherichia coli*-*Rhodococcus* shuttle vectors. *Microbiology*, 143, 3137-3147.
- DEGEN, O., KOBAYASHI, M., SHIMIZU, S. & EITINGER, T. (1999) Selective transport of divalent cations by transition metal permeases: the *Alcaligenes eutrophus* HoxN and the *Rhodococcus rhodochrous* NhlF. *Archives of Microbiology*, 171, 139-145.
- DREW, D., LERCH, M., KUNJI, E., SLOTBOOM, D. J. & DE GIER, J. W. (2006) Optimization of membrane protein overexpression and purification using GFP fusions. *Nature Methods*, 3, 303-313.
- EDWARDS, J. (2006) Biodegradation of the high explosive RDX by a cytochrome P450 from *Rhodococcus* sp., Department of Biology, University of York. Ref Type: Thesis/Dissertation.
- EGLAND, P. G. & HARWOOD, C. S. (1999) BadR, a New MarR Family Member, Regulates Anaerobic Benzoate Degradation by *Rhodospirillum rubrum* in Concert with AadR, an Fnr Family Member. *Journal of Bacteriology*, 181, 2102-2109.
- ERIKSSON, H. M., PERSSON, K., ZHANG, S. & WIESLANDER, A. (2009) High-yield expression and purification of a monotopic membrane glycosyltransferase. *Protein Expression and Purification*, 66, 143-148.
- ESTCP (2008) Treatment of RDX and/or HMX using Mulch Biowalls. U.S. Environmental Security Technology Certification Program. Ref Type: Technical report.



- ESTEVE-NUNEZ, A., CABALLERO, A. & RAMOS, J. L. (2001) Biological Degradation of 2,4,6-Trinitrotoluene. *Microbiol. Mol. Biol. Rev.*, 65, 335-352.
- EYERS, L., STENUIT, B. & AGATHOS, S. (2008) Denitration of 2,4,6-trinitrotoluene by *Pseudomonas aeruginosa* ESA-5 in the presence of ferrihydrite. *Applied Microbiology and Biotechnology*, 79, 489-497.
- FERNANDES, P. J., POWELL, J. A. C. & ARCHER, J. A. C. (2001) Construction of *Rhodococcus* random mutagenesis libraries using Tn5 transposition complexes. *Microbiology*, 147, 2529-2536.
- FLOKSTRA, B. R., AKEN, B. V. & SCHNOOR, J. L. (2008) Microtox® toxicity test: Detoxification of TNT and RDX contaminated solutions by poplar tissue cultures. *Chemosphere*, 71, 1970-1976.
- FOURNIER, D., HALASZ, A., SPAIN, J., FIURASEK, P. & HAWARI, J. (2002) Determination of key metabolites during biodegradation of hexahydro-1,3,5-trinitro-1,3,5-triazine with *Rhodococcus* sp strain DN22. *Applied and Environmental Microbiology*, 68, 166-172.
- FRENCH, C. E., HAILES, A. M., RATHBONE, D. A., LONG, M. T., WILLEY, D. L. & BRUCE, N. C. (1995) Biological production of semisynthetic opiates using genetically-engineered bacteria. *Bio-Technology*, 13, 674-676.
- FRENCH, C. E., NICKLIN, S. & BRUCE, N. C. (1998) Aerobic Degradation of 2,4,6-Trinitrotoluene by *Enterobacter cloacae* PB2 and by Pentaerythritol Tetranitrate Reductase. *Appl. Environ. Microbiol.*, 64, 2864-2868.
- FRENCH, C. E., ROSSER, S. J., DAVIES, G. J., NICKLIN, S. & BRUCE, N. C. (1999) Biodegradation of explosives by transgenic plants expressing pentaerythritol tetranitrate reductase. *Nature Biotechnology*, 17, 491-494.
- FUANGTHONG, M., ATICHARTPONGKUL, S., MONGKOLSUK, S. & HELMANN, J. D. (2001) OhrR Is a Repressor of ohrA, a Key Organic Hydroperoxide Resistance Determinant in *Bacillus subtilis*. *Journal of Bacteriology*, 183, 4134-4141.
- FULLER, M. E., HATZINGER, P. B., CONDEE, C. W. & TOGNA, A. P. (2007) Combined Treatment of Perchlorate and RDX in Ground Water Using a Fluidized Bed Reactor. *Ground Water Monitoring & Remediation*, 27, 59-64.
- GARCIA-GONZALEZ, V., GOVANTES, F., SHAW, L. J., BURNS, R. G. & SANTERO, E. (2003) Nitrogen Control of Atrazine Utilization in *Pseudomonas* sp. Strain ADP. *Appl. Environ. Microbiol.*, 69, 6987-6993.
- GONG, P., WILKE, B. M. & FLEISCHMANN, S. (1999) Soil-based phytotoxicity of 2,4,6-trinitrotoluene (TNT) to terrestrial higher plants. *Archives of Environmental Contamination and Toxicology*, 36, 152-157.
- GOVANTES, F., GARCÍA-GONZÁLEZ, V., PORRÚA, O., PLATERO, A. I., JIMÉNEZ-FERNÁNDEZ, A. & SANTERO, E. (2010) Regulation of the atrazine-degradative genes in *Pseudomonas* sp. strain ADP. *Fems Microbiology Letters*, 310, 1-8.

- GUNNISON, D., FREDRICKSON, H. L., RINGELBERG, D. B. & PERKINS, E. J. (1999) Implementation Guidance for Determining Suitability of Microorganisms for Explosives Degradation. U.S. Installation Restoration Research Program, Ref Type: Technical report.
- HANNINK, N., ROSSER, S. J., FRENCH, C. E., BASRAN, A., MURRAY, J. A. H., NICKLIN, S. & BRUCE, N. C. (2001) Phytodetoxification of TNT by transgenic plants expressing a bacterial nitroreductase. *Nature Biotechnology*, 19, 1168-1172.
- HANNINK, N. K., SUBRAMANIAN, M., ROSSER, S. J., BASRAN, A., MURRAY, J. A. H., SHANKS, J. V. & BRUCE, N. C. (2007) Enhanced transformation of TNT by tobacco plants expressing a bacterial nitroreductase. *International Journal of Phytoremediation*, 9, 385-401.
- HAWARI, J., HALASZ, A., SHEREMATA, T., BEAUDET, S., GROOM, C., PAQUET, L., RHOFIR, C., AMPLEMAN, G. & THIBOUTOT, S. (2000) Characterization of metabolites during biodegradation of hexahydro-1,3,5-trinitro-1,3,5-triazine (RDX) with municipal anaerobic sludge. *Applied and Environmental Microbiology*, 66, 2652-2657.
- HERVAS, A. B., CANOSA, I. & SANTERO, E. (2008) Transcriptome analysis of *Pseudomonas putida* in response to nitrogen availability. *Journal of Bacteriology*, 190, 416-420.
- HONEYCUTT, M. E., JARVIS, A. S. & MCFARLAND, V. A. (1996) Cytotoxicity and mutagenicity of 2,4,6-trinitrotoluene and its metabolites. *Ecotoxicology and Environmental Safety*, 35, 282-287.
- IIDA, T., MUKOUZAKA, Y., NAKAMURA, K., YAMAGUCHI, I. & KUDO, T. (2002) Isolation and characterization of dibenzofuran-degrading actinomycetes: Analysis of multiple extradiol dioxygenase genes in dibenzofuran-degrading *Rhodococcus* species. *Bioscience Biotechnology and Biochemistry*, 66, 1462-1472.
- INDEST, K. J., CROCKER, F. H. & ATHOW, R. (2007) A TaqMan polymerase chain reaction method for monitoring RDX-degrading bacteria based on the *xpIA* functional gene. *Journal of Microbiological Methods*, 68, 267-274.
- INDEST, K. J., JUNG, C. M., CHEN, H.-P., HANCOCK, D., FLORIZONE, C., ELTIS, L. D. & CROCKER, F. H. (2010) Functional characterization of pGKT2, a 182-kilobase plasmid containing the *xpIAB* genes, which are involved in the degradation of hexahydro-1,3,5-trinitro-1,3,5-triazine by *Gordonia* sp. strain KTR9. *Appl. Environ. Microbiol.*, 76, 6329-6337.
- JACKSON, R. G., RYLLOTT, E. L., FOURNIER, D., HAWARI, J. & BRUCE, N. C. (2007) Exploring the biochemical properties and remediation applications of the unusual explosive-degrading P450 system XpIA/B. *Proceedings of the National Academy of Sciences of the United States of America*, 104, 16822-16827.

- JAKOBY, M., NOLDEN, L., MEIER-WAGNER, J., KRAMER, R. & BURKOVSKI, A. (2000) AmtR, a global repressor in the nitrogen regulation system of *Corynebacterium glutamicum*. *Molecular Microbiology*, 37, 964-977.
- JOHNSTON, K., CLEMENTS, A., VENKATARAMANI, R. N., TRIEVEL, R. C. & MARMORSTEIN, R. (2000) Coexpression of Proteins in Bacteria Using T7-Based Expression Plasmids: Expression of Heteromeric Cell-Cycle and Transcriptional Regulatory Complexes. *Protein Expression and Purification*, 20, 435-443.
- JUNG, C. M., CROCKER, F. H., EBERLY, J. O. & INDEST, K. J. (2011) Horizontal gene transfer (HGT) as a mechanism of disseminating RDX-degrading activity among Actinomycete bacteria. *Journal of Applied Microbiology*, 110, 1449-1459.
- KITTS, C. L., CUNNINGHAM, D. P. & UNKEFER, P. J. (1994) Isolation of 3 hexahydro-1,3,5-trinitro-1,3,5-triazine-degrading species of the family Enterobacteriaceae from nitramine explosive-contaminated soil. *Applied and Environmental Microbiology*, 60, 4608-4611.
- KITTS, C. L., GREEN, C. E., OTLEY, R. A., ALVAREZ, M. A. & UNKEFER, P. J. (2000) Type I nitroreductases in soil enterobacteria reduce TNT (2,4,6-trinitrotoluene) and RDX (hexahydro-1,3,5-trinitro-1,3,5-triazine). *Canadian Journal of Microbiology*, 46, 278-282.
- KOMEDA, H., KOBAYASHI, M. & SHIMIZU, S. (1997) A Novel Transporter Involved in Cobalt Uptake. *Proceedings of the National Academy of Sciences of the United States of America*, 94, 36-41.
- KULAKOV, L. A., CHEN, S., ALLEN, C. C. R. & LARKIN, M. J. (2005) Web-Type Evolution of Rhodococcus Gene Clusters Associated with Utilization of Naphthalene. *Appl. Environ. Microbiol.*, 71, 1754-1764.
- KULAKOVA, A. N., LARKIN, M. J. & KULAKOV, L. A. (1997) The Plasmid-Located Haloalkane Dehalogenase Gene from *Rhodococcus rhodochrous* NCIMB 13064. *Microbiology*, 143, 109-115.
- LARKIN, M. J., KULAKOV, L. A. & ALLEN, C. C. R. (2005) Biodegradation and *Rhodococcus*-masters of catabolic versatility. *Current Opinion in Biotechnology*, 16, 282-290.
- LEMUH, N. D., DIALLINAS, G., FRILLINGOS, S., MERMELEKAS, G., KARAGOUNI, A. D. & HATZINIKOLAOU, D. G. (2009) Purification and partial characterization of the xanthine-uric acid transporter (UapA) of *Aspergillus nidulans*. *Protein Expression and Purification*, 63, 33-39.
- LEWIS, T. A., EDERER, M. M., CRAWFORD, R. L. & CRAWFORD, D. L. (1997) Microbial transformation of 2,4,6-trinitrotoluene. *Journal of Industrial Microbiology & Biotechnology*, 18, 89-96.
- LEWIS, T. A., NEWCOMBE, D. A. & CRAWFORD, R. L. (2004) Bioremediation of soils contaminated with explosives. *Journal of Environmental Management*, 70, 291-307.

- LOTUFO, G. R., GIBSON, A. B. & LESLIE YOO, J. (2010) Toxicity and bioconcentration evaluation of RDX and HMX using sheepshead minnows in water exposures. *Ecotoxicology and Environmental Safety*, 73, 1653-1657.
- LUCET, I., BORRIS, R. & YUDKIN, M. D. (1999) Purification, kinetic properties, and intracellular concentration of SpoIIIE, an integral membrane protein that regulates sporulation in *Bacillus subtilis*. *Journal of Bacteriology*, 181, 3242-3245.
- MASCHKE, H. E., KUMAR, P. K. R., GEIGER, R. & SCHÜGERL, K. (1992) Plasmid instabilities of single and three-plasmid systems in *Escherichia coli* during continuous cultivation. *Journal of Biotechnology*, 24, 235-251.
- MASI, M., PAGÈS, J.-M. & PRADEL, E. (2003) Overexpression and purification of the three components of the *Enterobacter aerogenes* AcrA-AcrB-TolC multidrug efflux pump. *Journal of Chromatography B*, 786, 197-205.
- MCCORMICK, N. G., CORNELL, J. H. & KAPLAN, A. M. (1981) Biodegradation of hexahydro-1,3,5-trinitro-1,3,5-triazine. *Applied and Environmental Microbiology*, 42, 817-823.
- MCLEOD, M. P., WARREN, R. L., HSIAO, W. W. L., ARAKI, N., MYHRE, M., FERNANDES, C., MIYAZAWA, D., WONG, W., LILLQUIST, A. L., WANG, D., DOSANJH, M., HARA, H., PETRESCU, A., MORIN, R. D., YANG, G., STOTT, J. M., SCHEIN, J. E., SHIN, H., SMAILUS, D., SIDDIQUI, A. S., MARRA, M. A., JONES, S. J. M., HOLT, R., BRINKMAN, F. S. L., MIYAUCHI, K., FUKUDA, M., DAVIES, J. E., MOHN, W. W. & ELTIS, L. D. (2006) The complete genome of *Rhodococcus* sp RHA1 provides insights into a catabolic powerhouse. *Proceedings of the National Academy of Sciences of the United States of America*, 103, 15582-15587.
- MCCORMACK, V., GARG, A., ALDRED, D., HOBBS, G., SMITH, R. & TOTHILL, I. E. (2008) Composting and bioremediation process evaluation of wood waste materials generated from the construction and demolition industry. *Chemosphere*, 71, 1617-1628.
- MIROUX, B. & WALKER, J. E. (1996) Over-production of proteins in *Escherichia coli*: Mutant hosts that allow synthesis of some membrane proteins and globular proteins at high levels. *Journal of Molecular Biology*, 260, 289-298.
- MOHANTY, A. K. & WIENER, M. C. (2004) Membrane protein expression and production: effects of polyhistidine tag length and position. *Protein Expression and Purification*, 33, 311-325.
- MOKHONOV, V., MOKHONOVA, E., YOSHIHARA, E., MASUI, R., SAKAI, M., AKAMA, H. & NAKAE, T. (2005) Multidrug transporter MexB of *Pseudomonas aeruginosa*: overexpression, purification, and initial structural characterization. *Protein Expression and Purification*, 40, 91-100.
- MULLIGAN, C. (2008) Functional characterisation of bacterial tripartite ATP-independent periplasmic (TRAP) transporters. Department of Biology, University of York. Ref Type: Thesis/Dissertation.

- MULLIGAN, C., GEERTSMA, E. R., SEVERI, E., KELLY, D. J., POOLMAN, B. & THOMAS, G. H. (2009) The substrate-binding protein imposes directionality on an electrochemical sodium gradient-driven TRAP transporter. *Proceedings of the National Academy of Sciences of the United States of America*, 106, 1778-1783.
- NEJIDAT, A., KAFKA, L., TEKOA, Y. & RONEN, Z. (2008) Effect of organic and inorganic nitrogenous compounds on RDX degradation and cytochrome P-450 expression in *Rhodococcus* strain YH1. *Biodegradation*, 19, 313-320.
- NIPPER, M., CARR, R. S., BIEDENBACH, J. M., HOOTEN, R. L., MILLER, K. & SAEPOFF, S. (2001) Development of marine toxicity data for ordnance compounds. *Archives of Environmental Contamination and Toxicology*, 41, 308-318.
- NUNEZ, M. F., KWON, O., WILSON, T. H., AGUILAR, J., BALDOMA, L. & LIN, E. C. C. (2002) Transport of L-lactate, D-lactate, and glycolate by the LldP and GlcA membrane carriers of *Escherichia coli*. *Biochemical and Biophysical Research Communications*, 290, 824-829.
- OKAMOTO, S., VAN PETEGEM, F., PATRAUCHAN, M. A. & ELTIS, L. D. (2010) AnhE, a metallochaperone involved in the maturation of a cobalt-dependent nitrile hydratase. *Journal of Biological Chemistry*, 285, 25126-25133.
- PAK, J. W., KNOKE, K. L., NOGUERA, D. R., FOX, B. G. & CHAMBLISS, G. H. (2000) Transformation of 2,4,6-Trinitrotoluene by Purified Xenobiotic Reductase B from *Pseudomonas fluorescens* I-C. *Appl. Environ. Microbiol.*, 66, 4742-4750.
- PAN, X. P., SAN FRANCISCO, M. J., LEE, C., OCHOA, K. M., XU, X. Z., LIU, J., ZHANG, B. H., COX, S. B. & COBB, G. P. (2007) Examination of the mutagenicity of RDX and its N-nitroso metabolites using the *Salmonella* reverse mutation assay. *Mutation Research-Genetic Toxicology and Environmental Mutagenesis*, 629, 64-69.
- PARK, H.-S. & KIM, H.-S. (2001) Genetic and Structural Organization of the Aminophenol Catabolic Operon and Its Implication for Evolutionary Process. *Journal of Bacteriology*, 183, 5074-5081.
- PERERA, I. C. & GROVE, A. (2010) Molecular Mechanisms of Ligand-Mediated Attenuation of DNA Binding by MarR Family Transcriptional Regulators. *Journal of Molecular Cell Biology*, 2, 243-254.
- PROVIDENTI, M. A. & WYNDHAM, R. C. (2001) Identification and Functional Characterization of CbaR, a MarR-Like Modulator of the cbaABC-Encoded Chlorobenzoate Catabolism Pathway. *Appl. Environ. Microbiol.*, 67, 3530-3541.
- QUICK, M. & WRIGHT, E. M. (2002) Employing *Escherichia coli* to functionally express, purify, and characterize a human transporter. *Proceedings of the National Academy of Sciences of the United States of America*, 99, 8597-8601.
- RO, K. S., PRESTON, K. T., SEIDEN, S. & BERGS, M. A. (1998) Remediation composting process principles: Focus on soils contaminated with explosive

- compounds. *Critical Reviews in Environmental Science and Technology*, 28, 253-282.
- RODIONOV, D. A., VITRESCHAK, A. G., MIRONOV, A. A. & GELFAND, M. S. (2003) Regulation of lysine biosynthesis and transport genes in bacteria: yet another RNA riboswitch? *Nucleic Acids Research*, 31, 6748-6757.
- ROSEN, G. & LOTUFO, G. R. (2007) Toxicity of explosive compounds to the marine mussel, *Mytilus galloprovincialis*, in aqueous exposures. *Ecotoxicology and Environmental Safety*, 68, 228-236.
- ROSENBERGER, R. F. & ELSDEN, S. R. (1960) The yields of *Streptococcus faecalis* grown in continuous culture. *Journal of General Microbiology*, 22, 726-739.
- ROSLONIEC, K. Z., WILBRINK, M. H., CAPYK, J. K., MOHN, W. W., OSTENDORF, M., VAN DER GEIZE, R., DIJKHUIZEN, L. & ELTIS, L. D. (2009) Cytochrome P450 125 (CYP125) catalyses C26-hydroxylation to initiate sterol side-chain degradation in *Rhodococcus jostii* RHA1. *Molecular Microbiology*, 74, 1031-1043.
- RUGH, C. L., SENECOFF, J. F., MEAGHER, R. B. & MERKLE, S. A. (1998) Development of transgenic yellow poplar for mercury phytoremediation. *Nature Biotechnology*, 16, 925-928.
- RYLOTT, E. L. & BRUCE, N. C. (2009) Plants disarm soil: engineering plants for the phytoremediation of explosives. *Trends in Biotechnology*, 27, 73-81.
- RYLOTT, E. L., JACKSON, R. G., EDWARDS, J., WOMACK, G. L., SETH-SMITH, H. M. B., RATHBONE, D. A., STRAND, S. E. & BRUCE, N. C. (2006) An explosive-degrading cytochrome P450 activity and its targeted application for the phytoremediation of RDX. *Nature Biotechnology*, 24, 216-219.
- RYLOTT, E. L., LORENZ, A. & BRUCE, N. C. (2011) Biodegradation and biotransformation of explosives. *Current Opinion in Biotechnology*, 22, 434-440.
- SABBADIN, F., JACKSON, R., HAIDER, K., TAMPI, G., TURKENBURG, J. P., HART, S., BRUCE, N. C. & GROGAN, G. (2009) The 1.5-angstrom structure of XplA-heme, an unusual cytochrome P450 heme domain that catalyzes reductive biotransformation of Royal Demolition Explosive. *Journal of Biological Chemistry*, 284, 28467-28475.
- SCHÄFER, A., TAUCH, A., JÄGER, W., KALINOWSKI, J., THIERBACH, G. & PÜHLER, A. (1994) Small mobilizable multi-purpose cloning vectors derived from the *Escherichia coli* plasmids pK18 and pK19: selection of defined deletions in the chromosome of *Corynebacterium glutamicum*. *Gene*, 145, 69-73.
- SETH-SMITH, H. M. B. (2002) Microbial Degradation of RDX. University of Cambridge, Institute of Biotechnology. Ref Type: Thesis/Dissertation.
- SETH-SMITH, H. M. B., EDWARDS, J., ROSSER, S. J., RATHBONE, D. A. & BRUCE, N. C. (2008) The explosive-degrading cytochrome P450 system is highly

conserved among strains of *Rhodococcus* spp. *Applied and Environmental Microbiology*, 74, 4550-4552.

SETH-SMITH, H. M. B., ROSSER, S. J., BASRAN, A., TRAVIS, E. R., DABBS, E. R., NICKLIN, S. & BRUCE, N. C. (2002) Cloning, sequencing, and characterization of the hexahydro-1,3,5-trinitro-1,3,5-triazine degradation gene cluster from *Rhodococcus rhodochrous*. *Applied and Environmental Microbiology*, 68, 4764-4771.

SETO, M., MASAI, E., IDA, M., HATTA, T., KIMBARA, K., FUKUDA, M. & YANO, K. (1995) Multiple polychlorinated biphenyl transformation systems in the Gram-positive bacterium *Rhodococcus* sp strain RHA1. *Applied and Environmental Microbiology*, 61, 4510-4513.

SHAO, Z. Q., SEFFENS, W., MULBRY, W. & BEHKI, R. M. (1995) Cloning and expression of the s-triazine hydrolase gene (*trzA*) from *Rhodococcus corallinus* and development of *Rhodococcus* recombinant strains capable of dealkylating and dechlorinating the herbicide atrazine. *Journal of Bacteriology*, 177, 5748-5755.

STUART-KEIL, K. G., HOHNSTOCK, A. M., DREES, K. P., HERRICK, J. B. & MADSEN, E. L. (1998) Plasmids responsible for horizontal transfer of naphthalene catabolism genes between bacteria at a coal tar contaminated site are homologous to pDTG1 from *Pseudomonas putida* NCIB 9816-4. *Applied and Environmental Microbiology*, 64, 3633-3640.

SYMONS, Z. (2005) The biotransformation of explosives by the Old Yellow Enzyme Family of Protein of Flavoenzymes. University of Cambridge, Institute of Biotechnology. Ref Type: Thesis/Dissertation.

THOMPSON, K. T., CROCKER, F. H. & FREDRICKSON, H. L. (2005) Mineralization of the cyclic nitramine explosive hexahydro-1,3,5-trinitro-1,3,5-triazine by *Gordonia* and *Williamsia* spp. *Applied and Environmental Microbiology*, 71, 8265-8272.

VAN DER GEIZE, R., HESSELS, G. I., VAN GERWEN, R., VAN DER MEIJDEN, P. & DIJKHUIZEN, L. (2001) Unmarked gene deletion mutagenesis of *kstD*, encoding 3-ketosteroid  $\Delta^1$ -dehydrogenase, in *Rhodococcus erythropolis* SQ1 using *sacB* as counter-selectable marker. *Fems Microbiology Letters*, 205, 197-202.

VAN HAM, N. H. A. (1998) Recycling and disposal of munitions and explosives. *Waste Management*, 17, 147-150.

WATERLAND, L. R., KING, C., RICHARDS, M. K. & THURNAU, R. C. (1991) Incineration treatment of arsenic-contaminated soil. *Remediation Journal*, 1, 227-237.

WHYTE, L. G., SMITS, T. H. M., LABBE, D., WITHOLT, B., GREER, C. W. & VAN BEILEN, J. B. (2002) Gene cloning and characterization of multiple alkane hydroxylase systems in *Rhodococcus* strains Q15 and NRRL B-16531. *Applied and Environmental Microbiology*, 68, 5933-5942.

- WIESMANN, U., CHOI, I. S. & DOMBROWSKI, E. (2007) Biodegradation of Special Organic Compounds. In *Fundamentals of Biological Wastewater Treatment*. Weinheim, Germany: Wiley-VCH, p195-222.
- WILBRINK, M. H., PETRUSMA, M., DIJKHUIZEN, L. & VAN DER GEIZE, R. (2011) FadD19 of *Rhodococcus rhodochrous* DSM43269: a steroid-CoA ligase essential for degradation of C24-branched sterol side chains. *Appl. Environ. Microbiol.*, AEM.00380-11.
- WILKINSON, S. P. & GROVE, A. (2005) Negative Cooperativity of Uric Acid Binding to the Transcriptional Regulator HucR from *Deinococcus radiodurans*. *Journal of Molecular Biology*, 350, 617-630.
- WILLIAMS, R. E., RATHBONE, D. A., SCRUTTON, N. S. & BRUCE, N. C. (2004) Biotransformation of Explosives by the Old Yellow Enzyme Family of Flavoproteins. *Appl. Environ. Microbiol.*, 70, 3566-3574.
- WILLIAMSON, N. R., FINERAN, P. C., LEEPER, F. J. & SALMOND, G. P. C. (2006) The biosynthesis and regulation of bacterial prodiginines. *Nat Rev Micro*, 4, 887-899.
- WITTICH, R.-M., HAÄ DOUR, A., VAN DILLEWIJN, P. & RAMOS, J.-L. (2008) OYE Flavoprotein Reductases Initiate the Condensation of TNT-Derived Intermediates to Secondary Diarylamines and Nitrite. *Environmental Science & Technology*, 42, 734-739.
- WITTICH, R.-M., RAMOS, J. L. & DILLEWIJN, P. V. (2009) Microorganisms and Explosives: Mechanisms of Nitrogen Release from TNT for Use as an N-Source for Growth. *Environmental Science & Technology*, 43, 2773-2776.
- YANG, X., LIU, X., SONG, L., XIE, F., ZHANG, G. & QIAN, S. (2007) Characterization and functional analysis of a novel gene cluster involved in biphenyl degradation in *Rhodococcus* sp strain R04. *Journal of Applied Microbiology*, 103, 2214-2224.
- YU, M., FAAN, Y. W., CHUNG, W. Y. K. & TSANG, J. S. H. (2007) Isolation and characterization of a novel haloacid permease from *Burkholderia cepacia* MBA4. *Applied and Environmental Microbiology*, 73, 4874-4880.
- ZHAO, J.-S., HALASZ, A., PAQUET, L., BEAULIEU, C. & HAWARI, J. (2002) Biodegradation of Hexahydro-1,3,5-Trinitro-1,3,5-Triazine and Its Mononitroso Derivative Hexahydro-1-Nitroso-3,5-Dinitro-1,3,5-Triazine by *Klebsiella pneumoniae* Strain SCZ-1 Isolated from an Anaerobic Sludge. *Appl. Environ. Microbiol.*, 68, 5336-5341.
- ZHAO, J. S., PAQUET, L., HALASZ, A. & HAWARI, J. (2003) Metabolism of hexahydro-1,3,5-trinitro-1,3,5-triazine through initial reduction to hexahydro-1-nitroso-3,5-dinitro-1,3,5-triazine followed by denitration in *Clostridium bifermentans*; HAW-1. *Applied Microbiology and Biotechnology*, 63, 187-193.
- ZOLOTAREV, A. S., UNNIKRISHNAN, M., SHMUKLER, B. E., CLARK, J. S., VANDORPE, D. H., GRIGORIEFF, N., RUBIN, E. J. & ALPER, S. L. (2008)



Increased sulfate uptake by *E. coli* overexpressing the SLC26-related SulP protein Rv1739c from *Mycobacterium tuberculosis*. *Comparative Biochemistry and Physiology - Part A: Molecular & Integrative Physiology*, 149, 255-266.